ปัจจัยที่มีผลต่อสภาพเลือกจำเพาะและค่าการแยกในไมเซลลาร์อิเล็กโทรไคเนทิก

โครมาโทกราฟีและคะพิลลารีอิเล็กโทรโครมาโทกราฟี

นางสาวชนิดา พวงพิลา

วิทยานิพนธ์นี้เป็นส่วนหนึ่งของการศึกษาตามหลักสูตรปริญญาวิทยาศาสตรดุษฎีบัณฑิต

สาขาวิชาเคมี ภาควิชาเคมี

คณะวิทยาศาสตร์ จุฬาลงกรณ์มหาวิทยาลัย

ปีการศึกษา 2554

FACTORS AFFECTING SELECTIVITY AND RESOLUTION IN
MICELLAR ELECTROKINETIC CHROMATOGRAPHY AND
CAPILLARY ELECTROCHROMATOGRAPHY

Miss Chanida Puangpila

A Dissertation Submitted in Partial Fulfillment of the Requirements
for the Degree of Doctor of Philosophy Program in Chemistry
Department of Chemistry
Faculty of Science
Chulalongkorn University
Academic Year 2011

Thesis Title   Factors Affecting Selectivity and Resolution in Micellar

                      Electrokinetic Chromatography and Capillary

                      Electrochromatography

By   Miss Chanida Puangpila

Field of Study   Chemistry

Thesis Advisor   Associate Professor Thumnoon Nhujak, Ph.D.

Accepted by the Faculty of Science, Chulalongkorn University in Partial Fulfillment of the Requirements for the Doctoral Degree

……………………………….. Dean of the Faculty of Science

(Professor Supot Hannongbua, Dr.rer.nat)

THESIS COMMITTEE

………………………………………….. Chairman

(Assistant Professor Suchada Chuanuwatanakul, Ph.D.)

……………………………………….……. Thesis Advisor

(Associate Professor Thumnoon Nhujak, Ph.D.)

……………………………………….. Examiner

(Associate Professor Amorn Petsom, Ph.D.)

……………………………………….. Examiner

(Assistant Professor Natchanun Leepipatpiboon, Dr.rer.nat)

……………………………………….. External Examiner

(Assistant Professor Somsak Sirichai, Ph.D.)

ชนิดา พวงพิลา : ปัจจัยที่มีผลต่อสภาพเลือกจำเพาะและค่าการแยกในไมเซลลาร์
อิเล็กโทรไดเนทิกโครมาโทกราฟีและคะพิลลารีอิเล็กโทรโครมาโทกราฟี.
(FACTORS AFFECTING SELECTIVITY AND RESOLUTION IN MICELLAR
ELECTROKINETIC CHROMATOGRAPHY AND CAPILLARY
ELECTROCHROMATOGRAPHY) อ.ที่ปรึกษาวิทยานิพนธ์หลัก: รศ. ดร. ธรรมนูญ
หนูจักร, 99 หน้า.

งานวิจัยนี้เกี่ยวข้องกับแบบจำลองทางทฤษฎีของสภาพเลือกจำเพาะของการแยก
สำหรับสารที่มีประจุในไมเซลลาร์อิเล็กโทรไดเนทิกโครมาโทกราฟี (MEKC) และการ
เปรียบเทียบสภาพเลือกจำเพาะของมอนอลิตที่ไม่มีประจุสำหรับการแยกเพปไทด์และโปรตีน
ในคะพิลลารีอิเล็กโทรโครมาโทกราฟี (CEC) ได้สร้างสมการและแบบจำลองทางทฤษฎี
สำหรับสภาพเลือกจำเพาะของการแยก (α_{MEKC}) ใน MEKC โดยที่ α_{MEKC} สัมพันธ์กับตัวแปรที่
ไม่มีหน่วยได้แก่ สภาพเลือกจำเพาะของการเคลื่อนที่ (α_{CZE}) ในคะพิลลารีโซน
อิเล็กโทรฟอริซิส (CZE) และสภาพเลือกจำเพาะของรีเทนชัน (α_k) ใน MEKC เมื่อ α_{CZE} และ
α_k นิยามเป็นอัตราส่วนของความสามารถในการเคลื่อนที่ทางไฟฟ้าใน CZE และอัตราส่วน
ของรีเทนชันแฟกเตอร์ใน MEKC สำหรับสารสองชนิดที่มีประจุ ตามลำดับ ตัวอย่างเช่น การ
แยกของสารที่มีประจุใน MEKC สามารถเพิ่ม α_{MEKC} ได้เมื่ออัตราส่วนของสภาพเลือกจำเพาะ
(ρ) มากกว่า 1.0 ($\rho = \alpha_k/\alpha_{CZE}$) ในขณะที่ α_{MEKC} ลดลงเมื่อ $\rho \leq 1.0$ เมื่อใช้อัลคิลเบนซีนเป็น
สารทดสอบพบว่าค่า α_{MEKC} ที่ได้จากการทดลองสอดคล้องกับการทำนายตามแบบจำลองของ
α_{MEKC}

นอกจากนี้ได้เตรียม CEC คอลัมน์ประเภทมอนอลิตที่ไม่มีประจุที่มีหมู่เกาะอัลคิลเป็น
C8-, C12- และ C16- โดยโคพอลิเมอไรเซชันของมอนอเมอร์ที่มีหมู่ฟังก์ชันเป็น
C8-เมทราคริเลต, C12-อะคริเลต และ C16-เมทราคริเลต ตามลำดับ กับสารเชื่อมโยงข้าม
เพนแทรีไทรทอลไทรอะคริเลต C16-มอนอลิตให้ประสิทธิภาพ (N) สำหรับแยกอัลคิล
เบนซีนดีกว่า (N เท่ากับ 200,000, 162,000, 150,000 เพลต/เมตร สำหรับ C16-, C12- และ C8-
มอนอลิต ตามลำดับ) และให้ประสิทธิภาพสำหรับแยกทริปทิกเพปไทด์แมปปิงดีกว่า
อย่างไรก็ตาม C8-มอนอลิตให้ประสิทธิภาพสำหรับแยกโปรตีนได้ดีกว่า (N เท่ากับ 332,000,
236,000, 225,000 เพลต/เมตร สำหรับ C8-, C12- และ C16-มอนอลิต ตามลำดับ)

ภาควิชา	เคมี	ลายมือชื่อนิสิต	
สาขาวิชา	เคมี	ลายมือชื่ออ.ที่ปรึกษาวิทยานิพนธ์หลัก	
ปีการศึกษา	2554		

497 22641 23 : MAJOR CHEMISTRY

KEYWORDS : CAPILLARY E LECTROCHROMATOGRAPHY/ CHARGED COMPOUNDS/ MICELLAR ELECTROKINETIC C HROMATOGRAPHY/ NEUTRAL MONOLITHS/ SEPARATION SELECTIVITY

CHANIDA PUANGPILA: FACTORS AFFECTING SELECTIVITY AND RESOLUTION IN MICELLAR ELECTROKINETIC CHROMATOGRAPHY AND CAPILLARY ELECTROCHROMATOGRAPHY. ADVISOR: ASSOC.PROF. THUMNOON NHUJAK, Ph.D., 99 pp.

This w ork involves the theoretical m odels of separation s electivity for charged an alytes in micellar electrokinetic ch romatography (MEKC), a nd comparison of selectivity of neutral monoliths for peptides and proteins separation in cap illary el ectrochromatography (CEC). Equations and t heoretical m odels for MEKC separation selectivity (α_{MEKC}) were established, in which α_{MEKC} is related to di mensionless va lues of mobility selectivity (α_{CZE}) in c apillary zone electrophoresis (CZE) and r etention s electivity (α_k) i n M EKC, an d w here α_{CZE} and α_k are defined as the ratio o f electrophoretic mobility in CZE and the ratio of retention f actor in M EKC f or t wo c harged a nalytes, r espectively. For ex ample, MEKC separation of two charged analytes can enhance α_{MEKC} when the selectivity ratio (ρ) i s greater t han 1.0 ($\rho = \alpha_k/\alpha_{CZE}$), w hile lo wer α_{MEKC} is o btained w ith $\rho \leq 1.0$. Using alkylparabens as t est an alytes, ex cellent a greement w as f ound between the observed α_{MEKC} and prediction according to the theoretical models of α_{MEKC}.

In a ddition, neutral mo nolithic CEC columns with C8-, C 12- and C 16-alkyl moieties were prepared by the copolymerization of the functional monomers C8-methacrylate, C 12-acrylate and C16-methacrylate, r espectively with the crosslinker pentaerythritol tr iacrylate. The C 16-monolith provided better separation e fficiency (N) for alkylbenzenes (N of 200,000, 162,000, 150,000 plates/m for C 16-, C 12- and C 8-monoliths, r espectively), a nd yielded better separation for tryptic peptide mapping. However, the C8-monolith provided better separation ef ficiency for pr oteins (N of 332,000 , 236,000, 225,000 plates/m for C8-, C12- and C16-monoliths, respectively).

Department : _____Chemistry_____   Student's Signature _____

Field of Study : _____Chemistry_____   Advisor's Signature _____

Academic Year : _____2011_____

ACKNOWLEDGEMENTS

First of all, I wish to express my gratitude to my advisor, Associate Professor Dr. Thumnoon Nhujak, for his professionalism, suggestion, and critical reading. My special thanks are extended to the thesis examiners for their valuable comments and suggestions.

I am grateful to Professor Dr. Ziad El Rassi for his instruction during my one year research on CEC work in his lab at the Department of Chemistry, Oklahoma State University. I am also grateful to the members of his research group for their support, cheerful and friendship.

Furthermore, I specially thank to all members of Separation and Chromatography Research Unit for their valuable suggestions. Also, I wish to thank all members of CE group for their helpfulness and encouragement. Moral supports and cheerful willingness of my friends are truly appreciated. Thanks are also extended to everyone who has contributed suggestions and supports throughout this research.

I thankfully acknowledge the Rachadaphiseksomphot Endowment and the Graduate School, Chulalongkorn University for the financial support and the Center for Petroleum, Petrochemicals, and Advanced Materials for international conference support. The financial support also imparted of the Institute for the Promotion of the Teaching Science and Technology, Thailand. All research facilities and partial grant, provided by the Department of Chemistry, Chulalongkorn University are appreciatively and thankfully acknowledge.

Finally, I am eternally grateful to my beloved parents and my brother for their love, encouragement and supports through to the end.

CONTENTS

LIST OF TABLES

LIST OF FIGURES

FIGURES **PAGE**

FIGURES   **PAGE**

FIGURES   **PAGE**

FIGURES **PAGE**

LIST OF ABBREVIATIONS AND SYMBOLS

ABs	alkylbenzene
ACN	acetonitrile
AIBN	2,2´-azobisisobutyronitrile
APKs	alkyl phenyl ketones
BGE	background electrolyte
BP	butylparaben
CE	capillary electrophoresis
CEC	capillary electrochromatography
CGE	capillary gel electrophoresis
CIEF	capillary isoelectric focusing
CITP	capillary isotachophoresis
CZE	capillary zone electrophoresis
C8-methacrylate	octyl methacrylate
C12-acrylate	dodecyl acrylate
C16-methacrylate	cetyl methacrylate
DAD	diode array detector
DB	dodecylbenzene
EDMA	ethylene dimethacrylate
EG	ethylene glycol
EOF	electroosmotic flow
EP	ethylparaben
EtOH	ethanol
GC	gas chromatography
HPLC	high-performance liquid chromatography
i.d.	internal diameter
IP	isomethylparaben
MEKC	micellar electrokinetic chromatography
NaOH	sodium hydroxide
NAs	nitroalkanes

NMM	naphthyl methacrylate monolith
ODM	octadecyl monolith
PETA	pentaerythritol triacrylate
pI	isoelectric point
PP	propylparaben
PTFE	polytetrafluoroethylene
RP-CEC	reversed-phase capillary electrochromatography
RSD	relative standard deviation
SDS	sodium dodecyl sulphate
[SDS]	concentration of sodium dodecyl sulphate
C	concentration of analyte
E	electric field strength
e	electronic charge
F_E	applied electric force
F_F	frictional force
H	plate height
H_{aq}	plate height due to intermicelle mass transfer in aqueous phase
H_{col}	plate height due to column
H_{det}	plate height due to detection
H_f	plate height due to maldistribution of flow
H_{inj}	plate height due to injection
H_{joule}	plate height due to thermal dispersion
H_l	plate height due to longitudinal diffusion
H_{mc}	plate height due to sorption-desorption kinetics in micelle phase
H_{min}	minimum plate height
H_p	plate height due to mass transfer resistance in the pore
H_{pd}	plate height due to polydispersity of micelle phase
H_t	plate height due to thermal dispersion
K	distribution constant
K_a	acid distribution constant

k	retention factor
L	total capillary length
l	length of capillary to detector
l_{inj}	length of analyte injected
N	number of theoretical plate, or peak efficiency
$\overline{N}$	average efficiency
n_{aq}	amount of analyte in aqueous phase
n_{mc}	amount of analyte in micelle phase
ΔP	pressure difference across the capillary
Q_{inj}	quantity of sample injected
R_s	resolution
r	internal capillary radius
r_h	hydrodynamic radius
t_{eo}	migration time of EOF
t_{ep}	migration time corresponding to the electrophoretic mobility of the charged analyte
t_{inj}	injection time
t_m	migration time
t_{mc}	migration times of micelle phase
t_o	retention time of EOF marker
u_{opt}	optimum flow velocity
V	applied voltage
V_{inj}	volume of sample injected
v_{eo}	electroosmotic velocity
v_{ep}	electrophoretic velocity
v_{net}	total electrophoretic velocity
v_s	observed velocity of the analyte
v_{sc}	observed velocity of micelle phase
w_b	peak width at base
w_h	peak width at half height
x_{aq}	mole fraction of analyte in aqueous phase

x_{mc}	mole fraction of analyte in micelle phase
z	charge of anion
α	selectivity
α_{CZE}	mobility selectivity in CZE
α_{dis}	degree of ionization
α_k	retention selectivity in MEKC
α_m	separation selectivity or mobility selectivity
α_{MEKC}	separation selectivity in MEKC
ε	permittivity
ϕ	volume of aqueous phase to pseudo stationary phase
η	viscosity
μ	electrophoretic mobility
μ_{eo}	electroosmotic mobility
μ_{eff}	effective electrophoretic mobility
μ_{mc}	mobility of micelle phase
μ_{MEKC}	effective electrophoretic mobility of fully charged analyte in MEKC
μ_{net}	total mobility
μ_0	electrophoretic mobility at CZE conditions
$\overline{\mu}$	average effective electrophoretic mobility
$\Delta\mu$	difference in the mobility for two analytes
σ	standard deviation of peak in distance unit
σ^2	peak variance
τ	standard deviation of peak in time unit
ζ	zeta potential
ρ	selectivity ratio

CHAPTER I

INTRODUCTION

1.1 Introduction to Capillary Electrophoresis

Capillary electrophoresis (CE) is a separation technique in which the analytes are separated in a capillary containing an electrolyte under the influence of applied electric field. The separation principle is based on the difference in electrophoretic mobility of analytes depending on the charged-to-size ratio [Khaledi, 1998; Camilleri, 1993]. The wide applications of CE have been demonstrated by its ability to separate both charged and neutral analytes, small and large molecules such as peptides and proteins. Several advantages of CE include high separation efficiency, simple sample preparation, short analysis time, and low sample and solvent consumption [Hansen *et al*., 2003; McEvoy *et al*., 2007].

According to separation mechanism [Grossman *et al*., 1992; Khaledi, 1998], CE can be classified into six basic modes including capillary zone electrophoresis (CZE), micellar electrokinetic chromatography (MEKC), capillary electrochromatography (CEC), capillary gel electrophoresis (CGE), capillary isotachophoresis (CITP) and capillary isoelectric focusing (CIEF). This work involves the first three modes that will be briefly mentioned in this section.

CZE is a basic mode of CE that commonly used for separation of charged analytes. Its separation mechanism is based on the difference in electrophoretic mobility of analytes due to their different charge-to-size ratio, as shown in Figure 1.1a. The background electrolytes (BGE) used in CZE are typically buffers such as phosphate, borate and acetate.

1.2 Introduction to Micellar Electrokinetic Chromatography

MEKC is another mode of CE in which BGE contains a surfactant, such as sodium dodecyl sulphate (SDS), to form micelles or micellar phase acting as a pseudo-stationary phase, similar to a stationary phase in high-performance liquid chromatography (HPLC). The major benefit of MEKC is that allows the separation of both neutral and charged analytes. The separation mechanism of neutral analytes depends only on the difference in partitioning of the analytes between an aqueous phase and a pseudo stationary phase of micelles while the separation of charged analytes in MEKC depends on the difference in either micellar partitioning or their electrophoretic mobilities.
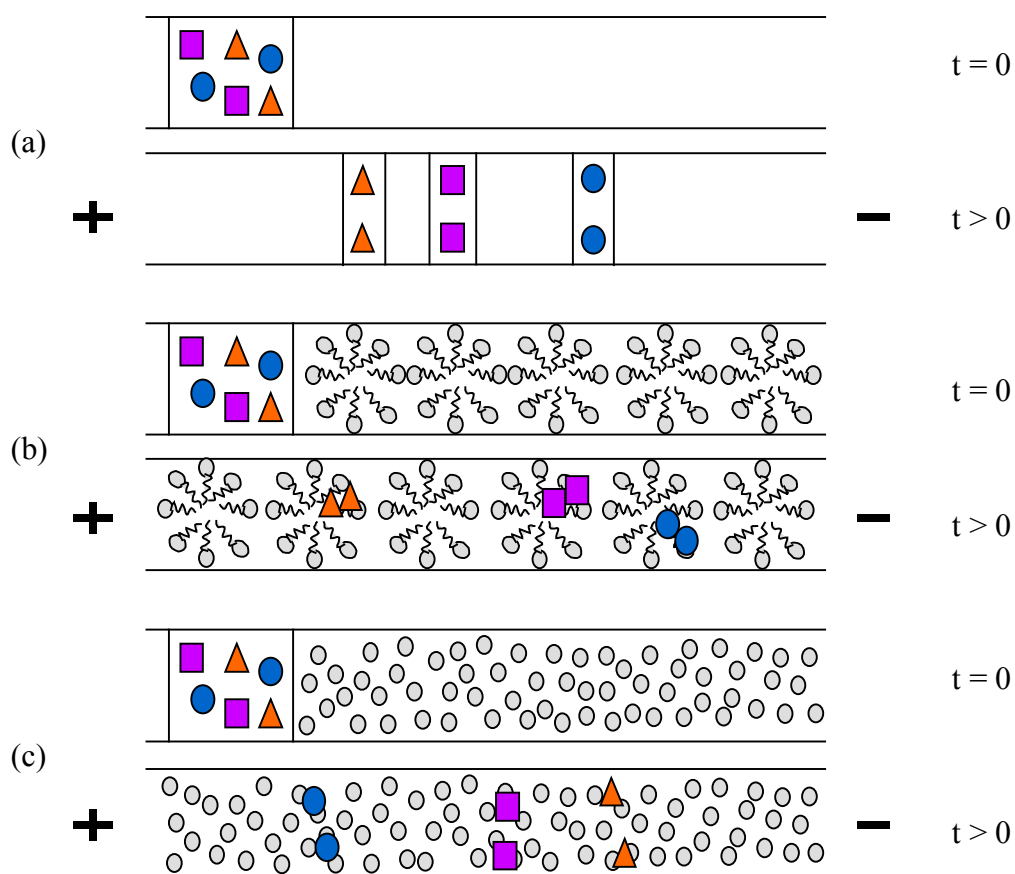
Figure 1.1 Separation mechanism in (a) CZE, (b) MEKC and (c) CEC. Adapted from Andrea and Brown [1997].

1.3 Introduction to Capillary Electrochromatography and Monolithic Columns

CEC is a separation technique combining the two modern liquid-phase separation techniques, namely HPLC and CE. Therefore, the separation principle is based on a dual mechanism whereby neutral analytes are separated according to different partitioning of the analytes between mobile phase and stationary phase while charged analytes additionally a separation mechanism based on the difference in their electrophoretic mobilities. Using the same stationary phase in a capillary column, CEC provides higher efficiency due to flat flow profile in CEC [Dittmann, and Rozing, 1997], while parabolic flow profile in HPLC. The columns used in CEC can be categorized into three types including the open-tubular columns, the packed columns and monolithic columns. There are limitations of the first two column types, such as tedious packing procedure for packed column, bubble formation due to the present of frits in packed column and low phase ratio for open-tubular columns [Dong *et al.*, 2009].

The monolithic columns are increasingly interested in recent years due in major part to the ease of the *in situ* polymerization in a capillary to form a continuous porous structure. Therefore, the monolithic columns can effectively overcome the above mentioned problems of packed columns. Furthermore, the much higher phase ratio of monolithic column than that of the open-tubular column [Dong *et al.*, 2009].

Monolithic columns can be classified into two main categories, i.e. silica-based monoliths and organic polymer-based monoliths. The former is prepared using the sol-gel technology creating a continuous sol-gel network throughout the column. The latter is usually prepared via vinyl polymerization in single step within a capillary column by the polymerization of an organic functional monomer in the presence of a crosslinker, initiator and porogens [Legido-Quigley *et al.*, 2003; Klodzinska *et al.*, 2006]. A wide variety of monomers can be used such as, acrylamide, acrylate, methacrylate and styrene [Stulik *et al.*, 2006; Eeltink *et al.*, 2006]. This provides monolithic stationary phases with difference in surface chemistries. The main benefit of using organic polymer-based monoliths is stable even under extreme pH

conditions, which could not tolerated by silica-based monoliths [Legido-Quigley *et al.*, 2003].

In this dissertation, we will focus on neutral organic polymer-based monoliths which are void of any fixed charges on the monolithic stationary phases. The neutral monolith without any charged monomers will prevent the electrostatic interaction between charged analytes and stationary phases that allows the separation of a wide range of neutral and charged analytes. The successful applications of CEC with neutral monolith to the separation of charged analytes especially for the proteins and peptides separation have been accomplished [Okanda, and El Rassi, 2005; Karenga, and El Rassi, 2008, 2010a, 2010b, 2011c].

1.4 Previous Work on Separation Selectivity in MEKC and RP-CEC of Proteins and Peptides Separation

Typically, the separation of two analytes in chromatography and electrokinetic chromatography such as MEKC can be expressed by separation selectivity (α) and resolution (R_s). In MEKC, R_s related to α, retention factor (k) and efficiency (N), therefore, the higher the separation selectivity, the greater the resolution of two analytes, resulting in the better separation. The separation mechanism of neutral analytes in MEKC depends only on the difference in micellar partitioning of the analytes. The MEKC separation selectivity (α_{MEKC}) for neutral analytes or retention selectivity (α_k) is defined as the ratio of k, i.e. $\alpha = k_2/k_1$ where $k_2 \geq k_1 > 0$. The higher the difference in k or higher separation selectivity provides the better separation. In case of charged analytes with a difference in electrophoretic mobility (μ_0) of analytes at CZE conditions, the MEKC separation is based on the differences in both k and μ_0. Therefore, α_{MEKC} for two charged analytes is defined as the ratio of effective electrophoretic mobility of two fully charged analytes, i.e. $\alpha_{MEKC} = \mu_{MEKC,2}/\mu_{MEKC,1}$ with $k_2 \geq k_1 > 0$. Factors affecting separation selectivity in MEKC include micellar buffer components, such as types and concentrations of surfactant,

organic s olvent, and p H, and p arameters o f CE i nstrument, s uch as t emperature [Riekkola *et al.*, 1997].

In pr evious w ork, the a ddition of s urfactant t o t he M EKC buf fer may r esult in improved s eparation f or amino aci ds [Iadarola *et a l.*, 2008], inorganic a nions [Riekkola *et al.*, 1997], dianisine [Mallampati *et al.*, 2005], anacardic acids [Česla *et al.*, 2006] and statins [Damić *et al.*, 2010], with respect to CZE separation. But the lower degree of separation in MEKC than that in CZE was reported for preservatives [Huang *et al.*, 2003]. These dual effects are similar to those seen in chiral separation using du al c yclodextrins a s reported i n our pr evious w ork [Nhujak *et a l.*, 2005]. However, s eparation s electivity and e lectrophoretic m obility or der i n MEKC f or charged analytes have not been explained.

CEC e mploying or ganic pol ymer-based m onolithic s tationary ph ases i s one of t he modes in CE that used as an effective separation method for charged species such as proteins and peptides. Customarily, the monolithic stationary phases with the fixed surface charges have been intentionally introduced to support the electroosmotic flow (EOF) [Bedair, and El Rassi, 2002, 2003; Augustin *et al.*, 2008; Feng *et al.*, 2009]. This l eads to the n uisance el ectrostatic i nteraction between charged an alytes and the stationary ph ases, w hich c aused e ither ba nd br oadening or i rreversible binding of charged an alytes. To ov ercome above pr oblems, t he ne utral nonpol ar m onoliths f or reversed-phase CEC (RP-CEC) have been developed for charged analytes separation [Okanda, and El Rassi, 2005; Karenga, and El Rassi, 2008, 2010a, 2010b, 2010c]. In this c ase, the E OF generated from the adsorption of mobile phase i ons to the neutral monolithic s urface. The m agnitude of t he E OF c an be c onveniently adjusted b y changing the p H a nd a cetonitrile c ontent of t he m obile pha se. In a ddition, t he separation s electivity, retention and magnitude o f the E OF ha ve be en m odulated b y mixed ligand m onolithic c olumns [Karenga, and E l R assi, 2011a] as w ell as segmented m onolithic c olumns c onsisting of o ctadecyl a nd na phthyl monolithic segments [Karenga, and El Rassi, 2011b].

In previous work, the neutral monoliths for RP-CEC have been developed in the aim of separating biomolecules, i.e. proteins and peptides, but these neutral monoliths were not effective in CEC of proteins and peptides [Dong *et al.*, 2005; Li *et al.*, 2004; Zhang *et al.*, 2003]. The success of preparing a series of neutral nonpolar monoliths with surface bond C17 [Okanda, and El Rassi, 2005], C18 [Karenga, and El Rassi, 2008] and naphthyl ligands [Karenga, and El Rassi, 2010c] for RP-CEC of proteins and peptides was reported. Up-to-date, the developing neutral nonpolar monoliths with varying *n*-alkyl chain lengths (i.e. C8, C12 and C16) for RP-CEC of charged analytes such as proteins and peptides have not been reported previously.

1.5 Aim and Scope

In this thesis, separation selectivity in MEKC and CEC was investigated for separation of particular analytes. As previous mentioned in Section 1.4, the better degree of separation in MEKC than that in CZE was obtained for some charged analytes, while the lower separation for other charged analytes was reported, as well as the reversed order of electrophoretic mobility for charged analytes in MEKC was obtained with respect to CZE separation. These dual effects are similar to those seen in chiral separation using dual cyclodextrins as reported in our previous work [Nhujak *et al.*, 2005]. The addition of surfactant to the MEKC buffer may result in improved or reduced separation for charged analytes. This behavior implies that an increase in the surfactant concentration in the MEKC buffer can affect the separation selectivity for the charged analytes separation. In preliminary study, it is interesting to establish theoretical models for separation selectivity in MEKC (α_{MEKC}) to explain a change in separation and electrophoretic mobility order of fully charged analytes in MEKC based on mobility selectivity in CZE (α_{CZE}), retention selectivity in MEKC (α_k), selectivity ratio ($\rho = \alpha_k/\alpha_{CZE}$) and the order of $|\mu|$ in CZE and k in MEKC. Therefore, the aims of this work are to develop theoretical models for α_{MEKC} of charged analytes and to compare the observed and the predicted α_{MEKC} over a wide range of SDS concentration ([SDS]) and k values. The experiment will be carried out using test analytes as four alkylparabens and MEKC buffer containing SDS surfactant

in a 10 mM disodium tetraborate buffer at pH 10.2 to afford almost fully negatively charged parabens. It is expected that this work will be very useful for explanation of a change, an increase or a decrease, of α_{MEKC} and electrophoretic mobility order of fully charged analytes in MEKC when SDS surfactant is added into the MEKC buffer. In recent year, the CEC employing organic polymer-based monolithic stationary phases is increasing used for separation of charged species i.e. proteins and peptides due to the ease of *in situ* polymerization in the capillaries. However, the potentials of CEC in the separation of proteins and peptides are still dormant due to the lack of suitable stationary phases. Since a few work have been reported the neutral nonpolar monoliths for RP-CEC of charged species including proteins and peptides in the absence of electrostatic interactions with the fixed surface charges. Therefore, further objective is to develop two differences neutral nonpolar monolithic column series which designated as A and B column series. Each series consisting of three columns at varying *n*-alkyl chain length such as C8, C12 and C16 which were prepared by the copolymerization of the functional monomers C8-methacrylate, C12-acrylate or C16-methacrylate with the crosslinking monomer pentaerythritol triacrylate and a ternary porogenic solvent made of cyclohexanol, ethylene glycol and water to yield monoliths with surface bound C8, C12 and C16 chains. In the A columns series, the composition of functional monomers and crosslinker was adjusted to yield comparable chromatographic retention while in the B columns series, the composition of functional monomers and crosslinker was kept constant yielding variable chromatographic retention.

In order to characterize the two difference series monolithic columns, the two columns series were demonstrated in the separation of neutral analytes such as alkylbenzenes, alkyl phenyl ketones, nitroalkanes, anilines and phenols as well as charged species such as proteins and peptide mapping. It is expected that some of these developed monolithic columns series will be suitable for proteins or peptides separation. In addition, the effect of different *n*-alkyl chain length monoliths with surface bound C8, C12 and C16 chains on the separation of proteins and peptide mapping will be clarified.

CHAPTER II

THREORY OF CE MEKC AND CEC

2.1 CE Instrumentation
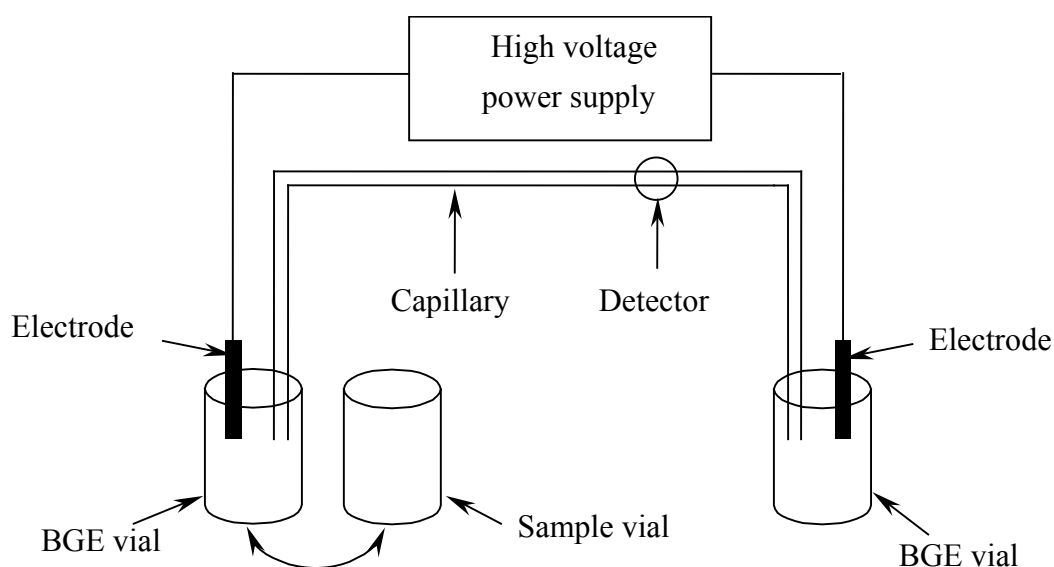
Figure 2.1 Schematic diagram of a basic CE instrument. Adapted from Weinberger [1993].

The schematic diagram of a typical CE instrument is shown in Figure 2.1. A CE system includes a capillary, high voltage power supply, electrodes, buffer vials and detector. The separation column is made of a narrow bore bare fused silica capillary for CZE and MEKC, and a narrow bore fused silica capillary containing the stationary phase in the case of CEC, ranging in diameter from 10 to 200 μm and length from 20 to 100 cm. The high voltage power supply is applied to drive the separation, allowing voltages up between -30 and + 30 kV. Two electrodes used commonly made of platinum wire. A UV-Vis detector with wavelength selection from 190 to 700 nm is widely used detector. A cooling system is required for controlling temperature of the capillary and reducing Joule heating.

Two di fferent m ethods a re ba sically us ed t o i ntroduce t he s ample i nto t he c apillary either hydrodynamic injection or electrokinetic injection. *The hydrodynamic injection is based on pr essure differences between t he i nlet an d outlet en ds o f t he cap illary.* This di fferent pr essure c an be a chieved by va rious methods s uch a s gravimetric, overpressure, a nd va cuum. The length of the s ample zone i njected (l_{inj}) into t he capillary by t he hydrodynamic method i s given by t he following e quation [Khaledi, 1998]

$$l_{inj} = \frac{\Delta P r^2}{8\eta L} t_{inj} \qquad (2.1)$$

where ΔP is the pressure difference between the inlet and outlet ends of capillary, r is the radius diameter of capillary, t_{inj} is the injection time, η is the liquid viscosity, and L is the capillary length. The volume (V_{inj}) and the amount (Q_{inj}) of analyte injected can be calculated using the following equations

$$V_{inj} = \frac{\Delta P \pi r^4}{8\eta L} t_{inj} \qquad (2.2)$$

and

$$Q_{inj} = \frac{\Delta P \pi r^4}{8\eta L} t_{inj} C \qquad (2.3)$$

where C is t he an alyte c oncentration. The p ressure i njection is w idely u sed i n C E. Since the injection is based on t he pressure di fference, it i s uni versally applied to all kinds o f s ample m atrices w ithout a ny bi as on t he s ample c ompounds. Therefore, pressure i njection h as b etter r eproducibility a nd gr eater control ov er t he a mount of sample injected into the capillary. *In electrokinetic injection*, the sample is introduced into the capillary by applying high voltage over a short period of time. Analyte ions will migrate into the capillary due to the combination of electrophoretic migration of the ions and electroosmotic flow of the sample solution. The length of sample zone introduced i nto t he c apillary du ring e lectrokinetic i njection i s g iven b y the e quation

$$l_{inj} = (v_{eo} + v_{ep})t_{inj} \qquad (2.4)$$

where v_{eo} is the electroosmotic velocity of the bulk solution and v_{ep} is the electrophoretic velocity. Since each analyte has a different mobility and electrokinetic injection is biased, therefore, this method gives the concentration of the injected sample is different from that of the original sample. However, the electrokinetic injection is preferable to introduce the analytes into the separation monolith with very low porosity to avoid the extremely high backpressure.

2.2 Electrophoretic Mobility [Grossman, and Colburn, 1992; Camilleri, 1993]

The two primary factors that affect electrophoretic migration in CE include the applied electric force (F_E) and the frictional force (F_F). When a voltage V is applied across a capillary of length L containing the BGE, each charged analytes will migrate toward the electrode in the direction opposite polarity to its direction of the electric force F_E

$$F_E = zeE \qquad (2.5)$$

where z is the charge of an ion, e is the fundamental electronic charge, and E is the electric field strength $(E = V/L$, where V is the applied voltage across L is the total length of capillary).

According to charged analytes migrate because of the applied electric force. This migration is resisted by the frictional force F_F

$$F_F = 6\pi r_h \eta v_{ep} \qquad (2.6)$$

where η is the viscosity of the medium, r_h is the hydrodynamic radius of the ion, and v_{ep} is the electrophoretic velocity of the ion. Then, the acceleration of the ion will proceed until F_E is balanced by F_F, giving the equation:

$$zeE = 6\pi r_h \eta v_{ep} \qquad (2.7)$$

The electrophoretic mobility, μ (m^2 V^{-1} s^{-1}) is defined as the electrophoretic velocity of anion migrating in BGE under the influence of an applied electric field and relates to parameters as the equation

$$\mu = \frac{v_{ep}}{E} = \frac{ze}{6\pi\eta r_h}$$

(2.8)

With respect to Equation 2.8, electrophoretic mobility depends on the charge-to-size ratio of an ion, z/r_h. Furthermore, it also depends on charge density of the analytes, ionic strength, viscosity of electrolyte, and temperature.

2.3 Electroosmosis [Grossman, and Colburn, 1992; Camilleri, 1993]

In addition to the electrophoretic mobility of analytes, the analytes will migrate along the capillary toward the detector by EOF. The EOF, as shown in Figure 2.2, is the movement of a medium toward the electrode when the voltage is applied. In the presence of the BGE, especially, a buffer at pH > 2, silanol groups at the surface of the bare fused silica capillary ionize to negatively charged (-Si-O$^-$) as the Equation 2.9 and 2.10. In cases of packed or monolithic columns, the charged may arise from charged moieties that might be intentionally incorporated to support the EOF. Furthermore, the adsorption of the ions from the mobile phase creates an adsorbed layer of ions on the solid surface.

$$\text{-SiOH } (s) + H_2O \ (l) \ \rightleftharpoons \ \text{-SiO}^- \ (s) + H_3O^+ \ (aq)$$

(2.9)

or

$$\text{-SiOH } (s) + OH^- \ (aq) \ \rightleftharpoons \ \text{-SiO}^- \ (s) + H_2O \ (l)$$

(2.10)
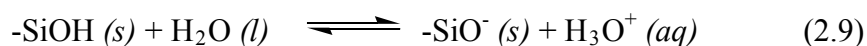
Under these conditions, and when the surface is in contact with a buffer, some BGE cations are attracted at the negative surface of the capillary to form an electrical double layer, as shown in Figure 2.2. One layer is tightly bound by electrostatic force, called the Stern layer, while other BGE cations are more loosely bound, called the diffusion layer. Moreover, the rest of the excess BGE cations are in the bulk solution. When the voltage is applied, the excess BGE cations both in the diffusion

layer and bulk solution migrate towards cathode and carry water or solvent molecules to the same direction. This phenomenon is called *electroosmosis*, and the migration of water or solvent molecules is called *electroosmotic flow* (EOF).
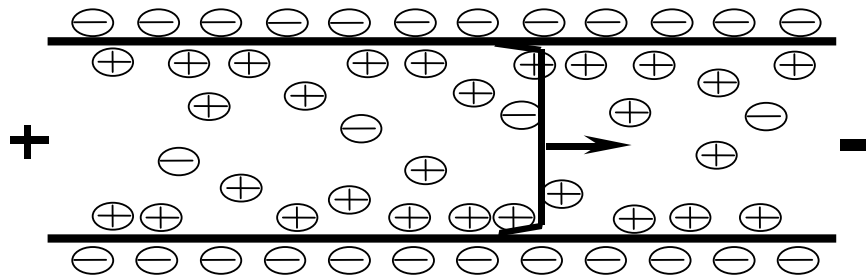
Figure 2.2 Electroosmotic flow (EOF). Adapted from Andrea *et al.* [1997].

The direction of EOF is influenced by sign of the zeta potential (ζ), the electric potential at the shear plane of the double layer. For a negatively charged solid surface, the zeta potential is negative and consequently, the EOF is cathodal and *vice versa*. The zeta potential is directly related to the velocity of electroosmotic flow, v_{eo}, as the equation

$$v_{eo} = -\frac{\varepsilon\zeta}{4\pi\eta}E \qquad\qquad (2.11)$$

where ε is the permittivity, and η is the viscosity of the liquid in the double layer. These values may be different from those in the bulk solution [Kenndler, 1998]. The electroosmotic mobility, μ_{eo}, can be defined as the velocity of electroosmotic flow versus the applied electric field as the equation

$$\mu_{eo} = \frac{v_{eo}}{E} = -\frac{\varepsilon\zeta}{4\pi\eta} \qquad\qquad (2.12)$$

In case of a bare fused silica capillary, the value of ζ is negative, and therefore, μ_{eo} has a positive sign. From the internal capillary surface, v_{eo} increases with increasing distance, and is constant at the distance of approximately 15 nm from the wall.

Typically, t he capillary used i n C E ha s 20 t o 1 00 μm i. d. (20000 t o 1 00000 nm). Thus, it can be said that v_{eo} is constant throughout the capillary radius [Grossman, and Colburn, 1992].

Since EOF is generated at the capillary wall, and it is uniformly distributed along the capillary, there is no pressure drop within the capillary. This results in a flat profile of the bulk flow which does not directly contribute to the zone broadening. The flat flow profile in CE contrasts to the parabolic profile generated by laminar flow driven by a pressure gradient in HPLC (Figure 2.3), resulting in high efficiency and resolution in CE than HPLC.
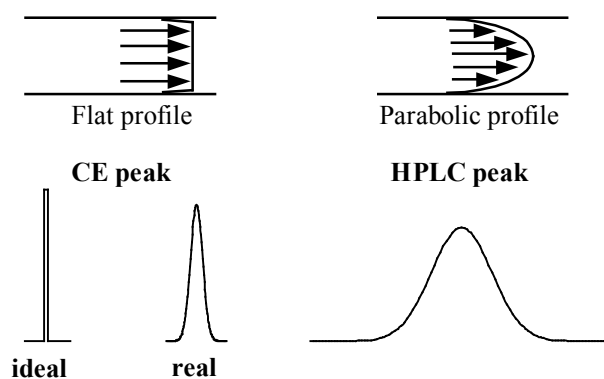
Figure 2.3 Flow profiles in CE and HPLC. Adapted from Chankvetadze [1997].

In t he p resence o f t he EOF, t he n et v elocity, v_{net}, of t he a nalyte i s t he s um of t he electrophoretic v elocity of t he analyte an d the e lectroosmotic ve locity as E quation 2.13 and Figure 2.4

$$v_{net} = v_{ep} + v_{eo} \qquad (2.13)$$

It s hould a lso be not ed that a t hi gh E OF, bot h a nions a nd c ations m igrate t o the detection window. For cations, $v_{ep,+}$ and v_{eo} are in the same direction to the cathode at the de tection window. The hi gher t he i on charges a nd t he s maller the i on s ize, t he faster the migration toward the cathode. For anions, $v_{ep,-}$ has the direction toward the anode. However, t he anions can migrate to t he cathode, b ecause $v_{eo} > v_{ep,-}$. The

higher th e io n c harges a nd th e s maller th e io n s ize, th e s maller th e n et velocity. Neutral mo lecules migrate toward t he cathode onl y due t o EOF, a nd cannot be separated.
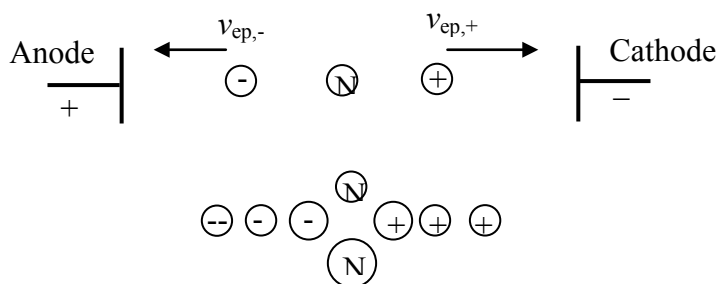
Figure 2.4 Migration behavior of the analytes. Adapted from Li [1992].

The net electrophoretic mobility ($\mu_{net} = \mu + \mu_{eo}$), μ_{eo} and μ can be calculated from an electropherogram using the following equations

$$\mu_{net} = \frac{v_{net}}{E} = \frac{lL}{Vt_m} \tag{2.14}$$

$$\mu_{eo} = \frac{v_{eo}}{E} = \frac{lL}{Vt_{eo}} \tag{2.15}$$

$$\mu = \mu_{net} - \mu_{eo} = \frac{lL}{V}\left(\frac{1}{t_m} - \frac{1}{t_{eo}}\right) \tag{2.16}$$

where t_m and t_{eo} are th e mig ration time s o f the a nalyte a nd th e E OF ma rker, respectively, l is the length of the capillary to detector, L is the total length of capillary and V is the applied voltage.

2.4 Retention and Separation Selectivity in MEKC

Overview of MEKC i s given in Section 1.2. In this s ection, more theoretical details of M EKC ar e d iscussed. A r etention f actor o r cap acity factor (k) i s one of t he characteristics t hat i ndicates r etention b ehavior of an alytes i n ch romatography an d

electrokinetic ch romatography s uch as M EKC. The r etention f actor in M EKC is defined as the ratio of total moles of analyte in the micelle phase (n_{mc}) versus those in the aqueous phase (n_{aq}) [Miola et $al.$, 1998] as the following equation

$$k = \frac{n_{mc}}{n_{aq}} = K\phi \qquad (2.17)$$

where K is t he di stribution c onstant be tween t he t wo ph ases, t he r atio of t he concentration of the solute in the micelle phase to that in the aqueous phase, and ϕ is the pha se r atio, t he r atio of t he vol ume of t he a queous pha se t o t hat of t he micelle phase. The higher the retention factor, the stronger the retention or the partitioning of analytes in the micelle phase.

In M EKC, t he obs erved e lectrophoretic m obility of analyte A (μ) i s a s um of the electrophoretic mo bility of a nalyte A (μ_A) a nd the e lectrophoretic mobility of t he micelle phase (μ_{mc}) [Camilleri, 1993] as the equation

$$\mu = x_{aq}\mu_A + x_{mc}\mu_{mc} \qquad (2.18)$$

where x_{aq} and x_{mc} are t he mole f ractions of an alyte in aq ueous and m icelle phase, respectively.

In the case of charged analyte A, μ is given by

$$\mu = x_{aq}\mu_A + x_{mc}\mu_{mc} = \frac{n_{aq}}{n_{aq} + n_{mc}} + \frac{n_{mc}}{n_{aq} + n_{mc}}\mu_{mc} \qquad (2.19)$$

From Equations 2.17 to 2.19, μ can be expressed by

$$\mu = \left(\frac{1}{1+k}\right)\mu_A + \left(\frac{k}{1+k}\right)\mu_{mc} \qquad (2.20)$$

In the presence of high EOF, the total mobility ($\mu_{net} = \mu_+ \mu_{eo}$) in Equation 2.20 is given by

$$\mu_{net} = \left(\frac{1}{1+k}\right)\mu_A + \left(\frac{k}{1+k}\right)\mu_{mc} + \mu_{eo} \qquad (2.21)$$

Therefore, the retention factor of the charged analyte in MEKC with high EOF can be calculated from an electropherogram using the equation [Téllez, Fuguet, and Rosés 2007a, 2007b; Camilleri, 1993]

$$k = \frac{\mu - \mu_A}{\mu_{mc} - \mu} \qquad (2.22)$$

where μ and μ_A are electrophoretic mobility of analyte in MEKC and at zero concentration of SDS or CZE, respectively, and μ_{mc} is the electrophoretic mobility of micelle marker. It should be mentioned that Equation 2.22 is written in terms of absolute rather than net electrophoretic mobility because μ_{eo} is a constant for all species.

It is important to note that MEKC has three different modes based on the direction of v_{eo}, the observed velocity of micellar phase (v_{sc}) and the observed velocity of the analyte (v_s). In the normal elution mode, v_{eo} and v_{sc} have identical direction and $|v_{eo}| > |v_{sc}|$. In the case that v_{eo} and v_{sc} have opposite direction and v_{eo} being opposite to v_s, this mode is called reversed elution mode. In the last mode, restricted elution mode in which v_s being opposite to v_{sc} and v_{eo} and v_{sc} have opposite direction [Pyell, 2006].

As previously mentioned in Section 1.4, separation selectivity (α) is another characteristic used for describing the degree of separation of two analytes in chromatography and electrokinetic chromatography such as MEKC. The separation selectivity in MEKC (α_{MEKC}) for two fully charged analytes is defined as the ratio of the effective electrophoretic mobilities, with $k_2 \geq k_1 > 0$.

$$\alpha_{\text{MEKC}} = \mu_{\text{MEKC},2}/\mu_{\text{MEKC},1} \qquad\qquad (2.23)$$

where $\mu_{\text{MEKC},1}$ and $\mu_{\text{MEKC},2}$ are the effective electrophoretic mobilities of the analyte 1 and analyte 2, respectively.

2.5 Retention in CEC [Dittmann *et al.*, 2000]

Although the concept of retention in CEC is similar to HPLC, it should be noted that the retention of solute in CEC depends on both partitioning and electromigration, while the retention in HPLC due only to the difference in stationary phase partitioning that can be described by following equation

$$t_{\text{R,LC}} = t_{\text{o}}(1 + k_{\text{LC}}) \qquad\qquad (2.24)$$

where $t_{\text{R,LC}}$ and t_{o} are the migration times of the retained analyte and unretained analyte in HPLC, respectively, and k_{LC} is the retention factor in HPLC. In CEC, the retention of analyte is based on partitioning and electrophoresis, therefore, Equation 2.20 needs to be modified to:

$$t_{\text{R,CEC}} = t_{\text{o}}(1 + k_{\text{LC}})\left(\frac{t_{\text{ep}}}{t_{\text{ep}} + t_{\text{o}}}\right) \qquad\qquad (2.25)$$

where $t_{\text{R,CEC}}$ and t_{o} are the migration times of the retained analyte and unretained or uncharged analyte in CEC separation, respectively, and k_{LC} is the retention factor associated with stationary phase and mobile phase partitioning, and t_{ep} is the migration time of analyte due to electrophoretic mobility. The first part of Equation 2.25 describes the chromatographic retention. The second part describes the modulation of analyte due to electromigration. In the case of neutral analytes, since they bear no charge, therefore, their retention depends only on the difference in partitioning between the stationary phase and mobile phase. The value of t_{ep} in Equation 2.25 is equal to infinity and Equation 2.25 is reduced to Equation 2.24. Therefore, the retention factor for neutral analyte in CEC is given by

$$k_{CEC} = \frac{t_{R,CEC} - t_o}{t_o}$$ (2.26)

The k values in CEC can be obtained in the range between -1 and ∞, where $k = 0$ refers to the analyte that not interacts with the stationary phase and migrates with the EOF, $k = -1$ refers to the analyte that retains in the stationary phase and migrates before the EOF, and $k = \infty$ refers to the analyte that more interacts with the stationary phase.

2.6 Resolution in CE

In CE, a resolution (R_s) of two analytes is defined as the ratio of the difference in their migration times to their peak width at base as the equation

$$R_s = \frac{t_{m2} - t_{m1}}{0.5(w_{b1} + w_{b2})}$$ (2.27)

It follows from Equations 2.27 and 2.16 that, R_s can be related to the mobility and the average number of theoretical plates, $\overline{N}$, as the equation

$$R_s = \frac{1}{4}\left(\frac{\Delta\mu}{\overline{\mu} + \mu_{eo}}\right)\sqrt{\overline{N}}$$ (2.28)

where $\Delta\mu$ is the difference in the mobility, $\mu_2 - \mu_1$, for two analytes, and $\overline{\mu}$ the average electrophoretic mobility of the analytes. For two analytes with same direction of μ Equation 2.28 may be rearranged to relate to the resolution R_s to the efficiency term, the selectivity term, and the mobility term as expressed in Equation 2.29

$$R_s = \left(\frac{\sqrt{\overline{N}}}{4}\right)\left(\frac{\alpha_m - 1}{\alpha_m}\right)\left|\frac{\mu_2}{\overline{\mu} + \mu_{eo}}\right|$$ (2.29)

where α_m is the separation selectivity or mobility selectivity, which is defined as the ratio of effective electrophoretic mobilities for two analytes such as μ_2/μ_1 for $|\mu_2| > |\mu_1|$. In MEKC with normal elution mode, the resolution equation for neutral analytes can be expressed to relate to the retention term in Equation 2.30

$$R_s = \frac{\sqrt{N}}{4}\left(\frac{\alpha_k - 1}{\alpha_k}\right)\left(\frac{k_2}{1 + k_2}\right)\left(\frac{1 - \dfrac{t_{eo}}{t_{mc}}}{1 + \left(\dfrac{t_{eo}}{t_{mc}}\right)k_1}\right) \tag{2.30}$$

where α_k is the retention selectivity which is defined as the ratio of the retention factor, e.g. k_2/k_1 and $k_2 \geq k_1 > 0$, t_{eo} and t_{mc} are the migration times of an EOF marker or an unretained compound and a micelle marker, respectively. With the normal elution mode of MEKC separation of fully charged analytes due only to the difference in micellar partitioning and not in their electrophoretic mobilities, the resolution equation is given by Equation 2.31:

$$R_s = \left(\frac{\sqrt{N}}{4}\right)\left(\frac{\alpha_k - 1}{\alpha_k}\right)\left(\frac{k_2}{1 + \bar{\bar{k}}}\right)\left(\frac{1 + t_{eo}/t_{ep} - t_{eo}/t_{mc}}{1 + t_{eo}/t_{ep} + (t_{eo}/t_{mc})\bar{\bar{k}}}\right) \tag{2.31}$$

where t_{ep} is the migration time corresponding to the electrophoretic mobility of the charged analyte, and $t_{ep} = t_{ep2} = t_{ep1}$ for this case.

Similar to the resolution in MEKC in Equation 2.30, the resolution in CEC for neutral analyte can be expressed to relate to the efficiency term, selectivity term and retention term in Equation 2.32

$$R_s = \frac{\sqrt{N}}{4}\left(\frac{\alpha - 1}{\alpha}\right)\left(\frac{k_2}{1 + k_2}\right) \tag{2.32}$$

where k_2 is the retention factor of more retained analyte, α is the selectivity which is defined as the ratio of the retention factor, e.g. k_2/k_1 and $k_2 \geq k_1 > 0$

2.7 Preparation and Factors Affecting Morphology and Porosity of Monoliths

Organic polymer-based monoliths are prepared in a single step within the confines of a capillary column by the polymerization of an organic functional monomer in the presence of a crosslinker, initiator and porogens [Merhar *et al.*, 2003]. The functional monomer defines the monolith polarity while the porogens, monomer-to-crosslinker ratio and polymerization temperature control the monoliths morphology [Urban, and Jandera, 2008]. Monoliths are associated with two main types of pores: (i) the flow-through pores and (ii) the mesopores filled with "stagnant" mobile phase in which the solute molecules migrate to access the active adsorption sites. To get large surface area and retention, a significant number of smaller pores should be incorporated into the polymer. Micropores with sizes smaller than 2 nm contribute most significantly to the overall surface area followed by mesopores ranging from 2 to 50 nm [Urban, and Jandera, 2008]. The larger flow-through pores (macropores) are essential to allow liquid to flow through at a reasonably low pressure and contribute very little to the overall surface area [Viklund *et al.*, 1996].

The polymerization can be initiated through the application of heat, UV radiation [Li, Tolley, and Lee 2009; Rohr *et al.*, 2003; Tan, Benetton, and Henion, 2003], gamma radiation [Sáfrány *et al.*, 2005; Beiler *et al.*, 2007] or redox reagents [Petra, Holdscaronvendová *et al.*, 2003; Cantó-Mirapeix *et al.*, 2008]. Once decomposed, the initiator initiates the polymerization and as the polymer chains grow, their solubility in the reaction mixture decreases and the polymer chains precipitate to form nuclei. Thermodynamically, the monomers are better solvents for the formed polymer than the porogens and the nuclei therefore become swollen with monomers. As a result of the monomer concentration in the nuclei being higher than in the surrounding solution, polymerization in the nuclei is kinetically preferred. Further polymerization leads to an increase in the size of the nuclei to microglobules, which then aggregate to form clusters. As the microglobules continue to grow and crosslink to each other the final morphological structure is formed. This process leads to two-phase system consisting of a white colored continuous solid monolith and inert liquid porogens filling the pores. Once the porogens are washed out, the volume occupied by the

porogens then corresponds to the volume of the macropores [Vlakh, and Tennikova, 2007]. While varying the monomer-crosslinker ratio or type of initiator can change the composition and rigidity of the monolith, the alteration of the porogen affects only the porous structure of the final polymer. The porogens can either be good or poor solvents for the polymer. The mechanism of pore formation using porogens has been described as follows. At the beginning of the polymerization, the solution is homogeneous until the growing and crosslinked polymer chains precipitates and falls out of the solution. If the porogen is a good solvent for the final polymer, phase separation is delayed and the resultant pores are smaller. Alternatively in the presence of a poor solvent, phase separation occurs early leading to large pores [Peters, Svec, and Fréchet, 1999]. While there is no standard way of choosing the right composition of porogens and the right porogen composition has to be based on trial and error, a reduction of monomer/crosslinker ratio represents a straight forward method to increase pore size and decrease pressure drop during operation (in HPLC), this approach however, decreases the homogeneity and rigidity of the macroporous polymer [Vlakh, and Tennikova, 2007].

2.8 Efficiency and Band Broadening in CE

The parameters of peak efficiency used in CE are characterized similarly to those in chromatography. Theoretically, an electrophoretic peak in CE are assumed to have a Gaussian peak with standard deviation, σ in the distance units and τ in time units, as shown in Figure 2.5. The width of the peak at base, w_b, may be obtained by drawing lines at tangents to the points of inflection, and measuring the separation between these two points. The w_b is given by

$$w_b = 4\sigma \quad \text{or} \quad w_b = 4\tau \tag{2.33}$$

and the peak width at half height, w_h, is given by

$$w_h = 2.354\sigma \quad \text{or} \quad w_h = 2.354\tau \tag{2.34}$$

Peak efficiency (N) is also related to σ and τ as the equation

$$N = \left(\frac{l}{\sigma}\right)^2 = \left(\frac{t}{\tau}\right)^2 \qquad (2.35)$$

It follow from Equations 2.33 to 2.35, N can be calculated from an electropherogram, according to the equation

$$N = 16\left(\frac{t_m}{w_b}\right)^2 = 5.54\left(\frac{t_m}{w_h}\right)^2 \qquad (2.36)$$
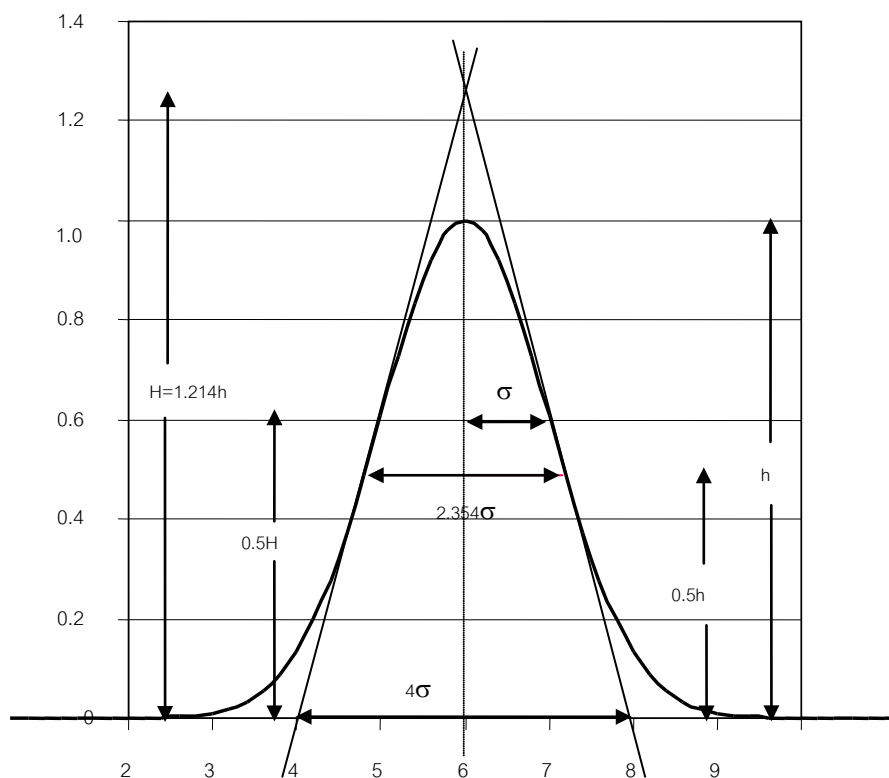
Figure 2.5 Gaussian peak.

In MEKC, peak broadening can be expressed by peak variance (σ^2) or theoretical plate height (H) as similarly explained in chromatography as the equation [Terabe *et al.*, 1989]

$$\sigma^2 = Hl \tag{2.37}$$

Analogous to chromatography, H in MEKC also relates to N and l as the equation [Khaledi, 1998]

$$H = \frac{l}{N} \tag{2.38}$$

According to Equation 2.38, the higher the efficiency, the smaller the plate height or peak broadening. In this work, peak broadening in MEKC will be discussed in terms of H. The total H can be described as the sum of plate height caused by five main contributions as the equation

$$H = H_l + H_{mc} + H_{aq} + H_t + H_{pd} \tag{2.39}$$

where H_l, H_{mc}, H_{aq}, H_t and H_{pd} are the plate height generated by longitudinal diffusion, sorption-desorption kinetics in the pseudo stationary phase solubilisation, intermicelle mass transfer in the aqueous phase, thermal dispersion and polydispersity of the pseudo stationary phase, respectively.

However, H_{mc} is negligible for analytes having strong partitioning into the pseudo stationary phase. H_l increases with increasing retention time and high diffusion coefficient of analytes. H_{aq} and H_{pd} decrease with increasing surfactant concentration. H_t increases with increasing the conductivity of BGE, capillary radius and applied voltage.

Similar to total H in MEKC, the total H in CEC can be expressed as

$$H = H_{inj} + H_{det} + H_{col} + H_{joule} \tag{2.40}$$

where H_{inj}, H_{det}, H_{col}, and H_{joule} are the plate height generated by injection, detection, column and thermal dispersion, respectively.

Joule heating causes non-uniform temperature gradients and local changes in viscosity that lead to band broadening. However, this effect can be minimized by using low conducting supporting electrolytes in the mobile phase, narrow bore capillaries for efficient heat dissipation, field strengths that are 1000 V/cm or less, and controlled column temperature. The contribution of band broadening in both pressure and electrodriven separations has been thoroughly studied and it has been reported that plate height contributions from H_{inj}, H_{det} and H_{joule} were all negligible compared to H_{det} [Wen, Asiaie, and Horváth, 1999]. Therefore, it can be assumed that the total plate height is determined by the passage of the sample through the column. In CEC, factors affecting H_{col} include; maldistribution of flow (H_f), longitudinal diffusion (H_l) and mass transfer resistance in the pore (H_p). After dropping the negligible terms and substituting these terms in Equation 2.40, total H can be expressed as

$$H = H_f + H_l + H_p \qquad (2.41)$$

On substituting the corresponding parameters that define plate height contributions into Equation 2.41, we obtain the van Deemter equation, which is usually represented in a simplified manner by summing up the constants (A, B and C) for a given set of conditions and relates each plate height contributor in terms of mobile phase velocity as:

$$H = A + \frac{B}{u} + Cu \qquad (2.42)$$

Figure 2.6 shows a typical van Deemter plot and the relative plate height contributions of each term in the van Deemter equation as a function of mobile phase velocity. As shown in Figure 2.6, the optimum flow velocity (u_{opt}) produces the minimum plate height (H_{min}). Longitudinal diffusion term, B/u, depends on the nature of the solute and an increase in the mobile phase flow velocity can minimize this term. The mass transfer resistance in the pores, Cu, increases with increasing mobile phase flow velocity. This diffusion mass transfer resistance is decreased in CEC due to the generated EOF within the flow through pores, which increases the kinetics of the mass transfer [Wen, Asiaie, and Horváth, 1999]. The highest gain in CEC separation

efficiency results from decreasing the maldistribution of flow (the A term) observed in pressure driven flow in packed columns, which is known as "Eddy diffusion" [Gidding, 1991]. The plug flow profile in CEC causes the "A" term to become negligible in determining the overall separation efficiency. Once the broadening effects in both the A and C terms of the van Deemter equation are reduced, efficiencies that are 5-10 times better than those obtained in pressure-driven mode under the same conditions are obtained.
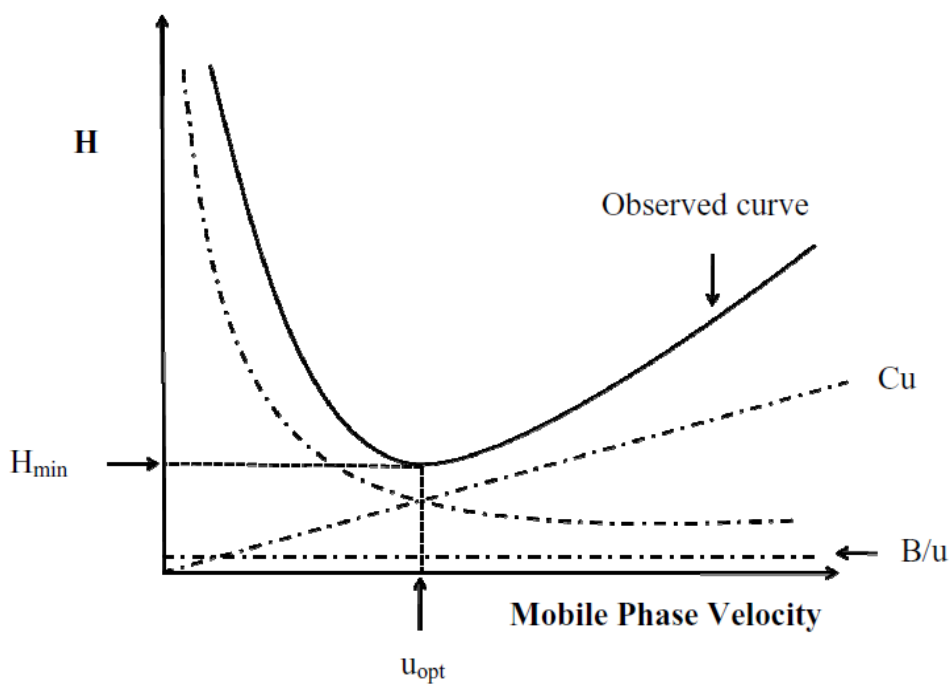
Figure 2.6 Illustration of the plate height (*H*) contribution to each van Deemter term and the resulting observed plot of *H* as a function of mobile phase linear velocity.

CHAPTER III

THEORETICAL MODELS OF SEPARATION SELECTIVITY FOR CHARGED COMPOUNDS IN MICELLAR ELECTROKINETIC CHROMATOGRAPHY

3.1 Introduction

In chromatography and electrokinetic chromatography such as MEKC, the degree of separation of two analytes can be described by separation selectivity and resolution. The higher the resolution, the better the separation. To obtain high resolution, the high difference in k or high separation selectivity is required. As described in Section 2.6, with the normal elution mode of MEKC separation for two neutral analytes, the separation depends only on a difference in their electrophoretic mobilities. The resolution of two analytes depends on the retention selectivity, α_k, which is defined as the ratio of k such as k_2/k_1. The higher the α_k, the better the resolution. In the case of MEKC separation of fully charged analytes due only to the difference in micellar partitioning and not in their electrophoretic mobilities, the resolution depends only on α_k as shown in Equations 2.30 and 2.31 in Section 2.6. The higher the difference in k or higher separation selectivity, the higher the resolution, resulting in the better separation.

It can be seen in Equations 2.30 and 2.31 that the separation selectivity may be now referred to the retention selectivity. In case of charged analytes with a difference in electrophoretic mobility (μ_0) of analytes at CZE conditions, the MEKC separation is based on the differences in both k and μ_0, and the separation selectivity for two charged analytes in MEKC, α_{MEKC}, is defined as the ratio of effective electrophoretic mobility of two fully charged analytes, i.e. $\alpha_{MEKC} = \mu_{MEKC,2}/\mu_{MEKC,1}$ with $k_2 \geq k_1 > 0$. Factors affecting separation selectivity in MEKC include micellar buffer components,

such as t ypes an d co ncentrations of s urfactant, or ganic s olvent, a nd pH , a nd parameters of CE instrument, such as temperature [Riekkola *et al.*, 1997].

Typically, sodium dode cyl s ulphate (SDS) is t he m ost w idely used as a n i onic surfactant i n M EKC be cause it i s i nexpensive and available in hi ghly pur ified form. Separation s electivity ca n b e al tered b y ad ding t he S DS s urfactant i nto t he M EKC buffer [Riekkola *et al.*, 1997; Mallampati *et al.*, 2005; Česla *et al.*, 2006; Iadarola *et al.*, 2008; Damić *et al.*, 2010].

In pr evious w ork, t he a ddition of s urfactant t o t he M EKC buf fer m ay r esult i n improved MEKC separation for amino acids [Iadarola *et al.*, 2008], inorganic anions [Riekkola *et al.*, 1997], dianisine [Mallampati *et al.*, 2005], anacardic acids [Česla *et al.*, 2006] and statins [Damić *et al.*, 2010], w ith r espect t o CZE s eparation. B ut the lower degree of separation in MEKC than that in CZE was reported for preservatives [Huang *et al.*, 2003]. These dual effects are similar to those seen in chiral separation using du al c yclodextrins a s reported in our pr evious w ork [Nhujak *et a l.*, 2005]. However, s eparation s electivity and e lectrophoretic m obility or der i n MEKC f or charged analytes have not been explained.

In o rder t o ex plain t he separation s electivity an d el ectrophoretic m obility o rder i n MEKC f or ch arged an alytes w ith d ifferences i n μ_0, th e a ims o f th is section are t o establish theoretical models of MEKC separation selectivity (α_{MEKC}) which is related to t he dimensionless va lues of mo bility s electivity (α_{CZE}) in C ZE and r etention selectivity (α_k) in M EKC, a nd t o c ompare t he observed and pr edicted separation selectivity in M EKC. The pr oposed α_{MEKC} models w ere c lassified ba sed on t he ranges of α_{CZE}, α_k, selectivity ratio ($\rho = \alpha_k/\alpha_{CZE}$) and the order of $|\mu|$ in CZE and *k* in MEKC. C E s eparations with nor mal e lution m ode were p erformed in t wo buf fer systems: (1) CZE with 10 mM disodium tetraborate buffer at pH 10.2, and (2) MEKC with 20 to 60 mM SDS surfactant in a 10 mM disodium tetraborate buffer at pH 10.2, and the test analytes used were alkylparabens.

isomethylparaben (IP)

ethylparaben (EP)

propylparaben (PP)
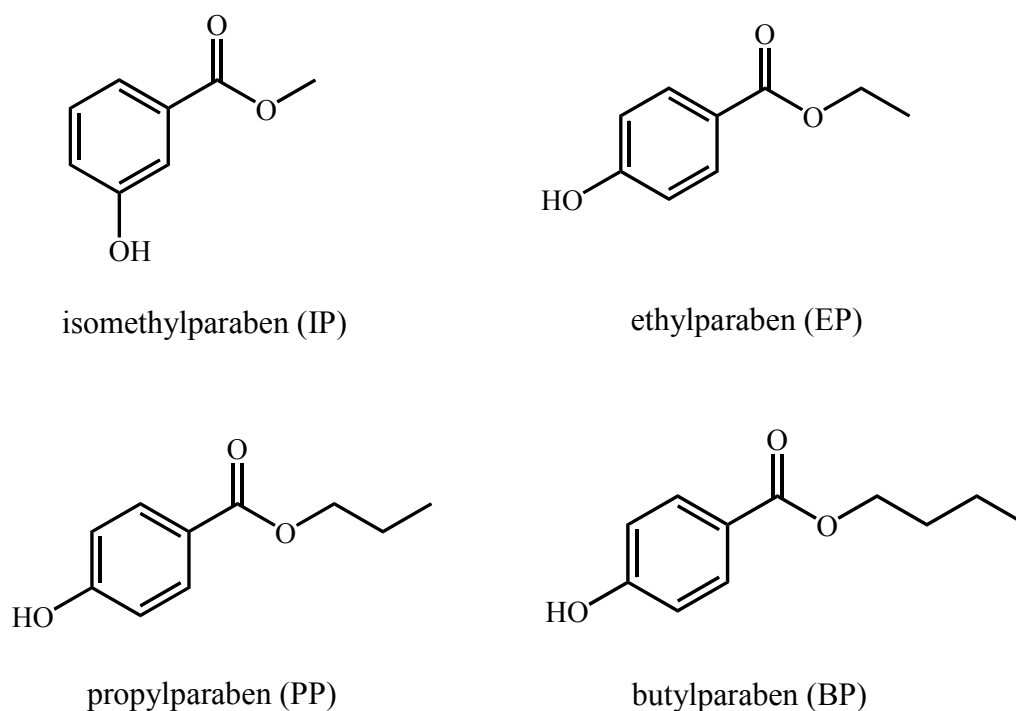
butylparaben (BP)

Figure 3.1 Chemical structures o f p arabens: is omethylparaben, e thylparaben, propylparaben and butylparaben.

3.2 Experimental

3.2.1 Chemicals

The following test analytes in a class of alkylparabens were purchased from Sigma-Aldrich (Steinheim, G ermany): is omethylparaben (methyl *m*-hydroxybenzoate; I P), ethylparaben (ethyl *p*-hydroxybenzoate; E P), pr opylparaben (propyl *p*-hydroxybenzoate; PP), and but ylparaben (butyl *p*-hydroxybenzoate; BP). Sodium hydroxide and disodium tetraborate decahydrate ($Na_2B_4O_7.10H_2O$) were supplied by Fluka (Buchs, S witzerland), S DS f rom S igma (St. L ouis, M O, U SA), all or ganic solvents obt ained f rom Merck (Dramstadt, G ermany), an d d odecylbenzene/micellar marker (M) from Sigma-Aldrich (Steinheim, Germany).

3.2.2 CE conditions

CE experiments were carried out with a Beckman Coulter MDQ-CE system equipped with a photo-DAD scanning from 190 to 300 nm and monitoring at 220 nm. The data handling system comprised an IBM PC and 32 Karat Software. The uncoated fused-silica c apillary 40.2 c m in le ngth (30 cm to d etector) × 50 μ m i.d. (Polymicro Technologies, AZ, USA) was used for CZE and MEKC separations, thermostated at 25 °C. V oltage w as s et a t 15 kV . A s ample solution w as i ntroduced b y 0.5 ps i pressure i njection f or 3 s. Prior to each d aily an alysis, t he cap illary was r insed sequentially for 15 m in with m ethanol, 0.1 M N aOH, w ater, a nd a r unning buffer. Between consecutive runs, the capillary was flushed with 0.1 M NaOH and then with a running bu ffer, each for 2 m in. After an alysis, each d ay, the capillary was r insed with water an d E tOH for 5 m in e ach, and t hen 0.1 M N aOH and water for 10 m in each. All experiment runs were performed in duplicate.

3.2.3 Preparation of buffer solutions

The e lectrophoretic mobilities were determined in two buffer systems: (1) CZE with 10 mM disodium tetraborate buffer, adjusted to pH 10.2 with 1.0 M NaOH, and (2) MEKC with 20 to 60 mM SDS in a 10 mM disodium tetraborate buffer at pH 10.2. All buffers were prepared using Milli-Q water, sonicated for 30 min, and then filtered through 0.45 μm PTFE filters prior to use.

3.2.4 Preparation of analytes

Each t est an alyte w as s eparately d issolved i n 5 m L o f a cetonitrile, an d t hen each analyte solution was diluted with Milli-Q water in a 10 mL volumetric flask to give 1000 ppm stock solutions. Stock solutions of DB and thiourea were also separately dissolved in ethanol, and then diluted to 20000 p pm with Milli-Q water. A working standard solution containing 20 to 60 ppm of each test analyte, 30 ppm thiourea and 150 ppm D B w ere pr epared b y di luting e ach of t he s tock s olutions w ith a 1.0 m M

borate buf fer.   All s olutions w ere f iltered t hrough 0.45   μm P TFE filters p rior to analysis.

3.2.5 Charged compounds separation in CZE

3.2.5.1 Determination of pK_a values of alkylparabens

Stock s olution of 100 m M disodium t etraborate was p repared b y w eighing an appropriate a mount of disodium te traborate and then di ssolved w ith Milli-Q wa ter, adjust to pH 10.2 with 1.0 M NaOH. Solution of 10 mM disodium tetraborate buffer was prepared by diluting appropriate amounts of 100 mM disodium tetraborate buffer with the Milli-Q water.

The borate buffers with vaious pHs from 7.8 to 10.2 were prepared by adjusting a 10 mM Na $_2$B$_4$O$_7$ buffer w ith a 1.0 M N aOH o r H$_3$BO$_3$ solution t o de sire pH . T he values of effective el ectrophoretic m obility, μ_{eff}, in C ZE c onditions of each pa raben were measured a nd calculated us ing E quation 2 .16.   The ap parent p K_a values of parabens w ere d etermined b y p lotting 1 /μ_{eff} versus 10 $^{-pH}$ ([H$_3$O$^+$]) a nd r esults ar e shown in Section 3.3.1.2.

3.2.5.2 Separation of alkylparabens in CZE at pH 10.2 of borate buffer

Simultaneous s eparation o f alkylparabens w as c arried o ut w ith a 10 m M disodium tetraborate buffer at pH 10.2 and other CE conditions as in Section 3.2.2. In the case of normal e lution mode, μ_{eff} of each p araben can b e cal culated f rom electropherograms u sing t he E quation 2.16 and t he r esults are s hown in S ection 3.3.1.3. Each v alue o f α_{CZE} was obtained from the ratio of μ_{eff} for t wo an alytes i.e. $\alpha_{CZE} = \mu_2/\mu_1$. Results are also shown in Section 3.3.1.3.

3.2.6 Charged compounds separation in MEKC

Equations and theoretical models w ere p roposed f or MEKC separation s electivity (α_{MEKC}) of two charged analytes using data of mobility selectivity in CZE, retention selectivity in MEKC, the order of $|\mu|$ in CZE and k in MEKC. Details are discussed in Section 3.3 .2. Experimental an d p redicted values o f α_{MEKC} for two ch arged analytes in MEKC were compared as shown in Section 3.3.2.3. The experiment was carried out using 10 mM $Na_2B_4O_7$ buffer at pH 10.2 and various concentrations of SDS. Results are shown in Figures 3.5.

3.3 Results and Discussion

3.3.1 Charged compounds separation in CZE

3.3.1.1 BGE conditions

All test analytes such as IP, BP, PP and EP are weak acid compounds (Figure 3.1) with pK_a values of 9.2 for IP [Piršelová, Baláž, and Schultz, 1996] and 8.4 for other parabens [Wilson, and Gisvold, 1998]. Therefore, a background electrolyte at basic pH was selected to allow separation of all parabens as negatively charged compounds. Typically, CZE separation of acid compounds is performed using a borate buffer at pH 8.2 to 10.2. In previous work, the separation of preservatives such as BP, PP and EP was carried out in the borate buffer at pH 9.0 [Huang *et al*., 2003]. In this work, borate bu ffer at pH 10 .2 w as chosen to a fford a lmost f ully ne gatively charged analytes, and the degrees of ionization of all parabens were determined and the details were discussed in Section 3.3.1.2.

3.3.1.2 Degrees of ionization and apparent pK_a values of alkylparabens

As previous mentioned in Section 3.2.5.1, the test analytes, parabens such as IP, BP, PP an d E P, ar e esters o f h ydroxybenzoic a cid w ith H O-C_6H_4COOR. T hese

compounds contain an –OH group that expresses a weak acid, and therefore they can be dissociated to carry a negative charge ($^-OC_6H_4COOR$), especially at $pH > pK_a$. The degree of ionization (α_{dis}) for each analyte depends on the pH of the BGE and the pK_a of the analyte in the BGE at the experimental ionic strength. The parabens in their fully charged form are separated in this experiment, in order to avoid interpretation of results of micelle partitioning for mixtures of neutral and ionic form of parabens. Therefore, the pK_a value of each paraben needs to be determined under these experimental conditions in order to choose particular pH of the buffer providing fully charged analytes.

In the case of a weak acid, HA, the protolysis of this neutral acid can be expressed by giving equation [Khaledi, 1998].

$$HA + H_2O = H_3O^+ + A^- \qquad (3.1)$$

The acid dissociation constant, K_a, at a given ionic strength is given by equation.

$$K_a = \frac{[H_3O^+][A^-]}{[HA]} \qquad (3.2)$$

The acid dissociation constant, K_a, may be determined by CE [Cai *et al.*, 1992]. When the weak acid analyte is partially ionized due to the equilibrium at a given pH, the effective electrophoretic mobility, μ_{eff}, depends on the degree of ionization, α_{dis}, and the electrophoretic mobility of fully charge, μ_0, as the equation.

$$\mu_{eff} = \alpha_{dis}\mu_0 \qquad (3.3)$$

For the case of a monovalent weak acid with a certain pK_a, the degree of ionization, α_{dis}, is connected to the pH of the BGE by

$$\alpha_{dis} = \frac{[A^-]}{[A^-]+[HA]} = \frac{1}{1+10^{pKa-pH}} \qquad (3.4)$$

From Equation 3.1 to 3.4, μ_{eff} of a monovalent weak acids depends on the pH of BGE by equation.

$$\mu_{eff} = \frac{\mu_0}{1+10^{pKa-pH}} \tag{3.5}$$

It is possible to obtain a linear Equation 3.6, by taking the inverse of Equation 3.5

$$\frac{1}{\mu_{eff}} = \frac{1}{K_a\mu_0}\left[H_3O^+\right]+\frac{1}{\mu_0} \tag{3.6}$$

Equation 3.6 is a linear relationship whereby a plot of $1/\mu_{eff}$ aginst $[H_3O^+]$ yield a straight line with a Y-intercept of $1/\mu_0$ and a slope of $1/K_a\mu_0$. The pK_a value follows using the equation

$$pK_a = \log\frac{slope}{intercept} \tag{3.7}$$

The apparent pK_a values of each paraben were determined by measuring μ_{eff} of each paraben in CZE as a procedure described in Section 3.2.5.1. From the linear fitting of $1/\mu_{eff}$ versus 10^{-pH} in Figure 3.2, Table 3.1 summarizes the values of slope, $1/K_a\mu_0$, and Y-intercept, $1/\mu_0$, experimental and the literature pK_a values of each paraben. The slightly smaller apparent pK_a than literature pK_a^o values are seen, where the latter is obtained from the zero ionic strength. Strictly speaking, $pK_a^o = pK_a + (-\log\gamma_{A-})$, where the γ_{A-} is activity coefficient for A⁻ at a given ionic strength, and always less than 1.0. Therefore, pK_a less than pK_a^o value is reasonable.

The borate buffer used in this work has the limit of buffering capacity in the pH range of $pK_a\pm1$, where the pK_a of boric acid is 9.2. Therefore, the pH 10.2 was chosen to obtain buffering capacity and afford almost fully charged analytes with the degrees of ionization of 0.96 for IP and 0.99 for other parabens, calculated using the apparent pK_a values in Table 3.1 and Equation 3.4.
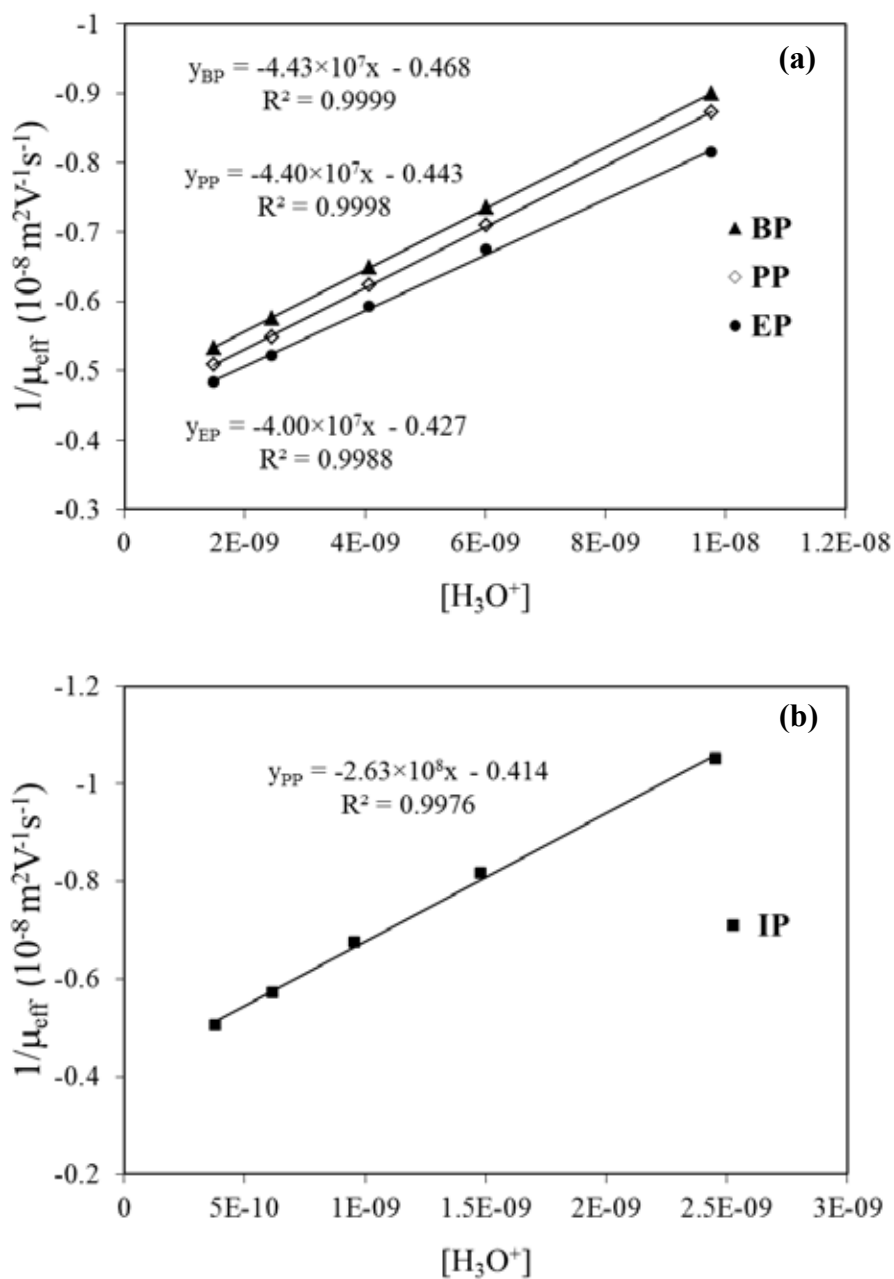
Figure 3.2 Plots of $1/\mu_{eff}$ as a function of $[H_3O^+]$ for BP, PP, and EP in (a), IP in (b). CE c onditions: uncoated f used s ilica 50 μm i .d. × 40.2 c m (30 c m t o de tector), temperature 2 5 °C, BGE, 10 m M disodium bor ate buf fer at a r ange of pH va lues, voltage 15 kV, 0.5 psi pressure injection for 3 s and UV detection at 220 nm.

Table 3.1 Slope, Y-intercept, experimental and the literature pK_a values of for each paraben

Analyte	Slope $(1/K_a\mu_0)$	Intercept $(1/\mu_0)$	pK_a	
			This work	Literature (at zero ionic strength)
IP	-2.63×10^8	-0.414	8.80	9.2
BP	-4.43×10^7	-0.468	7.98	8.4
PP	-4.40×10^7	-0.443	8.00	8.4
EP	-4.00×10^7	-0.427	7.97	8.4

3.3.1.3 Electrophoretic mobility and separation selectivity

Simultaneuos separation of IP, BP, PP and EP in CZE was carried out as a procedure described in Section 3.2.5.2. Figure 3.3 shows an example of electropherogram for separation of these parabens in CZE. As seen in Figure 3.3, the CZE separation, in which the electrophoretic mobility vectors of negatively charged parabens are opposite to an EOF vector, the migration time order EP > PP > BP > IP with the effective electrophoretic mobilities μ of -2.25, -2.13, -2.03 and -2.00 $10^{-8}m^2V^{-1}s^{-1}$, respectively, indicates the $|\mu|$ order EP > PP > BP > IP, in line with the charge-to-size ratio for homologous series EP > PP > BP. The smaller $|\mu|$ for IP than other parabens may be due to the smaller degree of ionization, and/or larger hydrodynamic size of IP. The values of α_{CZE} can be calculated from the ratio of μ for each pair of analytes, resulting in the α_{CZE} values of 0.888, 1.066 and 0.953 for IP/EP, PP/IP and BP/PP, respectively. It can be seen from Figure 3.3 that separation of BP, PP and EP was achieved under CZE conditions, while partial separation was obtained for IP and BP. It should be noted that each peak was identified by spiking standard analytes.
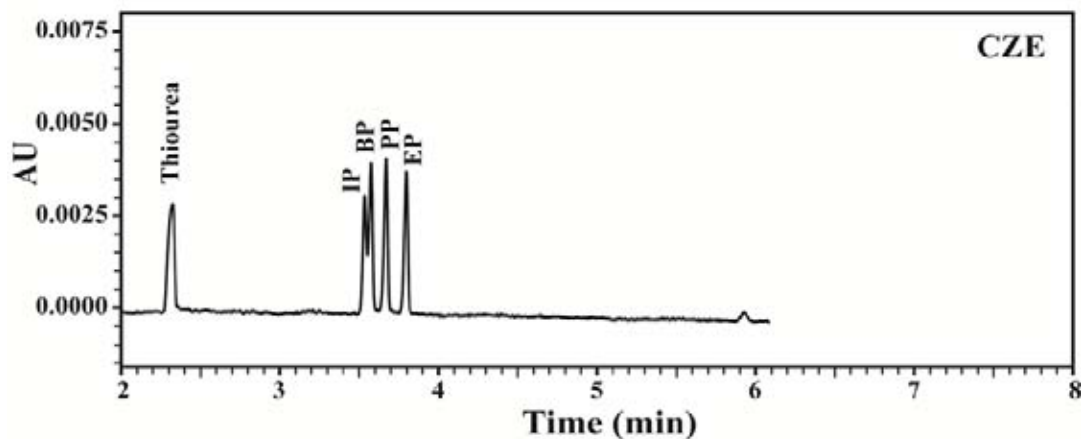
Figure 3. 3 Electropherogram of s eparation of IP, B P, PP a nd E P using CZE. CE c onditions: unc oated f used s ilica 50 μm i .d. × 40.2 c m (30 cm t o d etector), temperature 25 °C, BGE, 10 mM disodium borate buffer adjusted to pH 10.2 with 1.0 M Na OH, vol tage 15 kV, 0.5 ps i pressure i njection for 3 s and U V de tection at 220 nm.

3.3.2 Charged compounds separation in MEKC

3.3.2.1 Principle of charged compounds separation in MEKC

In MEKC, effective electrophoretic mobilities of two fully charged analytes, μ_{MEKC}, are given by Equations 3.8 and 3.9 [Camilleri, 1993].

$$\mu_{(MEKC,1)} = \left(\frac{\mu_{0,1} + k_1\mu_{mc}}{1 + k_1} \right) \tag{3.8}$$

$$\mu_{(MEKC,2)} = \left(\frac{\mu_{0,2} + k_2\mu_{mc}}{1 + k_2} \right) \tag{3.9}$$

where μ_0 is the electrophoretic mobility at zero concentration of SDS or under CZE conditions, and μ_{mc} is the electrophoretic mobility of the micelle marker. Subscripts 1 and 2 refer to the analytes 1 and 2, respectively.

As previously mentioned in Section 3.1, the retention selectivity (α_k) in MEKC is defined as the ratio of k, such as k_2/k_1, and therefore k_2 is given by Equation 3.10

$$k_2 = \alpha_k k_1 \qquad (3.10)$$

In CZE, the mobility selectivity (α_{CZE}) is defined as the ratio of μ_0, such as $\mu_{0,2}/\mu_{0,1}$, and therefore $\mu_{0,2}$ is given by Equation 3.11

$$\mu_{0,2} = \alpha_{CZE}\mu_{0,1} \qquad (3.11)$$

The separation selectivity in MEKC (α_{MEKC}) is the ratio of μ_{MEKC} with $k_2 \geq k_1 > 0$. From μ_{MEKC} values in Equations 3.8 and 3.9, α_{MEKC} can be rewritten as

$$\alpha_{MEKC} = \frac{\mu_{(MEKC,2)}}{\mu_{(MEKC,1)}} = \left(\frac{\mu_{0,2} + k_2\mu_{mc}}{\mu_{0,1} + k_1\mu_{mc}}\right)\left(\frac{1+k_1}{1+k_2}\right) \qquad (3.12)$$

From Equations 3.10 and 3.11, α_{MEKC} can be expressed by the equation

$$\alpha_{MEKC} = \left(\frac{\alpha_{CZE}\beta + \alpha_k k_1}{\beta + k_1}\right)\left(\frac{1+k_1}{1+\alpha_k k_1}\right) \qquad (3.13)$$

where $\beta = \mu_{0,1}/\mu_{mc}$

3.3.2.2 Theoretical models of separation selectivity

α_{MEKC} in Equation 3.1.3 may be rearranged to relate to the ratio of α_k/α_{CZE} as the equation

$$\alpha_{MEKC} = \alpha_{CZE}\left(\frac{\beta + \dfrac{\alpha_k}{\alpha_{CZE}}k_1}{\beta + k_1}\right)\left(\frac{1+k_1}{1+\alpha_k k_1}\right) \qquad (3.14)$$

Table 3.2 Types of theoretical models for α_{MEKC}

Type	Order of $|\mu|$ in CZE and k in MEKC	α_{CZE}	α_k	ρ	Assumed values	
					α_{CZE}	α_k
I	Same	$\alpha_{CZE} \geq 1$	$\alpha_k > \alpha_{CZE} \geq 1$	$\rho > 1$	1.1	1.2–3.3
II	Same	$\alpha_{CZE} > 1$	$\alpha_{CZE} \geq \alpha_k \geq 1$	$\rho \leq 1$	1.5	1.0–1.5
III	Reversed	$\alpha_{CZE} < 1$	$\alpha_k \geq 1 > \alpha_{CZE}$	$\rho > 1$	0.8	1.0–6.4
IV	Co-migration	$\alpha_{CZE} = 1$	$\alpha_k = \alpha_{CZE} = 1$	$\rho = 1$	–	–

In order to describe and predict separation of charged analytes in MEKC, theoretical models of α_{MEKC} for two charged analytes in Equation 3.14 are firstly proposed in this work, and classified into four types as listed in Table 3.2, based on the ranges of α_{CZE}, α_k, ρ and the order of $|\mu|$ in CZE and k in MEKC.

It should be noted that α_k is always ≥ 1.0. In the case of Types I and II where the value of $\alpha_{CZE} > 1.0$, the same order of $|\mu|$ in CZE and k in MEKC, e.g. $k_2 > k_1$ and $|\mu_2| > |\mu_1|$. In case of Type III, the value of $\alpha_{CZE} < 1.0$ refers to the reversed order of $|\mu|$ in CZE and k in MEKC, e.g. $k_2 > k_1$ and $|\mu_2| < |\mu_1|$. Type IV, where $\alpha_k = 1.0$ and $\alpha_{CZE} = 1.0$, indicates co-migration of two charged analytes and therefore, no resolution is obtained using either CZE or MEKC. In order to simply predict the values of α_{MEKC} for two charged analytes, the value of β in Equation 3.14 is assumed to be equal to 0.5. Figure 3.4 shows plots of the α_{MEKC} model of Types I–III over a wide range of k_1. Practically, an increase in k may be obtained by an increase in the concentration of SDS ([SDS]) in an MEKC buffer.

Figure 3.4a is firstly considered. At a fixed value ρ except in the case $\rho \approx 1.0$, for example, $\alpha_k = 1.2, 1.4, 1.7, 2.2$ and 3.3 respectively, the value of α_{MEKC} increases with an increase in k_1 to a maximum value, and then decreases at higher values of k_1. At a fixed value of k_1, the higher the value of α_k, the greater the value of α_{MEKC}. The k_1 giving the maximum α_{MEKC} value decreases as the value of α_k increases. It can be

concluded from the α_{MEKC} model of Type I, with the same order of $|\mu|$ in CZE and k in MEKC for charged analytes that higher α_k than α_{CZE} can improve α_{MEKC} for two charged analytes in MEKC.

In contrast to Type I, the α_{MEKC} model of Type II, where $\alpha_k \le \alpha_{CZE}$, in Figure 3.4b shows that the value of α_{MEKC} decreases with an increase in k_1, implying poorer separation for two charged analytes in MEKC. The addition of SDS surfactant in the BGE leads to a decrease of α_{MEKC} for two charged analytes.

Finally, the reversed order of $|\mu|$ in CZE and k in MEKC for two charged analytes as shown in Figure 3.4c is discussed. It is seen that, the theoretical α_{MEKC} for the Type III model starts from less than 1.0 ($1/\alpha_{MEKC} > 1.0$) to near 1.0 (poorer separation) with increasing k_1 and then higher than 1.0 (better separation) at higher k_1 values. At an α_{MEKC} of 1.0, the value of k_1 is given by Equation 3.15

$$k_1 = \frac{(1-\alpha_{CZE})}{(\alpha_{CZE}-\alpha_k)+(\alpha_k-1)/\beta} \qquad (3.15)$$

The small value of α_k gives a higher k_1 at α_{MEKC} 1.0, which is consistent with the bottom line for α_{MEKC} of 0.99 in Figure 3.4c. It should be noted that for a theoretical value of α_{CZE} or $\alpha_{MEKC} < 1.0$, the practical separation selectivity is equal to $1/\alpha_{CZE}$ or $1/\alpha_{MEKC}$. Therefore, an increase in k_1 may result in a reversed order of electrophoretic mobility for two charged analytes in MEKC.

As can be seen in Figure 3.4, the theoretical model of α_{MEKC} can be employed to describe the separation of two charged analytes. The greater the α_{MEKC} value ($\alpha_k > 1.0$), the greater the resolution. The better separation selectivity in MEKC over CZE can be obtained for the α_{MEKC} Type I ($\alpha_k > \alpha_{CZE}$), or Type III models ($\alpha_k \gg \alpha_{CZE}$, or $\alpha_k > 1/\alpha_{CZE}$) at appropriate values of k_1.

It should be noted that the direction of EOF velocity and total velocity does not affect the el ectrophoretic m obility o f an alytes an d m icelles, an d t he r etention f actor o f analytes i n M EKC. Owing to i ndependence o f t he v alues o f α_m and α_k with th e direction of these velocities, our proposed selectivity models can be used for MEKC with nor mal, r eversed a nd r estricted m odes c lassified b y t he di rection of E OF a nd total velocity as details given in Section 2.4.
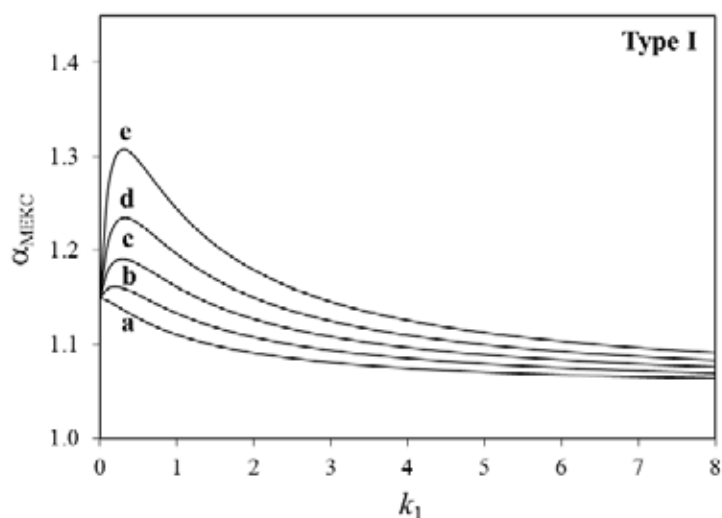
Figure 3.4a Theoretical models of α_{MEKC} of two charged analytes in MEKC. Type I: $\alpha_k > \alpha_{CZE} \geq 1.0$, $\rho > 1.0$. α_{MEKC} is obt ained us ing E quation 3.14 a nd da ta i n Table 3.2. a-e refer to the values of α_k for 1.2, 1.4, 1.7, 2.2, and 3.3, respectively.
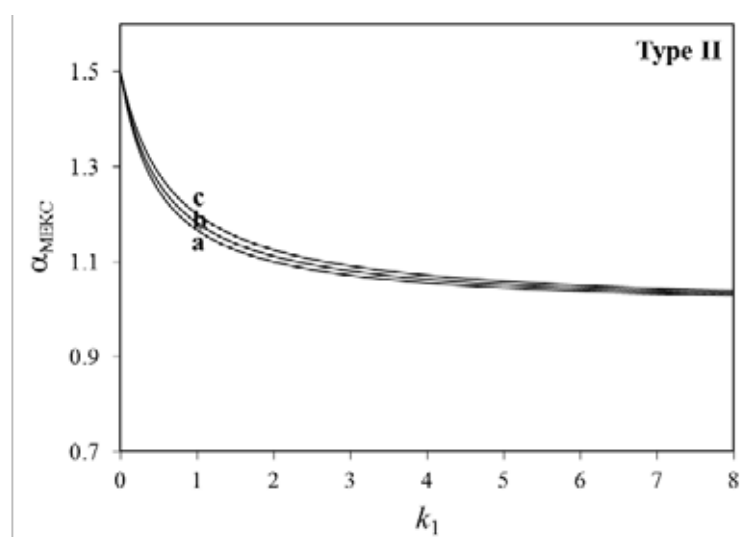
Figure 3.4b Continued. Type II: $\alpha_{CZE} \geq \alpha_k \geq 1.0$, $\rho \leq 1.0$. a-c refer to the values of α_k for 1.0, 1.2, and 1.5, respectively.
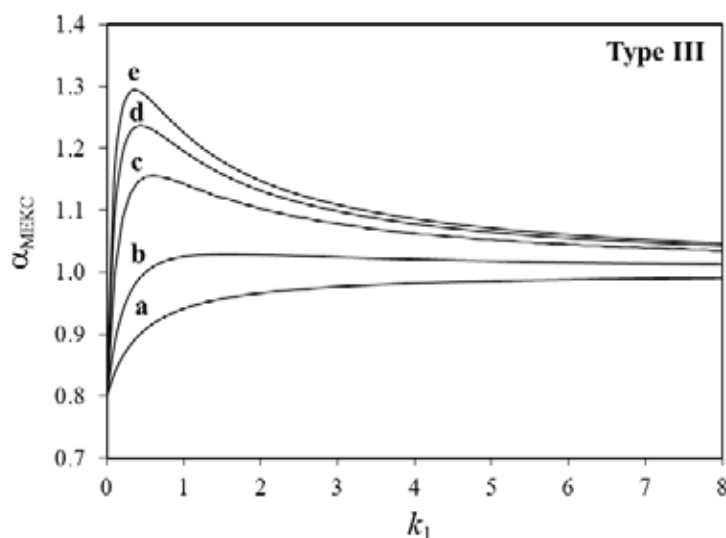
Figure 3.4c Continued. Type III: $\alpha_k \geq 1.0 > \alpha_{CZE}$, $\rho > 1.0$. a-e refer to the values of α_k for 1.0, 1.6, 3.2, 4.8 and 6.4, respectively.

3.3.2.3 Experimental and predicted values of α_{MEKC} in MEKC

Figure 3.5 shows an example of electropherograms of simultaneous separation of test analytes in MEKC using various concentrations of SDS. The retention factors for negatively charged parabens, calculated using Equation 2.22 and Figure 3.5, are shown in Table 3.3. The values of k were obtained in the order BP > PP > IP > EP, which are consistent with the magnitude order of octanol-water distribution constants in this series BP > PP > EP [Poouthree *et al.*, 2007; Golden, Gandy, and Vollmer, 2005; Tavares *et al.*, 2009]. As seen in Figure 3.5c for MEKC separation with 60 mM SDS, the order of migration time or $|\mu_{MEKC}|$ is obtained to be BP > PP > IP > EP, while different orders are obtained in MEKC at 20 mM SDS (Figure 3.5a): BP > PP > EP > IP, and in CZE (Figure 3.3): EP > PP > BP > IP. These differences in migration behavior can be explained using the separation selectivity models in Section 3.3.2.2.

Figure 3.6 shows the observed and predicted values of α_{MEKC} for parabens in MEKC over a wide range of [SDS] (Figure 3.6a) and k_1 values (Figure 3.6b). The former is useful to consider the [SDS] giving the achieve resolution of all solutes and the reversed migration, whereas the latter is useful to compare the observed and the

predicted m odel w ithout know n [SDS]. T he pr edicted va lues of α_{MEKC} at d ifferent [SDS] (6.0 t o 60 m M) were c alculated us ing d ata i n T able 3. 3 and Equation 3.14. Table 3 .3 also lis ts th e mo bility s electivity, r etention s electivity, r etention factor, selectivity ratio, a nd p redicted mo dels o f α_{MEKC}. As pr eviously m entioned, f or MEKC s eparation o f a particular analyte p air, s uch as P P an d IP, k_1 refers t o t he retention f actor f or th e solute w ith s maller k, s uch a s k_{IP}. U sing a w ide r ange o f [SDS] (20 to 60 mM), the observed k_1 can be plotted against [SDS] to derive a linear calibration pl ot, a llowing pr edicted values o f k_1 at va rious [SDS] t o b e obt ained. Using d ata i n T able 3 .3 and E quation 3.14, t he o bserved v alues of α_{MEKC} in F igure 3.6 were found t o b e i n g ood a greement w ith t he pr edicted v alues, i ndicating t hat Equation 3.14 c an b e us ed f or pr ediction of the α_{MEKC} values o ver a w ide r ange o f [SDS] and k_1.

Table 3.3 Mobility selectivity (α_{CZE}), retention selectivity (α_k), retention factor (k_1), selectivity ratio (ρ), and types of α_{MEKC} model

Pair	Solute	$k_1 = a[SDS]+b$	α_{CZE}	α_k	β	ρ	Types of model for α_{MEKC} in MEKC
IP/EP	EP	0.00236[SDS]-0.013	0.888	k_{IP}/k_{EP}	0.575	$\rho > 1.0$	III
PP/IP	IP	0.00871[SDS]-0.028	1.066	k_{PP}/k_{IP}	0.511	$\rho > 1.0$	I
BP/PP	PP	0.01004[SDS]-0.035	0.953	k_{BP}/k_{PP}	0.544	$\rho > 1.0$	III
	BP	0.03068[SDS]-0.057	-	-	-		-
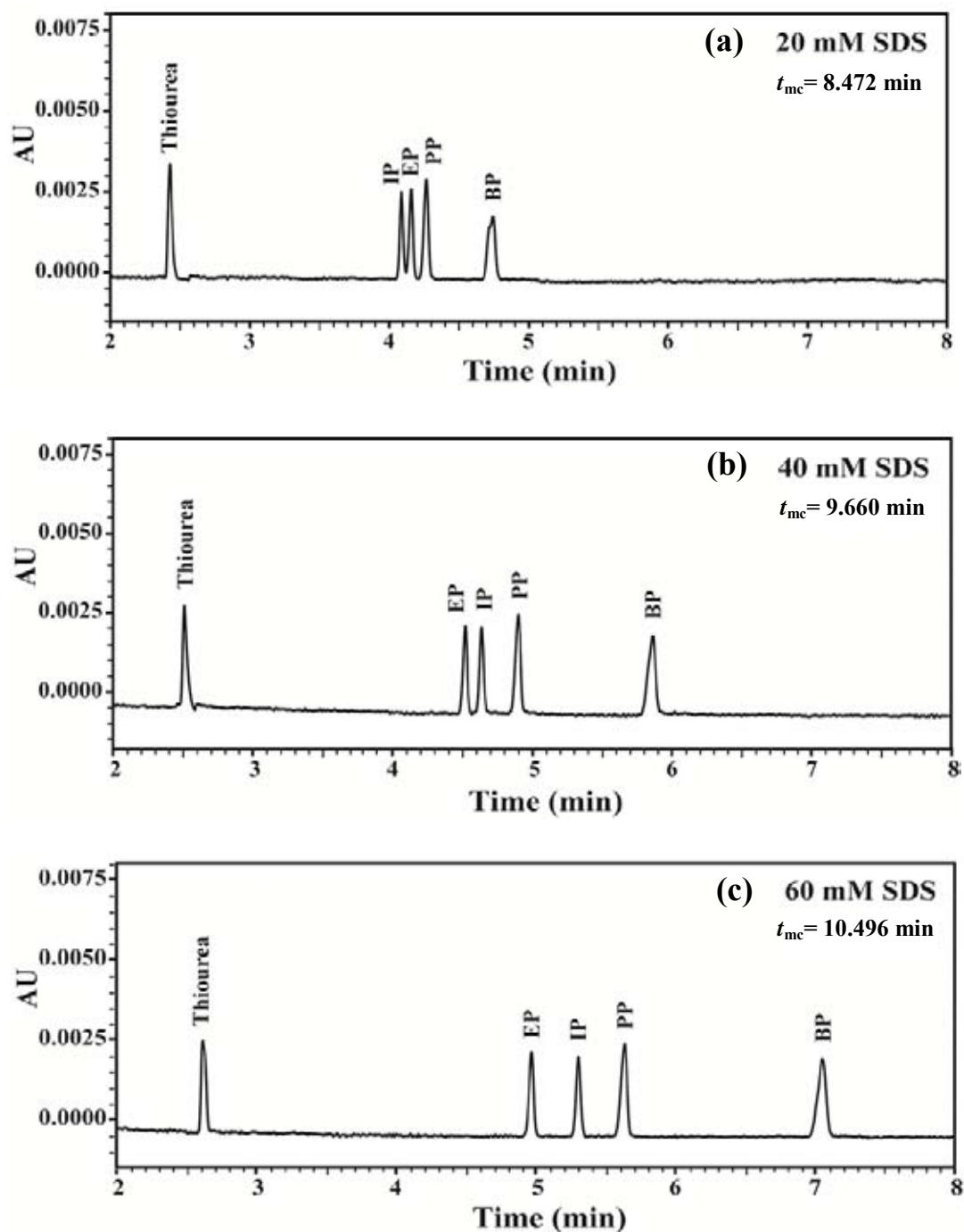
Figure 3.5 Electropherograms of separation of IP, BP, PP and EP in MEKC using (a) 20, (b) 40, and (c) 60 mM SDS in a 10 mM $Na_2B_4O_7$ buffer adjusted to pH 10.2 with 1.0 M NaOH. CE conditions: uncoated fused silica 50 μm i.d. × 40.2 cm (30 cm to detector), temperature 25 °C, voltage 15 kV, 0.5 psi pressure injection for 3 s and UV detection at 220 nm.
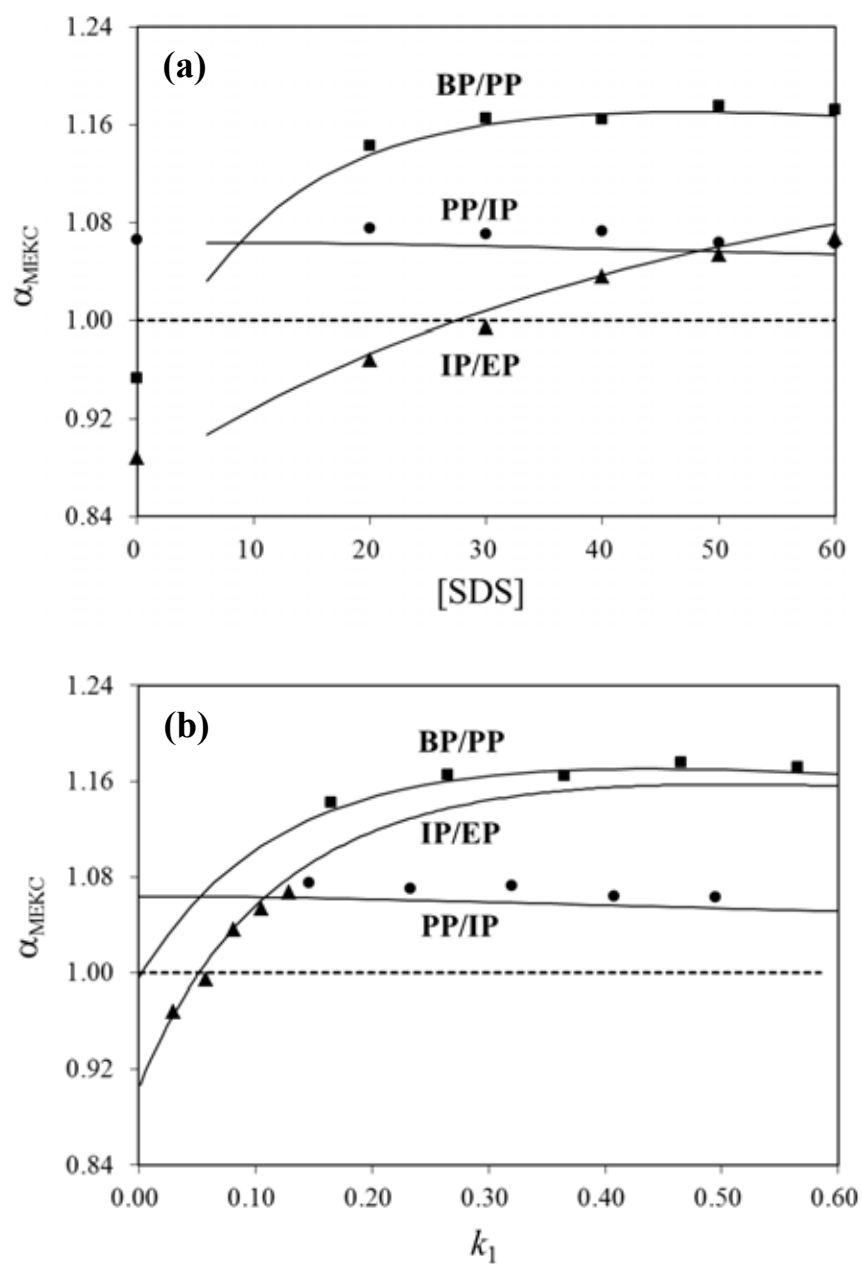
Figure 3.6 Observed (symbols) and predicted (solid lines) values of α_{MEKC} for two charged analytes in MEKC. (a) Various concentrations of SDS and (b) various values of k_1. Symbols ■, ●, and ▲ refer to pairs of BP/PP, PP/IP, and IP/EP, respectively. Predicted values are obtained using Equation 3.14 and data as listed in Table 3.3.

According to electropherograms in Figure 3.5 and data in Table 3.3, the same order of $|\mu|$ in CZE and k in MEKC was obtained for PP/IP, and therefore $\alpha_{CZE} > 1.0$ and $\alpha_{MEKC} > 1.0$. Although the ρ value is greater than 1.0, a slight decrease in the observed and predicted values of α_{MEKC} with an increase in [SDS] and k_1 is due to small calculated values of ρ between 1.032 and 1.072 for 10 to 60 mM SDS. Therefore, a change in α_{MEKC} for PP/IP in MEKC is consistent with the α_{MEKC} model of Type I described in Section 3.3.2.2 with small values of ρ.

Owing to the reversed order of $|\mu|$ in CZE and k in MEKC for IP/EP and BP/PP, and the theoretical value of α_{CZE} being less than 1.0, the reversed $|\mu|$ order for IP/EP and BP/PP at high [SDS] and at low or zero [SDS] is consistent with the α_{MEKC} Type III model. At an α_{MEKC} value of 1.0, the predicted values of k_1 in Figure 3.6b are estimated to be 0.003 for BP/PP at very low [SDS], and 0.052 for IP/EP which is in good agreement with the observed k_1 of 0.064. It should be noted that, employing Equation 3.15 with an average α_k of 3.831 for IP/EP at 6.0 to 60 mM SDS, the predicted values of k_1 of 0.057 giving α_{MEKC} of 1.0 are found to be good agreement with value of k_1 of 0.052 in Figure 3.6b.

3.4 Conclusion

Micellar electrokinetic chromatography (MEKC) is one of the modes in capillary electrophoresis which is performed by the addition of a surfactant into the running buffer, to form micelles acting as a pseudo-stationary phase. The separation of charged compounds in MEKC depends on the difference in either micellar partitioning or their electrophoretic mobilities (μ). MEKC separation selectivity (α_{MEKC}), defined as the ratio of their μ, is one of the characteristics used to describe separation of two analytes. In order to explain the separation selectivity and electrophoretic mobility order of fully charged analytes in MEKC, equations and theoretical models for α_{MEKC} which is related to the dimensionless values of mobility selectivity (α_{CZE}) in capillary zone electrophoresis (CZE) and retention selectivity

(α_k) in MEKC were established, where α_{CZE} and α_k are defined as the ratio of μ in CZE and the ratio of retention factor (k) in MEKC for two charged analytes, respectively. Theoretical models for α_{MEKC} can be classified into four types based on the order of $|\mu|$ in CZE, k in MEKC and the selectivity ratio ($\rho = \alpha_k/\alpha_{CZE}$). The α_{MEKC} Type I (the same order of $|\mu|$ in CZE and k in MEKC with $\rho > 1.0$), MEKC separation of two charged analytes can enhance α_{MEKC} up to the maximum value with increasing the SDS concentration, while the α_{MEKC} Type II (the same order of $|\mu|$ in CZE and k in MEKC), lower separation selectivity in MEKC than CZE is obtained with $\rho \leq 1.0$ ($\alpha_{CZE} \geq \alpha_k \geq 1.0$). The α_{MEKC} Type III (the reversed order of $|\mu|$ in CZE and k in MEKC with $\rho > 1.0$) can give the reversed order of the μ in MEKC results in worse separation in MEKC than CZE. For the α_{MEKC} Type IV with α_{CZE} of 1.0 and α_k of 1.0 ($\rho = 1.0$), no resolution is obtained in either CZE or MEKC. Using four alkylparabens as test analytes, excellent agreement was found between the observed α_{MEKC} and the proposed α_{MEKC} models of test analytes in MEKC over a wide range of SDS concentrations and values of k.

CHAPTER IV

INVESTIGATION OF NEUTRAL MONOLITHIC CAPILLARY COLUMNS WITH VARYING *n*-ALKYL CHAIN LENGTHS IN CAPILLARY ELECTROCHROMATOGRAPHY

4.1 Introduction

CEC employing organic polymer-based monolithic stationary phases is increasingly used as an effective separation method due in major part to the ease of the *in situ* polymerization of vinyl-based monomers in capillaries and microchannels [Eeltink, and Svec, 2007; Karenga, and El Rassi, 2011c; Svec, 2009, 2010], which has allowed the realization of tailor made stationary phases for the separation of a wide range of species [Faure *et al.*, 2008; Karenga, and El Rassi, 2010a; Lu *et al.*, 2009]. Recently, and to widen the scope of applications of CEC to encompass biomolecules i.e. peptides and proteins, El Rassi's research group has introduced a series of neutral nonpolar monoliths with surface bound C 17, C 18 and naphthyl ligands for RP-CEC of charged species (including proteins and peptides) in the absence of electrostatic interactions with fixed surface charges while affording relatively moderate EOF velocity [Karenga, and El Rassi, 2008, 2010a, 2010b, 2010c; Okanda, and El Rassi, 2005]. Customarily, the fixed surface charges have been intentionally introduced to support the EOF [Lu *et al.*, 2009; Augustin *et al.*, 2008; Bedair, and El Rassi, 2002, 2003], a fact that led to the nuisance electrostatic interactions, which caused either band broadening or irreversible binding of charged solutes such as proteins and peptides. In the new generation of neutral nonpolar monoliths [Karenga, and El Rassi, 2008, 2010a, 2010c; Okanda, and El Rassi, 2005], the EOF resulted from the adsorption of mobile phase ions to the neutral monolithic surface, thus imparting this surface with the zeta potential required to support the EOF necessary for solute transport across the column. The magnitude of the EOF has been conveniently adjusted by the pH and ACN content of the mobile phase. The

separation s electivity, r etention a nd m agnitude of t he E OF ha ve be en f urther modulated b y m ixed ligands (i.e. C18/naphthyl ligands) m onolithic c olumns [Karenga, and E l R assi, 2011a] as w ell a s by s egmented mo nolithic c olumns consisting of oc tadecyl a nd na phthyl m onolithic s egments [Karenga, and E l R assi, 2011b]. Although ot her r esearchers ha ve a lso d eveloped n eutral m onoliths f or R P-CEC [Dong *et a l.*, 2004; Li *et a l.*, 2004; Zhang *et a l.*, 2003], t hese w ere s parse attempts a nd t he de scribed ne utral m onoliths were not e ffective i n t he C EC of peptides and pr oteins. Briefly, in the first attempt, Zhang *et al.* [Zhang *et al.*, 2003] developed a ne utral m onolith, w hich w as pr epared by t he c opolymerization of but yl methacrylate and ethylene dimethacrylate (EDMA). This neutral monolith exhibited a w eak E OF, and t herefore, t he s eparation o f small aci dic s olutes w as ach ieved through th eir d ifferential e lectromigration. Similarly, a n eutral mo nolithic c olumn was p repared b y the copolymerization o f l auryl m ethacrylate and E DMA t hat w as applied to RP-CEC of ionic analytes whereby their separation was realized with their electrophoretic mobility as the driving force [Dong *et al.*, 2004]. In another report, a monolithic c apillary c olumn whose i nner w all grafted with p olyethyleneimine to support the generation of an annular EOF was developed [Li *et al.*, 2004]. The actual monolith was made by *in situ* copolymerization of vinylbenzene chloride and EDMA. This monolith permitted the separation of short peptides at pH 2.5 where the peptides are also p ositively charged as t he an nular p olyethyleneimine co ating t o avoid electrostatic attractions between the peptides and the annular coating.

As a continuation of this recent e fforts in developing n eutral nonpol ar m onoliths for the R P-CEC o f ch arged s pecies i n t he ab sence o f electrostatic i nteractions, t wo different neutral nonpolar monolithic columns series (designated as A and B columns series) each consisting of three columns at varying *n*-alkyl chain length (i.e. C8, C12 and C 16) w ere pr epared a nd c haracterized ove r a w ide r ange of m obile pha se composition. In the A columns s eries, the c omposition of the functional m onomers and c rosslinker w as a djusted t o yield c omparable c hromatographic r etention regardless of the alkyl chain length while in the B columns series, the composition of the f unctional m onomers a nd c rosslinker w as ke pt c onstant yielding va riable chromatographic r etention. The t wo c olumns s eries were d emonstrated in th e

separation of neutral (nonpolar and polar) and charged species such as proteins and peptide mapping.

4.2 Experimental

4.2.1 Reagents and materials

Pentaerythritol triacrylate (PETA), dodecyl acrylate (C12-acrylate), 2,2´-azobisisobutyronitrile (AIBN), 3-(trimethoxysilyl)propyl methacrylate, benzene, alkylbenzenes (ABs), alkyl phenyl ketones (APKs), nitroalkanes (NAs), phenols, anilines, and analytical-grade acetone were purchased from Aldrich (Milwaukee, WI, USA). Octyl methacrylate (C8-methacrylate) and cetyl methacrylate (C16-methacrylate) were from Polysciences (Warrington, PA, USA). Cyclohexanol was purchased from J.T. Baker (Phillipsburg, NJ, USA). Ethylene glycol (EG), HPLC-grade acetonitrile (ACN), and nitric acid were from Fischer Scientific (Fair Lawn, NJ, USA). The following proteins were purchased from Sigma (St. Louis, MO, USA): chicken egg white lysozyme, equine heart cytochrome C, bovine pancreas ribonuclease A, ov albumin, and bovine pancreas α-chymotrypsin. TPCK trypsin from bovine pancreas was also purchased from Sigma (St. Louis, MO, USA). Equine heart cytochrome C tryptic digestion was performed after protein reduction and alkylation using the Promega protocol. Buffer solutions were prepared using sodium phosphate monobasic from Mallinckrodt (Paris, KY, USA).

4.2.2 CE conditions

The instruments used in this investigation were a P/ACE 2200 and P/ACE 5510 system CE from Beckman (Fullerton, CA, USA) equipped with a fixed wavelength UV detector, and a photodiode array detector, respectively. All electrochromatograms were recorded with a personal computer running Gold P/ACE software. The uncoated fused-silica capillary 27 cm in length (20 cm to detector) $\times$ 100 μm i.d. (Polymicro Technologies, AZ, USA) was used for CEC separations, thermostated at 25 °C. The samples were injected electrokinetically at

various times and applied voltages, which are stated in the figure captions. Prior to CEC separation each day, the monolithic column was conditioned with the running buffer using a syringe pump for 30 min. Thereafter, the column was placed in the CEC instrument for conditioning at the running voltage until a stable current and baseline were observed.

4.2.3 Column fabrication

The fabrication of organic polymer based-monolithic column can be divided into two main steps and the details as describes in Sections 4.2.3.1 and 4.2.3.2. The monomers used in the process of column fabrication are shown in Figure 4.1

octyl methacrylate
(C8-methacrylate)

dodecyl acrylate
(C12-acrylate)

cetyl methacrylate
(C16-methacrylate)

pentaerythritol triacrylate (PETA)

3-(trimethoxysilyl)propyl methacrylate
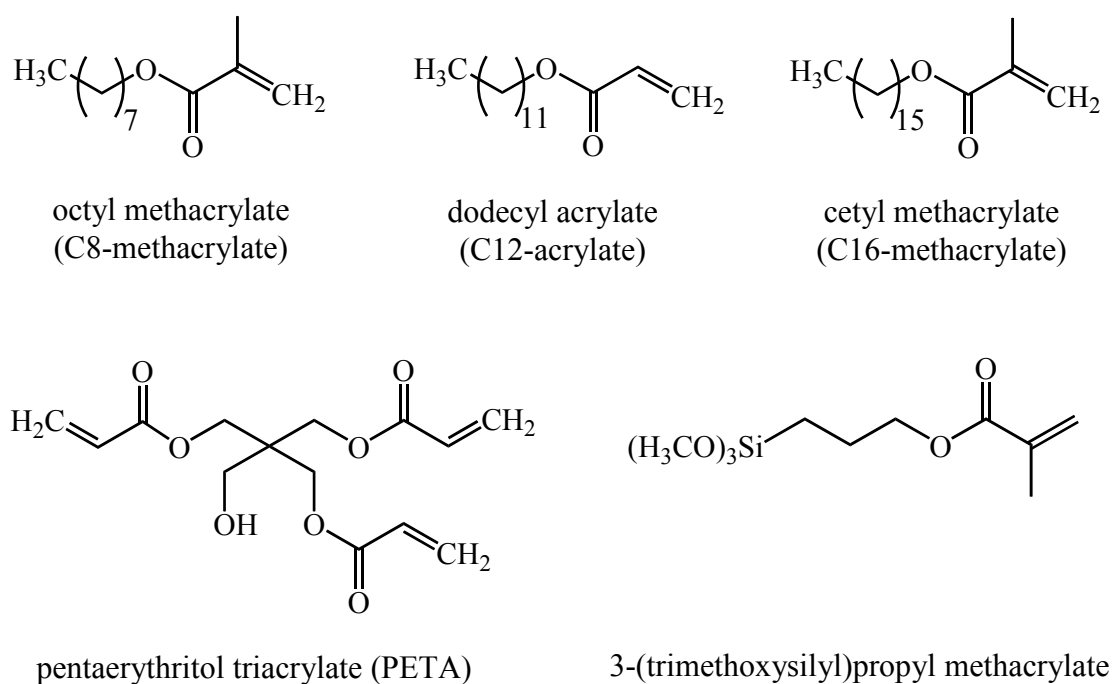
Figure 4.1 Chemical structures of monomers used in the column fabrication: octyl methacrylate (C8-methacrylate), dodecyl acrylate (C12-acrylate), cetyl methacrylate (C16-methacrylate), pentaerythritol triacrylate (PETA), and 3-(trimethoxysilyl)propyl methacrylate.

4.2.3.1 Column pretreatment

Prior to the polymerization step, the inner wall of the fused-silica capillary was treated with 1.0 M sodium hydroxide for 30 min, flushed with 0.1 M hydrochloric acid for 30 min, a nd t hen r insed with w ater f or 30 m in. The c apillary i nner w all w as t hen allowed to react with a solution of 50% v/v of 3-(trimethoxysilyl)propyl methacrylate in acet one f or 6 h at r oom t emperature t o v inylize t he i nner wall o f th e c apillary. Finally, t he c apillary w as r insed w ith a cetone a nd t hen dr ied with a s tream of nitrogen. The process of column pretreatment is shown in Figure 4.2.

Rinsed with 1.0 M NaOH for 30 min

↓

Rinsed with 0.1 M HCl for 30 min

↓

Rinsed with H_2O for 30 min

↓

Reacted with a solution of 50% (v/v)
3-(trimethoxysilyl)propyl methacrylate
in acetone for 6 h

↓

Rinsed with acetone

↓

Dried with a stream of nitrogen for 1 h
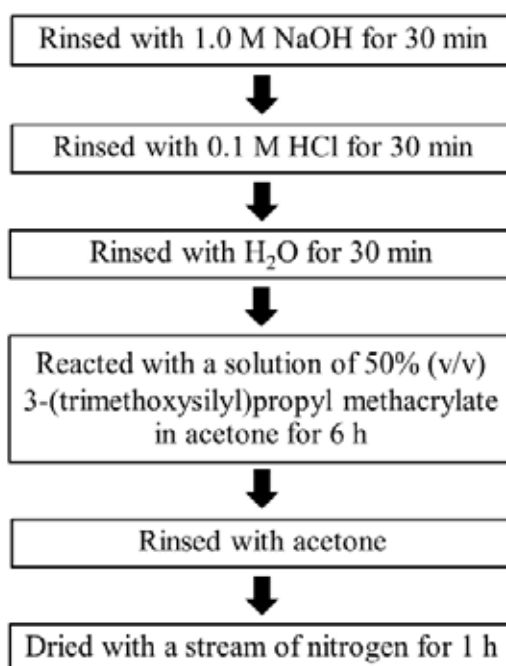
Figure 4.2 Schematic diagram of column pretreatment procedure.

4.2.3.2 *In situ* polymerization

Polymerization s olutions w ere pr epared f rom *n*-alkyl a crylate o r m ethacrylate functional m onomers w ith C 8, C 12, or C 16 a lkyl c hains, t he c rosslinking m onomer PETA a nd po rogenic s olvents, a nd all m ixed i n t he r atio o f 20:80 w /w monomers/porogenic solvents. The mixtures of monomers were weighed in different ratios, and then di ssolved in a t ernary por ogenic s olvent c onsisting of c yclohexanol and ethylene glycol in various ratios at constant 3.6 w t% water, the details as shown in Table 4.1. AIBN (1.0 wt% with respect to monomers) was added to the solution as the free radical initiator. The polymerization solutions was then mixed with a vortex mixer t o ob tain c lear s olutions, a nd de gassed w ith ni trogen f or 10 m in. A 30 c m pretreated c apillary (see Section 4.2.3.1) w as filled w ith the pol ymerization solution up to 21 c m by immersing the inlet of the capillary in the solution vial and applying vacuum to the capillary outlet. T he capillary ends were then sealed using GC septa, and the capillary was put in a 60 °C GC oven for 12 h. The resulting monolith was washed w ith a n 80: 20 v/v a cetonitrile:water m ixture us ing a n H PLC pum p. A detection window was created at 1 to 2 mm after the end of the polymer bed using a thermal wire stripper. Finally, the column was cut to a total length of 27 cm with an effective length of 20 cm. The overall process is shown in Figure 4.3.

Table 4.1 Composition o f t he pol ymerization s olutions us ed i n the pre paration of t he different mo nolithic c olumns. Capillary c olumn, 27 c m t otal l ength, 20 c m e ffective length × 100 μm i.d.; mobile phase, 75% ACN (v/v) in 1.0 mM sodium phosphate buffer, pH 7.0; voltage, 15 kV.

Column/monolith designation	*n*-Alkyl chain length monomer		Plates/m[b]	EOF (mm/s)	k		
	designation	mmol[a]			pentyl benzene	hexyl benzene	heptyl benzene
1A[c]	C8	0.58	150,000	1.15	1.94	2.71	3.82
2A[c]	C12	0.47	162,000	1.10	1.86	2.64	3.75
3A[c]	C16	0.26	200,000	1.03	1.62	2.42	3.40
1B[d]	C8	0.48	128,000	0.90	1.58	2.21	3.12
2B[d]	C12	0.48	93,000	0.90	1.94	2.78	4.01
3B[d]	C16	0.48	62,000	0.86	2.52	3.66	5.35

[a]Amount of *n*-alkyl monomer used in the polymerization mixture.
[b]The average values taken for benzene and the first seven alkylbenzenes series.
[c]Polymerization solutions contained 0.07, 0.13, and 0.15 mmol PETA for the monolithic columns 1A, 2A, and 3A, respectively (i.e. the A columns series).
[d]Polymerization solutions contained 0.07 mmol PETA (i.e. the B columns series).
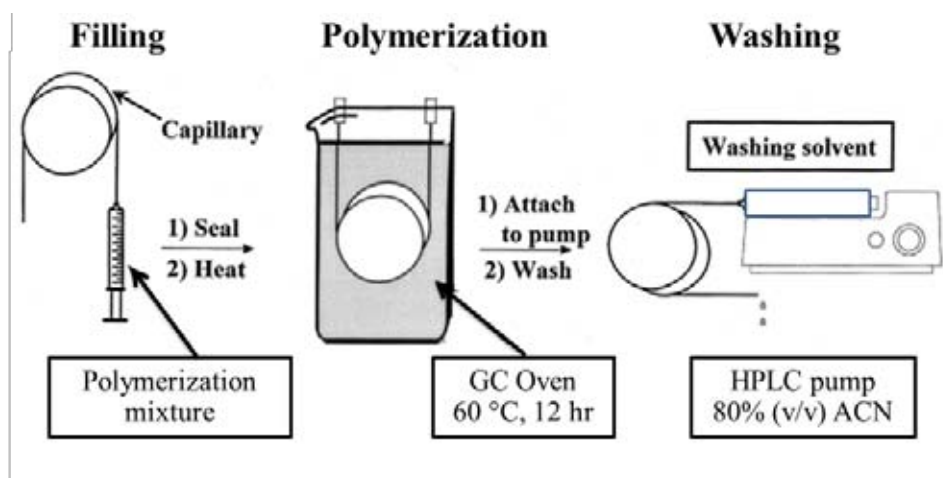
Figure 4.3 Schematic diagram of column fabrication. Adapted from Svec *et al.* [2000].

4.2.4 Preparation of mobile phase

The CEC mobile phase solutions were prepared by pipetting the appropriate amounts of stock aqueous solution of 100 mM phosphate buffer into a 25 mL volumetric flask, followed by adding appropriate volumes of ACN. Thereafter, the final solution was made up to 25 mL with DI water. All buffers were sonicated for 30 min prior to use. It should be note that the stock aqueous solution of 100 mM phosphate buffer was prepared by adjusting a phosphate buffer with a 1.0 M phosphoric acid or 1.0 M NaOH solution to desire pH.

4.2.5 Preparation of analytes

An appropriate amount of each analytes was separately dissolved in ACN in a 5 mL volumetric flask to give 0.1 M stock solutions. Stock solution of thiourea was also separately dissolved in DI water in a 5 mL volumetric flask to give 0.1 M stock solutions. Each protein was separately dissolved at a concentration of 5.0 mg/mL in DI water. The mixture of proteins at the concentration of 1.0 mg/mL was obtained by diluting 5.0 mg/mL of each proteins and and 1.0 mM thiourea, and then diluting the

mixture with a running mobile phase. Other working standard solutions of each set of test analytes containing 2.0 mM of each test analytes and 1.0 mM thiourea were also prepared by diluting each of the stock solutions with a running mobile phase. All solutions were sonicated for 10 min prior to CEC analysis.

The preparation of the samples of peptides was done by tryptic digestion of cytochrome *C* after reduction and alkylation following the Promega protocol. The stock solution of the digest protein was made in DI water before diluting it in a concentration of 1.0 mg/mL for CEC analysis.

4.3 Results and Discussion

4.3.1 Column fabrication and characterization

4.3.1.1 Porogens and monomers composition

Very recently, a neutral octadecyl monolith (ODM) with C18 chains for enhanced retention and selectivity has developed [Karenga, and El Rassi, 2008]. In their work, a ternary porogenic solvent made of cyclohexanol, ethylene glycol (EG), and water in the ratio 75.7: 20.7:3.6 wt% proved to be the optimal porogen to obtain an ODM monolith with reasonable EOF and high separation efficiency. Initially, in the present investigation, the C16 monolith was prepared by free radical polymerization using two different initiators, AIBN (1.0 wt% with respect to monomers) and nitric acid [Wang *et al.*, 2010] (0.06 mmol), and a ternary porogenic solvent introduced by Karenga and El Rassi [Karenga, and El Rassi, 2008] and made of cyclohexanol, EG, and water in the ratio 75.7: 20.7:3.6 wt% for the former initiator and in the ratio 82.5:14.9:2.5 wt% for the latter initiator. Using 30:70 %wt of monomers (functional monomer and PETA crosslinker) to porogen, the latter monolithic column with the nitric acid initiator provided high separation efficiency of 145,000 plates/m for benzene and ABs (Figure 4.4a), and up to 204,000 plates/m for proteins (Figure 4.4b), while the former column with the AIBN initiator gave very low permeability in a pressure driven flow and low separation efficiency in CEC. However, the latter

—

monolithic column (i.e. that prepared in the presence of nitric acid) was not stable, and therefore, AIBN was chosen as the free radical initiator for fabricating further columns throughout the study.

In an attempt to produce C8-, C12-, and C16- monolithic columns with acceptable permeability using a pressure driven flow, polymerization solutions with higher content in porogen in the ratio of monomers to porogen of 20:80 %wt were used. Table 4.1 shows the results of C8-, C12-, and C16- monolithic columns prepared using constant and different amounts (mmol) of the functional monomers (C8, C12 and C16 acrylate or methacrylate monomers) and the crosslinking monomer PETA. On the other hand, the optimum composition of the ternary porogenic solvent was determined by increasing the %wt of macroporogen EG while decreasing the %wt of microporogen cyclohexanol. These attempts resulted in the monoliths with higher separation efficiency in CEC and higher permeability using a pressure driven flow. The optimal column efficiency and reasonable EOF were obtained with a porogen composed of 68.8 wt% cyclohexanol, 27.7 wt% EG, and 3.6 wt% water. The C8-, C12-, and C16- monoliths prepared from variable monomer composition are referred to as 1A, 2A, and 3A columns (the A columns series), respectively, the details are shown in Table 4.1. The amount of functional monomer for the A monoliths series was increased in the order C8 > C12 > C16, resulting in the slightly higher retention factor (k) of ABs on C8 and C12 than on C16. The longer alkyl chain length monolith yielded the higher separation efficiency. Figure 4.5 a shows the EOF velocity increased with increasing the macroporogen content (i.e. EG content) of the monolith most likely due to the reduction of the electric double layers overlap as a result of the increased macroporosity of the monoliths. As shown in Table 4.1 and Figure 4.5a, the shorter the alkyl chain length, the higher the EOF velocity. This indicates stronger mobile phase ions adsorption as the alkyl chain length decreases. As can be seen in Figure 4.5b, increasing the macroporogen content in the polymerization mixture increases the separation efficiency. This may be due to increasing the monolith pore size with higher macroporogen content that leads to reducing the mass transfer resistance and consequently increasing the separation efficiency. It should be noted that in the A columns series, the compositions of the monomers were adjusted to yield

a chromatographic retention of more or less the same order of magnitude, see Table 4.1.

Another set of the C 8-, C 12-, and C 16- monoliths was prepared by keeping the composition of the functional monomers and the crosslinker PETA constant, and the resulting monoliths are referred to as 1B, 2B, and 3B columns (the B columns series), respectively (see Table 4.1). In all cases, the porogen was composed of 72.8 wt% cyclohexanol, 23.7 wt% EG, and 3.6 wt% water. The k values of ABs increased with increasing the alkyl chain length as in principle should be the case. As shown in Table 4.1, the separation efficiency obtained on the monolithic columns with the same composition of the polymerization mixture (i.e. the B columns series) was lower than that of the variable ones (i.e. the A columns series). In the B columns series, the column made with the shorter alkyl chain length yielded higher separation efficiency than the longer one. This is due primarily to the fact that a shorter analysis time would allow less band spreading that arises from longitudinal molecular diffusion assuming that everything else has remained the same.
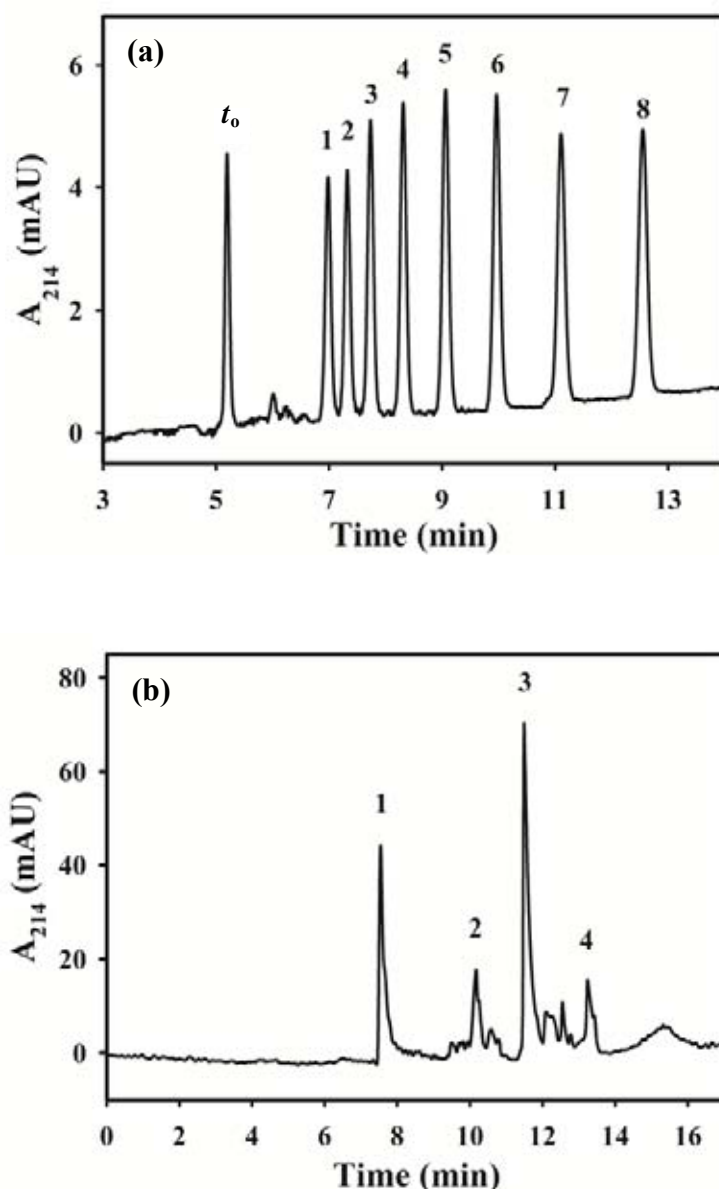
Figure 4.4 Electrochromatograms of benzene and AB homologous series in (a) and some standard proteins in (b). C16 capillary column for which nitric was used as initiator, 20 cm effective length, 27 cm total length × 100 μm i.d.; mobile phase, 1.0 mM in (a) and 10 mM in (b) sodium phosphate monobasic, pH 7.0, at 65 % ACN (v/v) in (a) and 45% ACN (v/v) in (b), running voltage 15 kV in (a) and 10 kV in (b); EOF tracer, thiourea; electrokinetic injection for 3 s at 10 kV. Solutes in (a): 1, benzene; 2, toluene; 3, ethylbenzene; 4, propylbenzene; 5, butylbenzene; 6, pentylbenzene; 7, hexylbenzene; 8, heptylbenzene. Solutes in (b): 1, lysozyme; 2, cytochrome *C*; 3, ribonuclease A; 4, α-chymotrypsin.
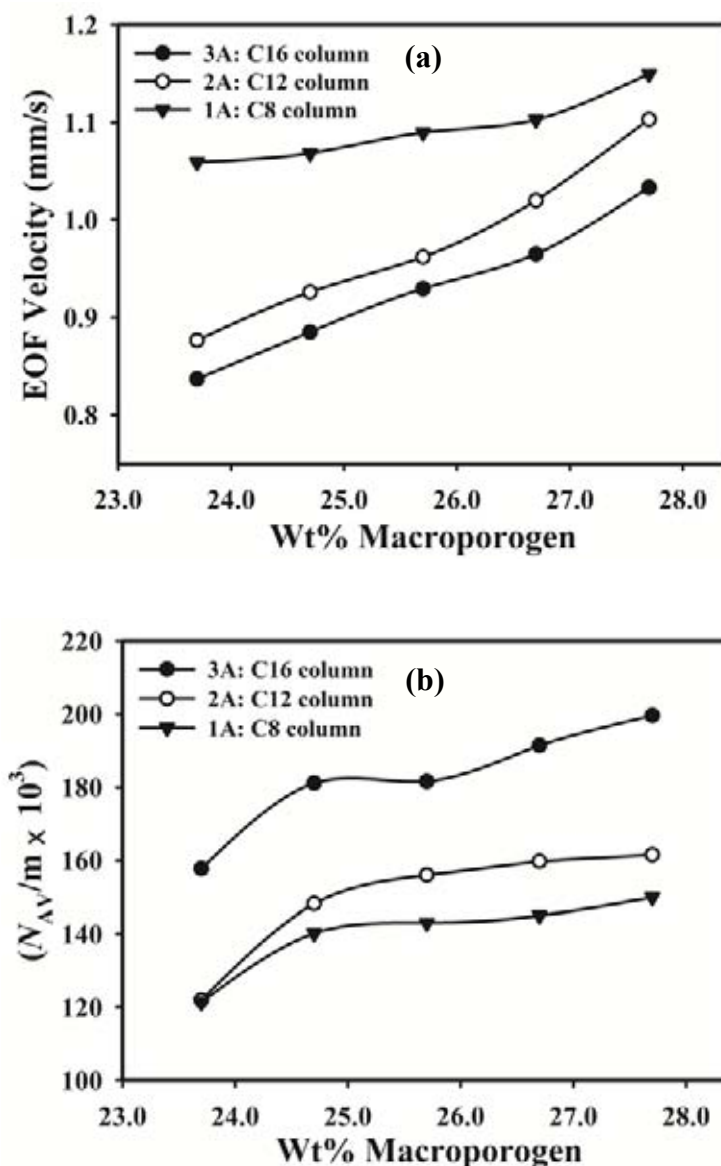
Figure 4. 5 Effect o f w t% m acroporogen i n t he pol ymerization s olution f or t hree monolithic columns prepared from polymerization solution at different *n*-alkyl chain length on the apparent EOF velocity in (a) and the average plate number per meter in (b). 1A, 2A, and 3A capillary columns, 20 cm effective length, 27 cm total length × 100 μm i.d.; m obile pha se, 1.0 m M sodium pho sphate m onobasic, pH 7.0, a t 75 % ACN (v/v), r unning vol tage 15 kV ; electrokinetic i njection f or 3 s a t 10 kV . The average p late n umber p er m eter i s t he av erage t aken f or benzene an d the first e ight AB homologous series: benzene, toluene, ethylbenzene, propylbenzene, butylbenzene, pentylbenzene, hexylbenzene, and heptylbenzene. EOF tracer, thiourea.

4.3.1.2 Van Deemter plots

The A columns series i.e. 1A, 2A and 3A columns were further evaluated in terms of the plate height versus linear flow velocity by varying the operating voltage from 8 to 25 kV. Figure 4.6 shows the van Deemter plots obtained with benzene and the first seven ABs series on the three monolithic columns at varying alkyl chains length in their polymeric networks (i.e. columns 1A, 2A, and 3A). Columns 1A, 2A and 3A were prepared from polymerization solutions at 0.58, 0.47, and 0.26 mmol functional monomers, respectively. The curves show that the H_{min} value has nearly stabilized over the velocity range from ~1.0 to ~1.5 mm/s, which corresponds to little or no variation in the separation efficiency over this linear flow velocity range. This may be an indication of an efficient solute mass transfer characteristic within the porous monoliths. The monolithic column 3A (C16 ligand) seems to be a good compromise as far as the efficiency and EOF velocity are concerned. This column exhibited the highest separation efficiency reaching a value of 209,000 plates/m at about 1.33 mm/s.
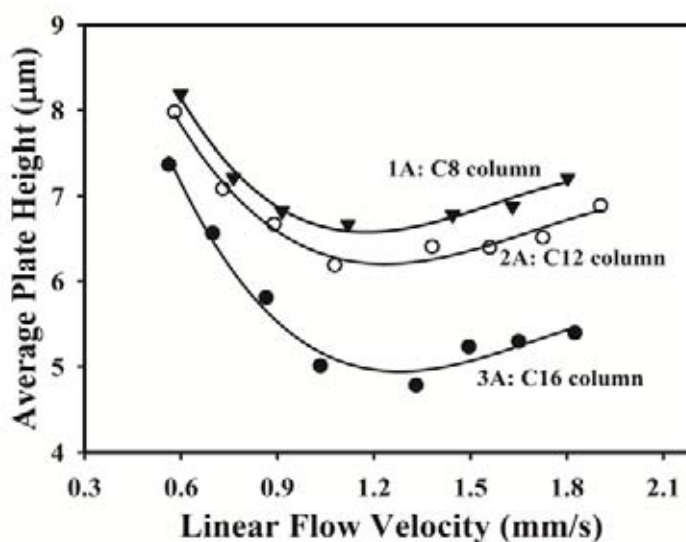
Figure 4.6 van Deemter plots showing average height as a function of apparent EOF velocity for 1A, 2A, and 3A capillary columns, 20 cm effective length, 27 cm total length × 100 μm i.d.; mobile phase, 1.0 mM sodium phosphate monobasic, pH 7.0, at 75 % ACN (v/v), electrokinetic injection for 3 s at 10 kV. The plate height is the average taken for the first eight AB homologous series: benzene, toluene, ethylbenzene, propylbenzene, butylbenzene, pentylbenzene, hexylbenzene, heptylbenzene. EOF tracer, thiourea.

4.3.1.3 Reproducibility of column fabrication

The reproducibility of column production was assessed through the percent relative standard deviation (%RSD) for the retention time of EOF marker (t_o), retention factor (k) of heptylbenzene, and the separation efficiency (N) of benzene and the first seven of the ABs series using a mobile phase containing 75% v/v ACN in 1.0 mM sodium phase buffer, pH 7.0. Table 4.2 shows the overall %RSD from column-to-column (n=3) for the EOF velocity, retention factor, and separation efficiency on columns 1A, 2A, and 3A. These reproducibility data agree with those previously reported for other monoliths [Karenga, and El Rassi, 2010a, 2010b].

Table 4.2 The overall %RSD from column-to-column ($n = 3$) of velocity (t_o), retention factor (k), and separation efficiency (N) reproducibilities.

Column	RSD (%)		
	t_o (min)	k	N (plates/m)
1A (C8)	2.3	4.1	11
2A (C12)	1.4	1.4	9.3
3A (C16)	2.1	2.3	10

4.3.1.4 The driving force of EOF

The A columns series are void of fixed charges, and therefore, they have no zeta potential with respect to water. As can be seen in Figure 4.7, the magnitude of the EOF depends on the pH and the ACN content of the mobile phase. This is indicative of the adsorption of electrolyte ions of the mobile phase to the monolithic surface, which imparts the monoliths with the zeta potential necessary to support the EOF. The ability of the monoliths to adsorb phosphate ions from the mobile phase can be traced to the presence of polar ester groups in the C8, C12, and C16 monomers and the crosslinker PETA as well as the hydroxyl group in PETA. Under the mobile phase conditions used, the direction of the EOF is from anode to cathode, indicating that the zeta potential is negative. Figure 4.7a shows the EOF is somewhat increased in the pH range 4.0 to 5.0 and then increased sharply at pH 5.0 to 7.0. In the pH range 5.0 to 7.0, the amount of the adsorbed phosphate ions are more ionized, carrying each

ion a double negative charge thus producing the sharp rise in EOF, while at pH 4.0 most of the phosphate ions have a single negative charge, thus explaining the relatively lower EOF. Good agreement was found between this observation and that reported earlier with C17, C18, and NMM neutral monoliths based on pentaerythritol diacrylate monostearate, octadecyl acrylate, and naphthyl methacrylate monomers, respectively [Okanda, and El Rassi, 2005; Karenga, and El Rassi, 2008, 2010b].

As can be seen from Figure 4.7b, the A columns series exhibited an increase in EOF velocity upon increasing the ACN content of the mobile phase due to an increases in phosphate ions adsorption to the monolithic surface. The shorter is the alkyl chain length the higher is the EOF velocity. This indicates stronger mobile phase ions adsorption as the alkyl chain length decreases. Despite the fact that increasing the ACN content decreases the dielectric constant of the mobile phase, which may diminish the ionization of the adsorbed phosphate ions, the concomitant decrease in the viscosity of the mobile phase and increase in the amount of adsorbed phosphate ions to the monolithic surface would be the two major contributors to increasing the EOF velocity at high ACN concentration in the mobile phase. It is believed that the adsorption of the phosphate ions to the monolith surface is of a polar type and the extent of which would increase with the ACN content of the mobile phase. This observation is similar to that previously reported with different neutral monoliths. [Okanda, and El Rassi, 2005; Karenga, and El Rassi, 2008, 2010a, 2010b, 2010c]

4.3.2 Evaluation of chromatographic retention

4.3.2.1 Neutral nonpolar solutes

The A columns series were evaluated for their performance with three homologous series including ABs, APKs, and NAs, which are typical model solutes of high, moderate, and low hydrophobic character, respectively. Figure 4.8 shows typical electrochromatograms for benzene and its alkyl derivatives which are the first seven ABs homologous series obtained on the three columns. Column 3A bearing the longest C16 chain on its surface yielded the highest theoretical plate count for the

separation of benzene and the first seven ABs series in less than 14 min. Under the same mobile phase composition and applied voltage, the magnitude of retention order was ABs > APKs > NAs, which is consistent with that of the hydrophobic order of the homologous ABs > APKs > NAs. In fact, whereas the rapid separation of AB's necessitated the use of 75% (v/v) ACN in the mobile phase, that of APKs and NAs required 70% (v/v) ACN and 35% (v/v) ACN in the mobile phase, respectively. Under these conditions, for APKs (up to heptanophenone) the analysis time was slightly less than 6.0 min on C16 column, and approximately 6.5 min on C8 and C12 columns while for NAs (up to nitrohexane) the analysis time was approximately 11.3 min on C16 column, approximately 11.5 min on C12 column and approximately 11.8 min on C8 column. These observations, which are indicative of a typical reversed phase chromatographic retention mechanism, were further confirmed by the linearity of the plots of logarithmic k (log k) versus % ACN in the mobile phase for ABs, APKs, and NAs over a wide range of ACN concentration on the 3A monolithic column, the results are shown in Figure 4.9. Furthermore, the magnitude order of k values ABs > APKs > NAs were in accordance to their relative hydrophobicity order ABs > APKs > NAs. This is another indicative of a reversed phase retention mechanism. The slopes of the lines in each set of solutes increased with increasing the size of the solute. These behaviors were also observed with 2A and 1A monoliths, results are shown in Figures 4.10 and 4.11, respectively. It should be noted that the amount of the functional monomers for the A series such as 1A, 2A, and 3A monoliths, increased in the order C8 > C12 > C16, and the shorter alkyl chain length the higher is the EOF velocity (see Figure 4.7). This explains the slightly higher k values or slightly longer separation time on C8 and C12 than on C16 monoliths. In short, a monolith with short alkyl chain (i.e. C8 or C12) at relatively high functional monomer content would accomplish as much retention as a longer alkyl chain length such as C16. But, this would be at the expense of lower separation efficiency. Therefore, and for difficult separations that would require high separation efficiency, one would consider a longer alkyl chain monolith at optimal functional monomer content (i.e. C16) with slightly lower retention and faster analysis time.
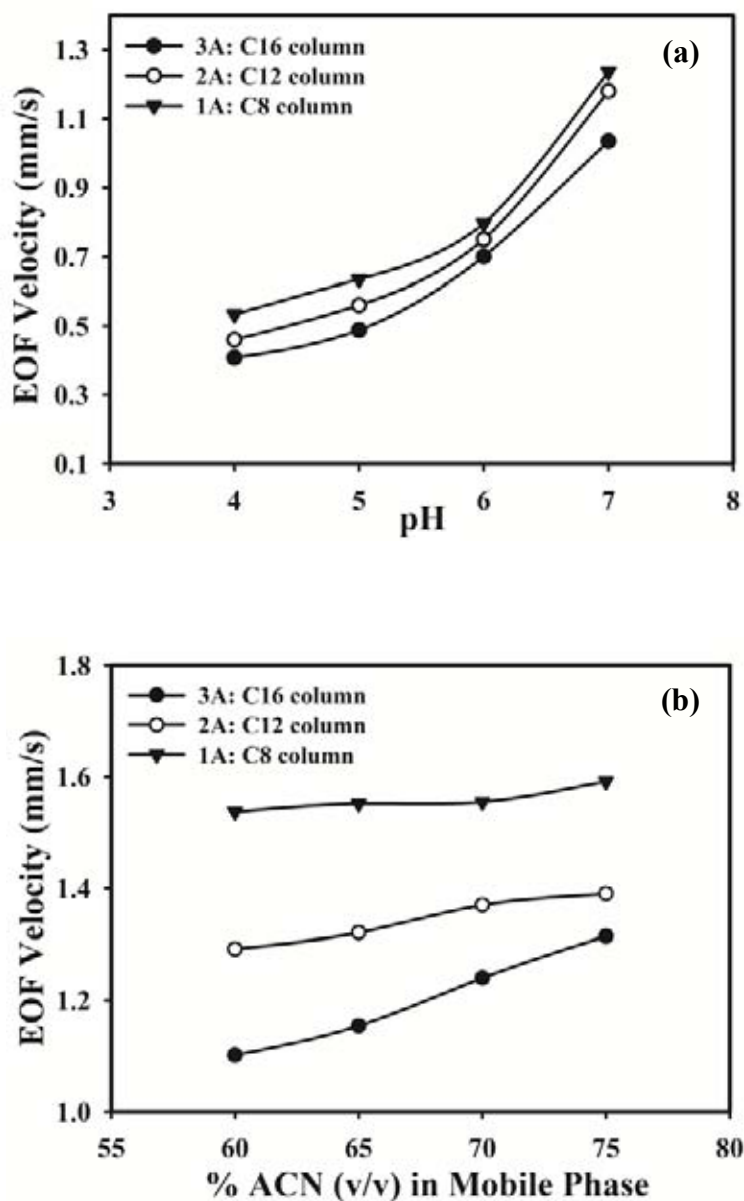
Figure 4.7 Plots of the apparent EOF velocity versus the pH of the mobile phase in (a) and the % ACN (v/v) in the mobile phase in (b) for 1A, 2A, and 3A monolithic columns, 20 cm effective length, 27 cm total length × 100 μm i.d.; mobile phase, 1.0 mM sodium phosphate monobasic at various pHs and 50 % ACN (v/v) in (a) and various % ACN (v/v) in 1.0 mM sodium phosphate monobasic, pH 7.0, in (b); running voltage 25 kV, electrokinetic injection for 3 s at 10 kV. EOF tracer, thiourea.
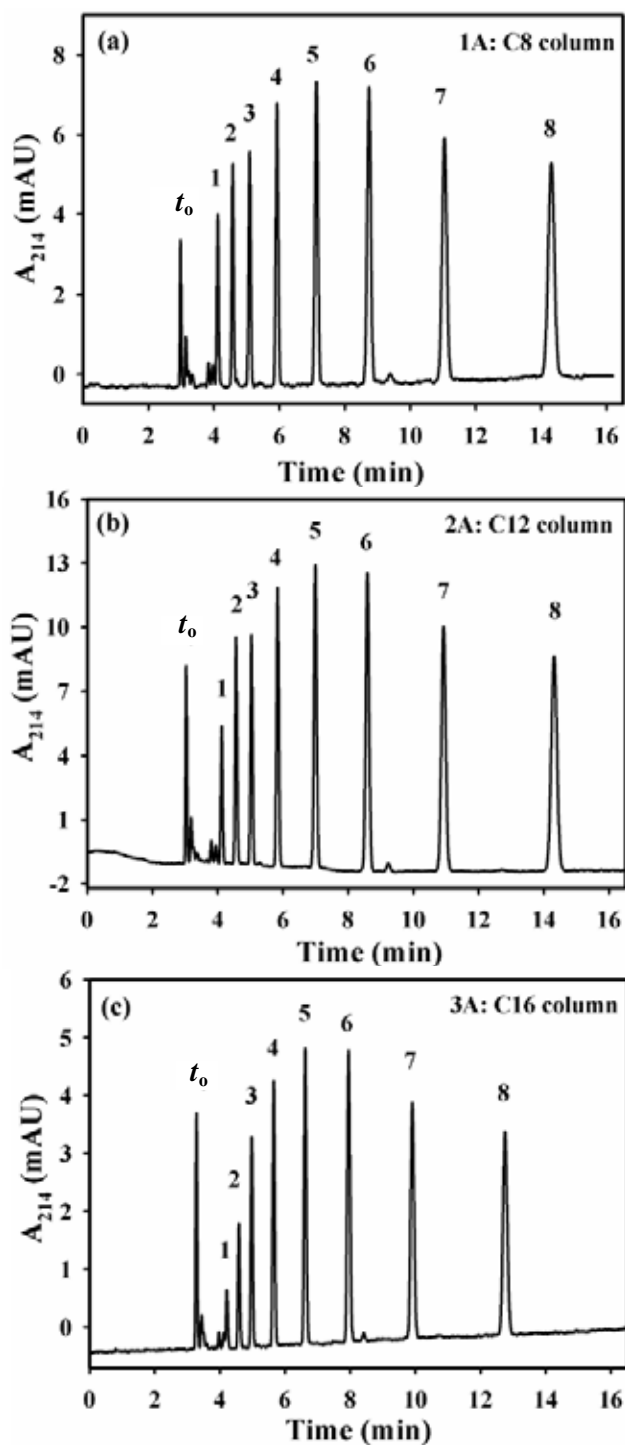
Figure 4.8 Electrochromatograms of benzene and AB homologous series using columns with different *n*-alkyl chain length, 20 cm effective length, 27 cm total length × 100 μm i.d., 1A: C8 column in (a), 2A: C12 column in (b) and 3A: C16 column in (c); mobile phase, 1.0 mM sodium phosphate monobasic, pH 7.0, at 75 % ACN (v/v), running voltage 15 kV; electrokinetic injection for 3 s at 10 kV. EOF tracer, thiourea, solutes: 1, benzene; 2, toluene; 3, ethylbenzene; 4, propylbenzene; 5, butylbenzene; 6, pentylbenzene; 7, hexylbenzene; 8, heptylbenzene.
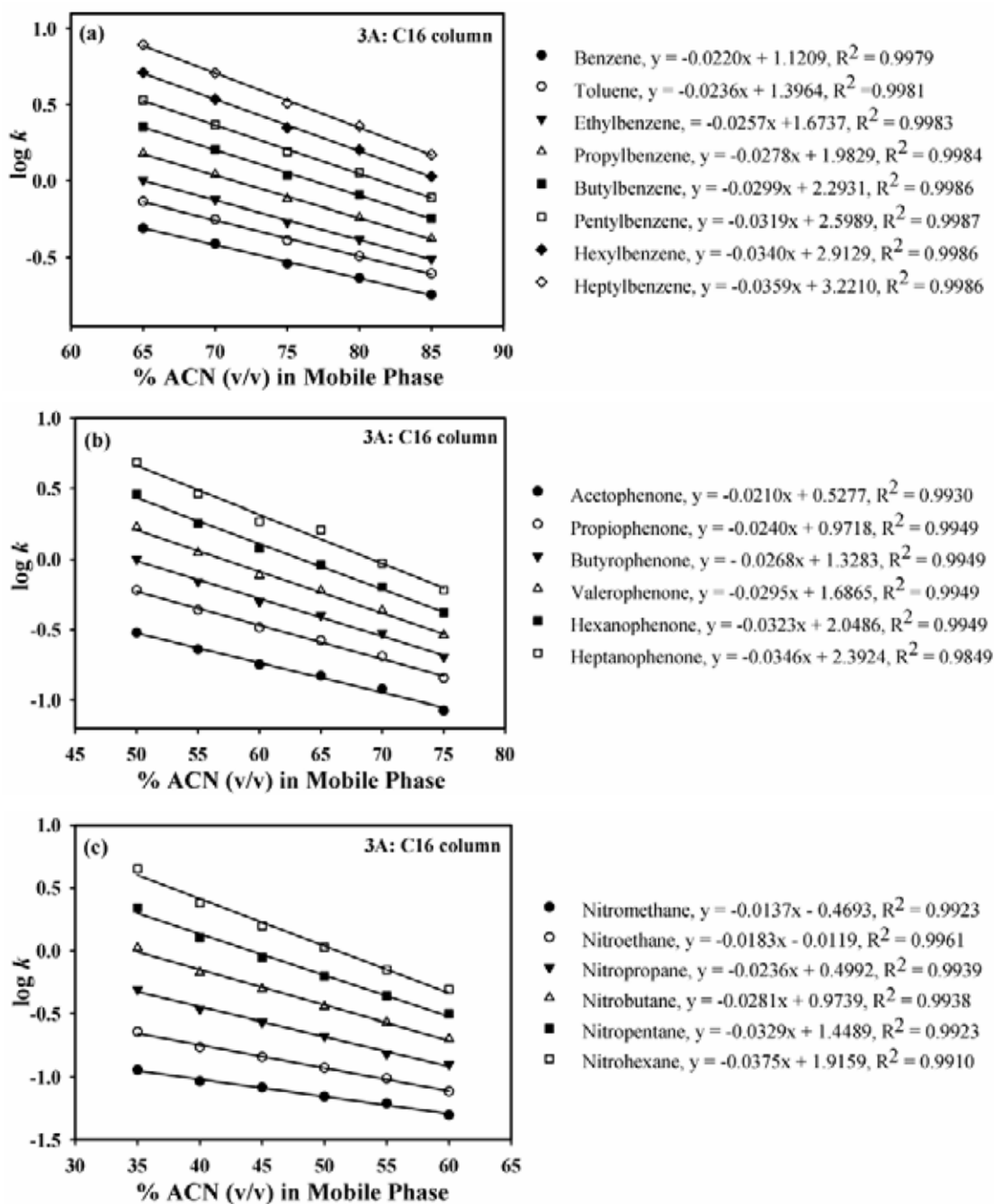
Figure 4.9 Plots of log *k* for (a) ABs, (b) APKs, and (c) NAs versus % ACN (v/v) in the mobile phase for 3A: C16 capillary column, 20 cm effective length, 27 cm total length × 100 μm i.d.; mobile phase, 1.0 m M sodium phosphate monobasic, pH 7.0, running voltage 25 kV, electrokinetic injection for 3 s at 10 kV. EOF tracer, thiourea. Solutes i n (a) 1, b enzene; 2, t oluene; 3, e thylbenzene; 4, pr opylbenzene; 5, butylbenzene; 6, pe ntylbenzene; 7, he xylbenzene; 8, he ptylbenzene; (b) 1, acetophenone; 2, pr opiophenone; 3, but yrophenone; 4, va lerophenone; 5, hexanophenone; 6, he ptanophenone; (c) 1, ni tromethane; 2, ni troethane; 3 , nitropropane; 4, nitrobutane; 5, nitropentane; and 6, nitrohexane.
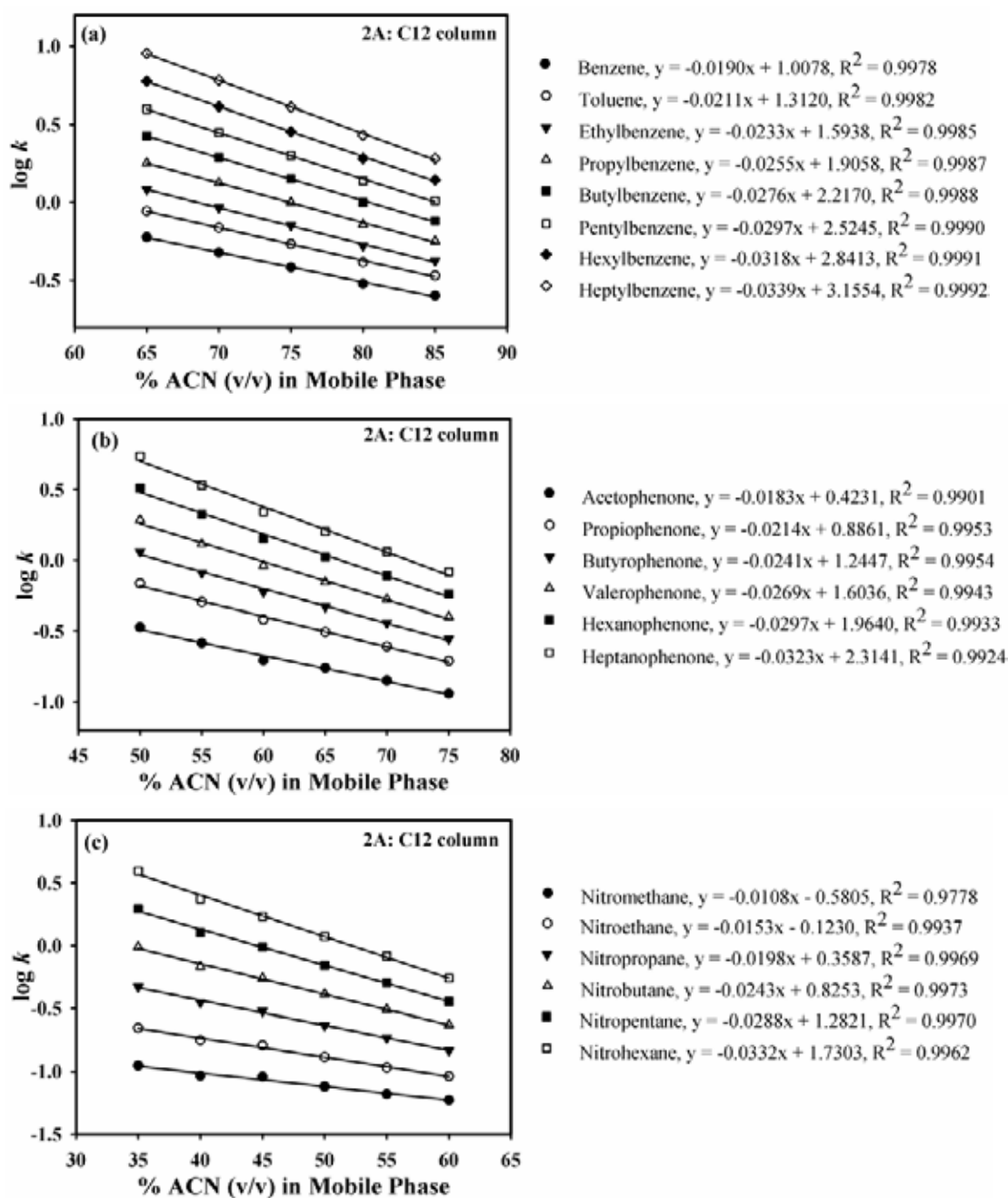
Figure 4.10 Plots of log *k* for (a) ABs, (b) APKs, and (c) NAs versus % ACN (v/v) in the mobile phase for 2A: C12 capillary column, 20 cm effective length, 27 cm total length × 100 μm i.d.; mobile phase, 1.0 m M sodium phosphate monobasic, pH 7.0, running voltage 25 kV, electrokinetic injection for 3 s at 10 kV. EOF tracer, thiourea. Solutes i n (a) 1, b enzene; 2, t oluene; 3, e thylbenzene; 4, pr opylbenzene; 5, butylbenzene; 6, pe ntylbenzene; 7, he xylbenzene; 8, he ptylbenzene; (b) 1, acetophenone; 2, pr opiophenone; 3, bu tyrophenone; 4, va lerophenone; 5, hexanophenone; 6, he ptanophenone.; (c) 1, ni tromethane; 2, ni troethane; 3, nitropropane; 4, nitrobutane; 5, nitropentane; and 6, nitrohexane.
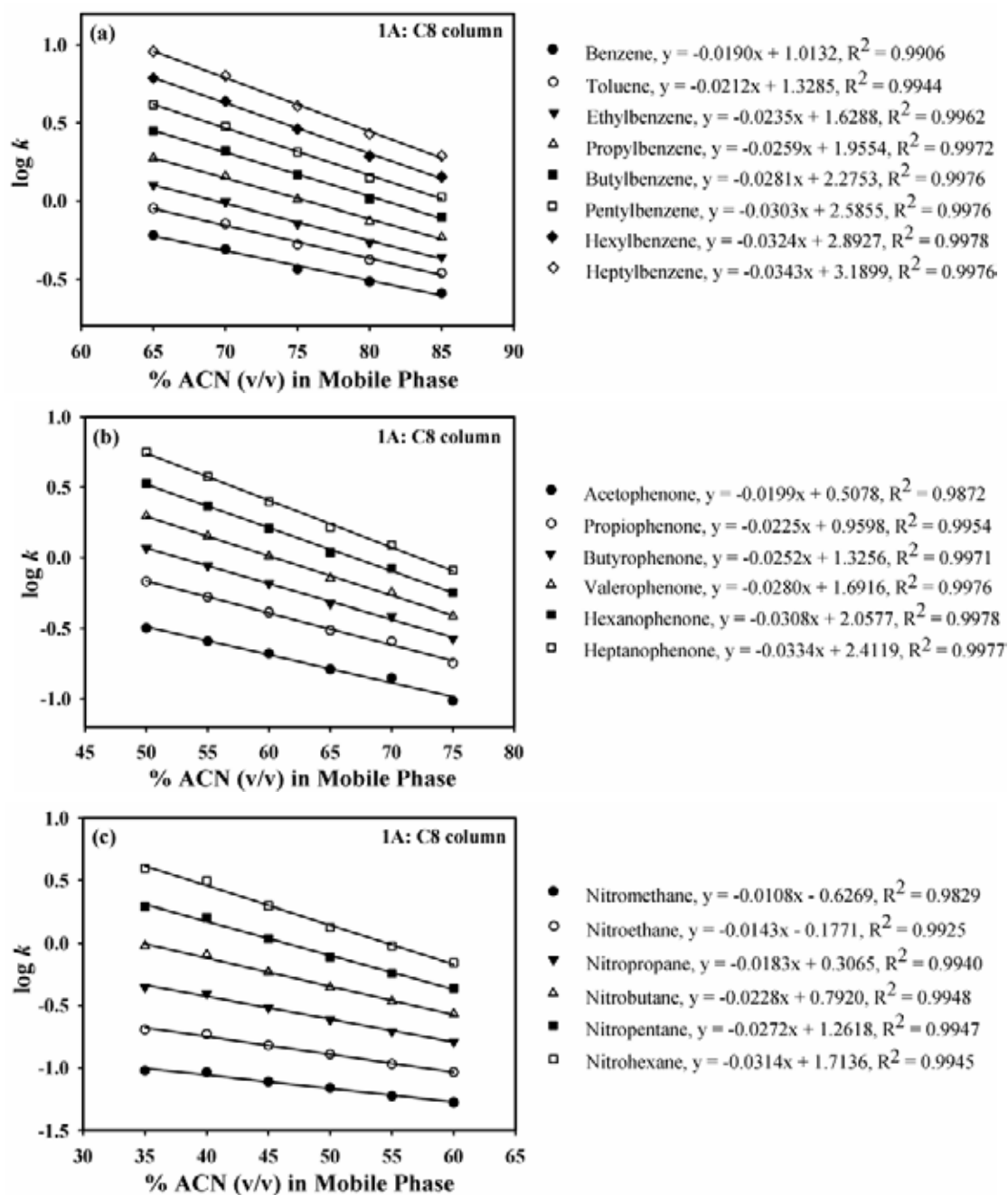
Figure 4.11 Plots of log *k* for (a) ABs, (b) APKs, and (c) NAs versus % ACN (v/v) in the mobile phase for 1A: C8 capillary column, 20 cm effective length, 27 cm total length × 100 μm i.d.; mobile phase, 1.0 mM sodium phosphate monobasic, pH 7.0, running voltage 25 kV, electrokinetic injection for 3 s at 10 kV. EOF tracer, thiourea. Solutes in (a) 1, benzene; 2, toluene; 3, ethylbenzene; 4, propylbenzene; 5, butylbenzene; 6, pentylbenzene; 7, hexylbenzene; 8, heptylbenzene; (b) 1, acetophenone; 2, propiophenone; 3, butyrophenone; 4, valerophenone; 5, hexanophenone; 6, heptanophenone.; (c) 1, nitromethane; 2, nitroethane; 3, nitropropane; 4, nitrobutane; 5, nitropentane; and 6, nitrohexane.

4.3.2.2 Slightly polar solutes

Figure 4.12 illustrates the separation of six phenols on the A columns series using a mobile phase at 50% v/v ACN for 1A column and 45% v/v ACN for 2A and 3A columns, and at pH 7.0 to bring about similar analysis time and base line resolution among the three columns. One of these phenols, namely 2,4-dichlorophenol (last eluting solute) with pK_a of 7.85, is very slightly ionized at the operating pH, while all other phenols under investigation with p$K_a \geq 8.5$ are largely undissociated and can be considered as neutral solutes. 2,4-Dichlorophenol seems to broaden (noticeably on the 1A column) may be due to its relatively higher migration time, which would translate into increased longitudinal molecular diffusion. The phenols investigated eluted in the order of decreasing polarity on the three columns, a behavior that is typical of RP-CEC. For instance, phenol and hydroxyphenol (i.e. quinol < phenol) are less retained than monochlorophenols (4-chlorophenol < 3-chlorophenol) and 2,4-dichlorophenol.

Another class of slightly polar solutes consisting of seven anilines including aniline (pK_a = 4.70), 3-methylaniline (pK_a = 4.91), 4-isopropylaniline (pK_a = 5.0), 4-chloroaniline (pK_a = 4.06), 4-bromoaniline (pK_a = 3.86), 3-chloro-4-methylaniline (pK_a = 4.05), and 3,4-dichloroaniline (pK_a = 3.33), were used to evaluate the retention property of the A columns series. The seven anilines were baseline separated in ca. 12 min on the 1A, 2A, and 3A columns (see Figure 4.13) at 45 % v/v ACN in the mobile phase affording a theoretical plate count of 96,000, 108,000, and 108,000 plates/m, respectively. The elution order of the anilines on 1A, 2A and, 3A columns was the same, and in the order of increasing of nonpolar character of the solutes. This retention behavior is typical to RP-CEC where halogenated anilines are more retained than methyl-substituted anilines and di-substituted anilines are more retained than mono-substituted anilines.
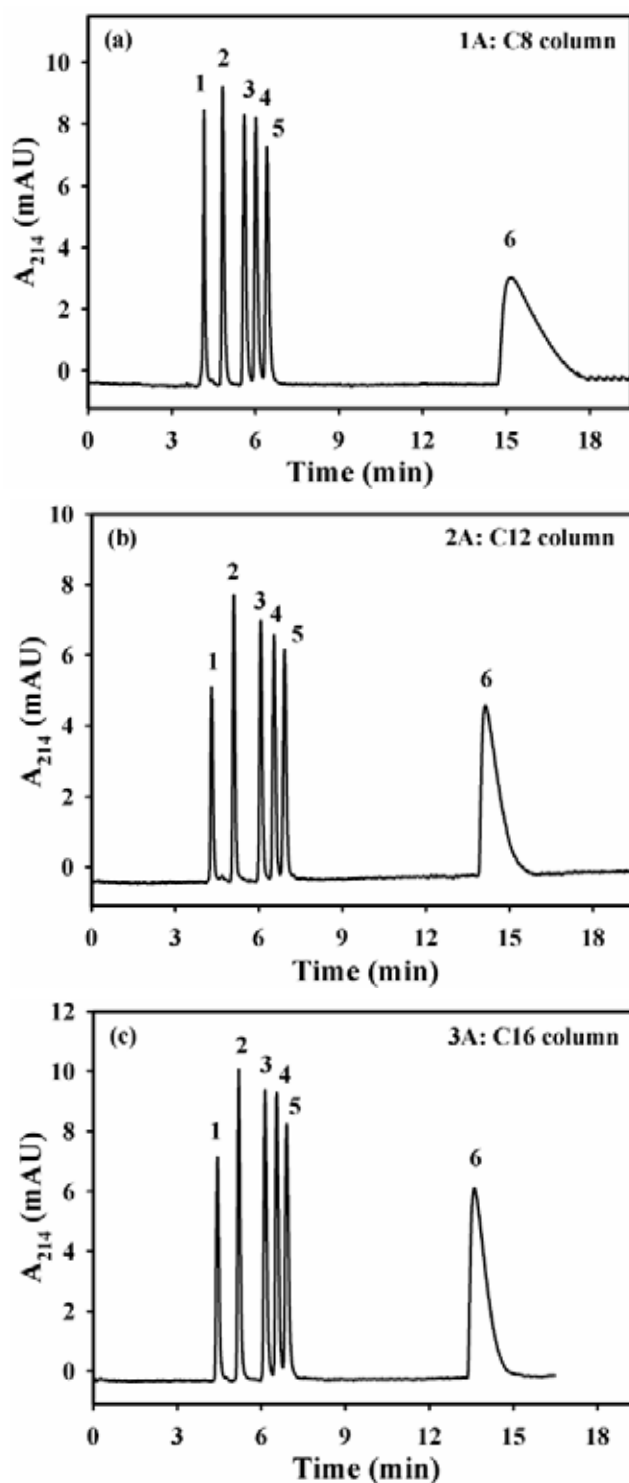
Figure 4. 12 Electrochromatograms of s ome p henols f or t hree c olumns, 20 c m effective le ngth, 2 7 c m total le ngth × 100 μm i.d., 1A: C 8 c olumn i n (a), 2A : C 12 column in (b) and 3A: C 16 column in (c); hydro-organic mobile phase at 50 % ACN (v/v) in (a), 45 % ACN (v/v) in (b and c); 1.0 mM sodium phosphate, pH 7.0; running voltage 15 kV; electrokinetic injection for 3 s at 10 kV. Solutes: 1, quinol; 2, phenol; 3, 3,4-dimethylphenol; 4, 4-chlorophenol; 5,3-chlorophenol; 6, 2,4-dichlorophenol.
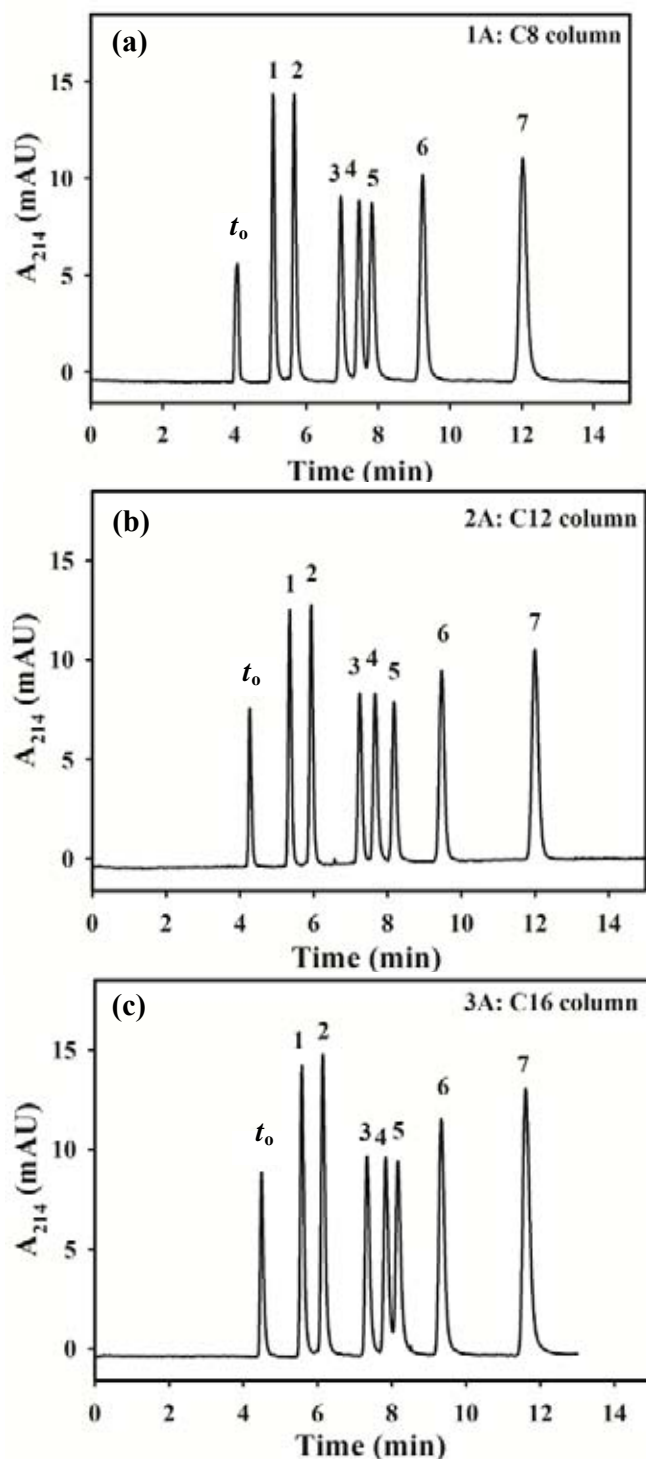
Figure 4. 13 Electrochromatograms of s ome a nilines f or t hree columns, 20 c m effective le ngth, 2 7 c m total le ngth × 100 μm i.d., 1A: C 8 c olumn i n (a), 2A: C 12 column in (b) and 3A: C 16 column in (c); hydro-organic mobile phase at 45 % ACN (v/v), 1.0 m M sodium phos phate, pH 7.0; r unning vol tage 15 kV ;electrokinetic injection f or 3 s a t 10 kV . EOF t racer, t hiourea. Solutes: 1, a niline; 2, 3 - methylaniline; 3 , 4-chloroaniline; 4, 4 -isopropylaniline; 5, 4-bromoaniline; 6, 3 - chloro-4-methylaniline; 7, 3,4-dichloroaniline.

4.3.2.3 Peptides and proteins

The B monolithic columns series were further evaluated in the separation of polyionic solutes such as proteins and tryptic peptide mapping whose retention is based on their electrophoretic migration and chromatographic partitioning. Figure 4.14 shows the separation of four standard proteins of various sizes and charges (i.e. isoelectric points, pIs), namely lysozyme (pI = 11.1), cytochrome C (pI = 10.2), ribonuclease A (pI = 9.3), and ovalbumin (pI = 4.7) obtained on the B columns series, using a hydro-organic mobile phase consisting of 10 mM sodium phosphate, pH 7.0 at 45% (v/v) ACN. As can be seen in Figure 4.14a-c, the proteins migrated in the order of decreasing pI values with the most acidic protein (ovalbumin) eluting last while the most basic protein (lysozyme) eluted first. On the 1B column, the four proteins were eluted in 14.8 min with an average theoretical plate count of 332,000 plates/m, while on 2B and 3B columns, the four proteins were eluted at about 18 min with an average theoretical plate count of 236,000 and 225,000 plates/m, respectively. The observed cathodal EOF velocity under the condition used was about 0.39, 0.34, and 0.32 mm/s on 1B, 2B, and 3B, respectively. The slight decrease in the EOF velocity when going from C8 to C16 corroborates with the slight increase in the analysis time in the order C16 ≥ C12 > C8. In comparison with 2B and 3B monoliths, the 1B monolith seems to be the best column for the separation of the four standard proteins under investigation with the highest separation efficiency and the shortest analysis time (see Figure 4.14a). Kinetically speaking, for large molecules such as proteins, energetically "softer" surfaces such as C8 would allow faster sorption kinetics and in turn improved efficiency. Thus, a short alkyl chain monolith such as C8 at sufficient surface ligand density (i.e. 1B column) is preferred for protein separation.

In addition, the monoliths prepared from polymerization mixtures at the same amount of functional monomer (i.e. the B monoliths series) performed better in protein separation than the A monolithic series. The A columns series gave broad peaks and much longer analysis time (results not shown). This may be due to the pore morphology.

In another s et of experiments, a c omplex p eptide mix ture c onsisting o f th e tr yptic digest of cytochrome *C* was separated on the B columns series. Figure 4.15 shows the tryptic peptide map of cytochrome *C* obtained on the B columns series using a hydro-organic m obile pha se c ontaining 35% (v/v) A CN i n 10 m M s odium phos phate concentration, pH 6.0. Increasing t he phos phate i on c oncentration i n t he m obile phase t o 15 m M a nd 20 m M di d not i mprove t he pe ptide m ap pr ofile i n t erms of resolution among the various peaks but resulted in decreasing substantially the EOF velocity a nd c onsequently i ncreasing t he an alysis t ime, results are shown in Figure 4.16. This behavior is due to the decrease in the thickness of the electric double layer at the liquid-solid interface as the ionic strength is increased. For instance, the EOF velocity decreased from 0.16 mm/s at 10 m M sodium phosphate to 0.13 mm/s at 15 mM, and to 0.12 mm/s at 20 mM on the C16 column (i.e. 3B column). Increasing the % ACN in the mobile phase from 35% to 45% (v/v) increased the EOF velocity by a factor o f approximately 1.2, 1.5 and 1.3 on C 8, C 12 a nd C 16, respectively, but resulted in decreasing the overall resolution of the CEC systems, results are shown in Figure 4.17. As can be seen in Figure 4.18, keeping the ACN content of the mobile phase at 35% (v/v) and that of the sodium phosphate at 10 mM, but decreasing the pH of t he m obile pha se from 6.0 t o 4.0 de creased t he a nalysis t ime b y m ore t han 50%. Although de creasing t he pH of t he m obile p hase de creased t he E OF ve locity substantially, the fact that decreasing the pH of the mobile phase increases the amount of pos itive c harges on t he pe ptide fragments r esulted i n de creasing the pe ptide m ap retention.

Although, t he obs erved c athodal E OF unde r a ll c onditions us ed f or pr oteins a nd peptide mapping separation is very small and not strong, proteins and peptides eluted from t he B c olumns series i n a few m inutes. This m ay in dicate th at th e chromatographic partitioning contribution to proteins and peptides migration is much less i n m agnitude t han t he e lectrophoretic contribution. Figure 4.1 9a s hows t he separation of tryptic peptide mapping of cytochrome *C* on 3B column using a hydro-organic m obile ph ase c ontaining 10 m M s odium phos phate, pH 6.0 a t 35% (v/v) ACN, and a running voltage of 10 k V, the peptide fragments were eluted in 23 m in. The r emaining p eptide f ragments w ere completely el uted in 7 m in (Figure 4.1 9b)

using reversed polarity at the same mobile phase compositions. Using the same CEC conditions as Figure 4.19, the separation of cytochrome *C* tryptic map on 3A column was examined, resulting in the peptide fragments eluted in 30 min and the remaining peptide fragments eluted in 6 min using reversed polarity as shown in Figure 4.20. The 3A monolith, which prepared from polymerization mixtures at the optimal amount of functional monomer (Figure 4.20) performed better in cytochrome *C* tryptic map separation than those at the same amount of functional monomer, 3B monolith (Figure 4.19).

Furthermore, the A columns series were also evaluated in the separation of cytochrome *C* tryptic digest using the same elution conditions as in Figure 4.15. As can be seen in Figure 4.21a-c, the shorter the alkyl chain length of the functional monomer, the higher is the EOF velocity. In comparison with 1A and 2A monoliths, the 3A monolith seems to be the best column for the separation of cytochrome *C* tryptic digest (see Figure 4.21c). In short, while an energetically soft surface (C8-monolith) is optimal for protein separation, an energetically "harder" surface (C16-monolith) is more favorable for the separation of smaller size solutes such as peptides.
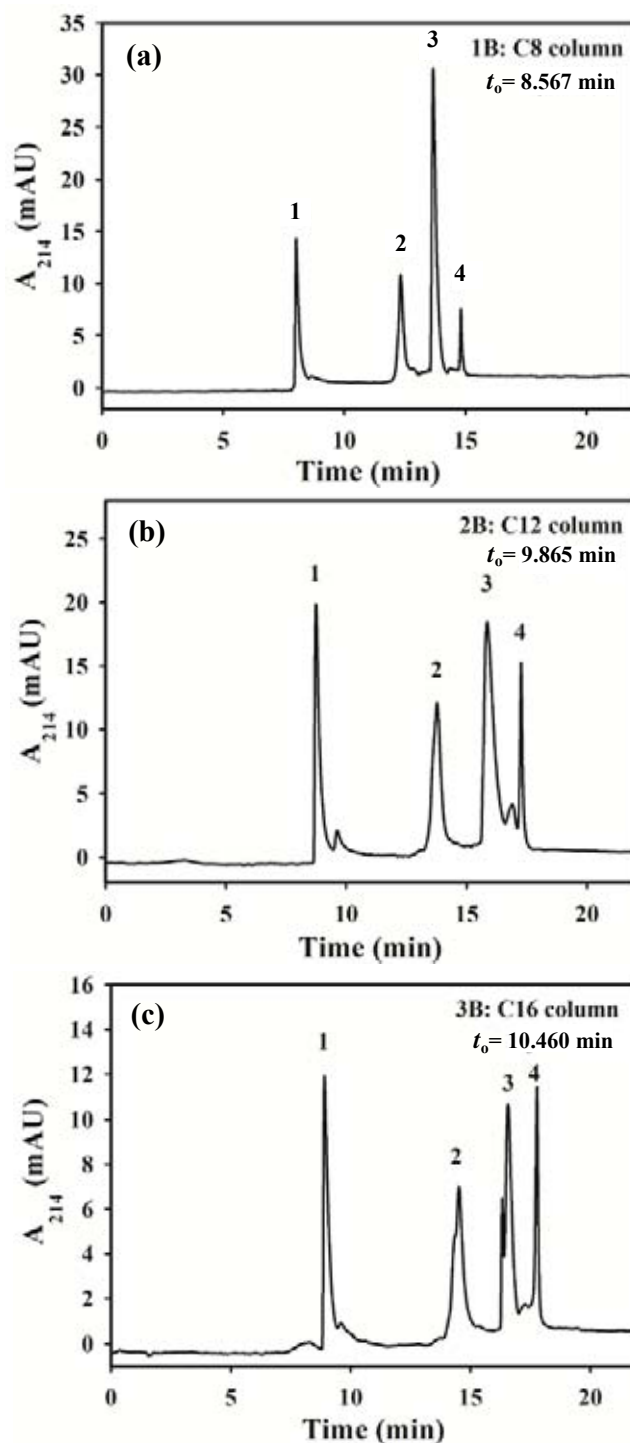
Figure 4.14 Electrochromatograms of some standard proteins for three monolithic capillary columns prepared from polymerization solution at different *n*-alkyl chain length, 20 cm effective length, 27 cm total length × 100 μm i.d., 1B: C8 column in (a), 2B: C12 column in (b) and 3B: C16 column in (c); mobile phase, 10 mM sodium phosphate monobasic, pH 7.0, at 45% ACN (v/v), running voltage 10 kV, electrokinetic injection for 3 s at 10 kV; EOF tracer, thiourea; solutes: 1, lysozyme; 2, cytochrome *C*; 3, ribonuclease A; 4, ovalbumin.
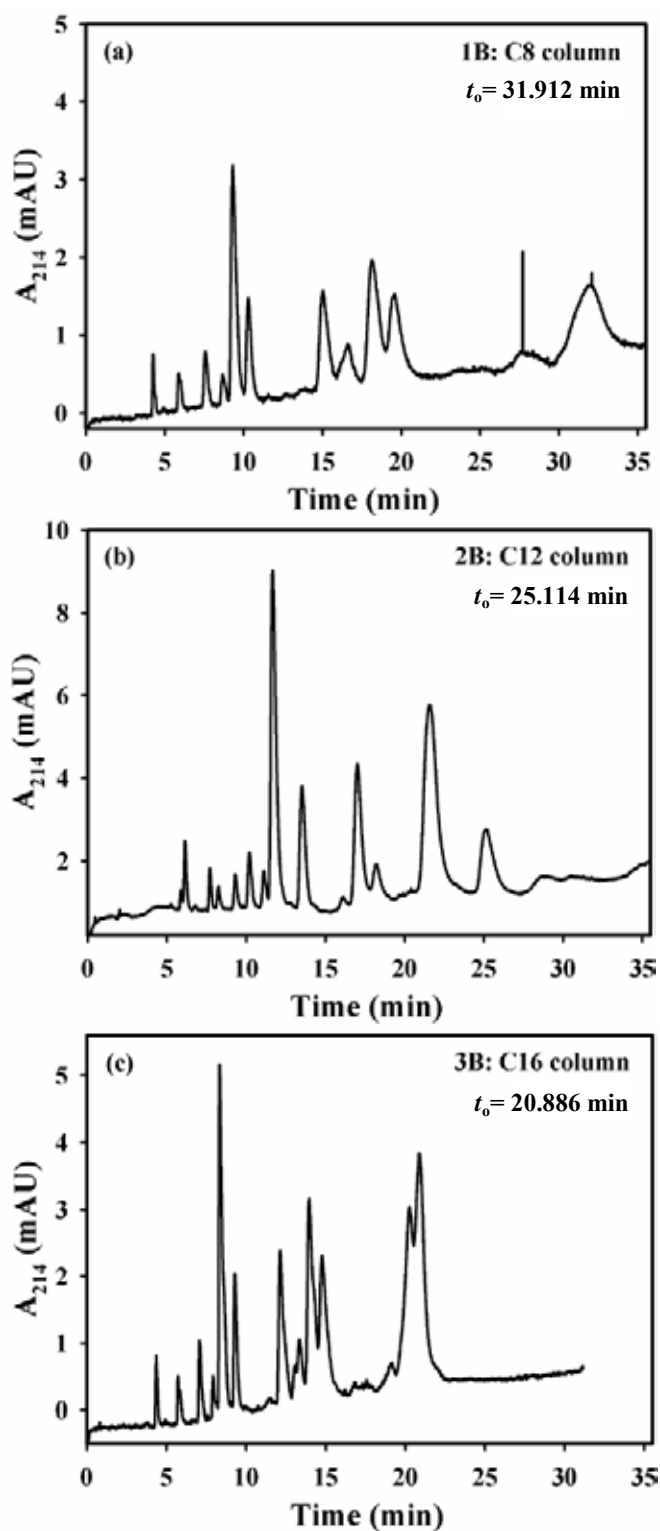
Figure 4.1 5 Electrochromatograms o f th e tr yptic d igest o f cytochrome *C*. 1B: C 8 column in (a), 2B : C 12 column in (b) a nd 3 B: C 16 column i n (c), 20 c m e ffective length, 27 cm t otal l ength × 100 μm i.d.; h ydro-organic mobile ph ase, 35 % A CN (v/v), 10 m M i n s odium phos phate m onobasic, pH 6.0, r unning vol tage 10 kV ; electrokinetic injection for 5 s at 10 kV.
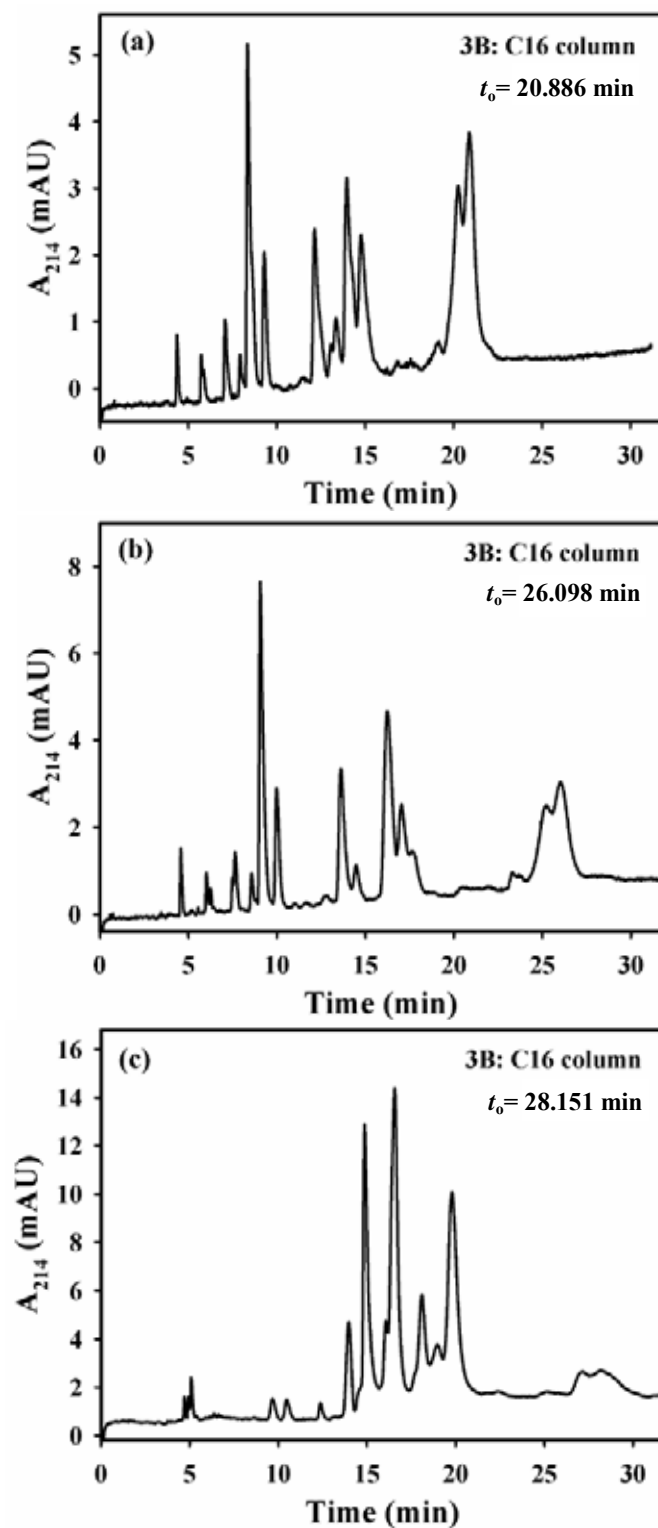
Figure 4.1 6 Electropherograms of t he t ryptic digest of c ytochrome *C*. 3 B: C 16 capillary c olumn, 2 0 c m e ffective le ngth, 2 7 c m to tal le ngth × 100 µm i.d.; hy dro-organic mobile phase, 35 % ACN (v/v), 10 mM in (a), 15 mM in (b), and 20 mM in (c) s odium phos phate monobasic, pH 6.0, running vol tage 10 kV , electrokinetic injection for 5 s at 10 kV.
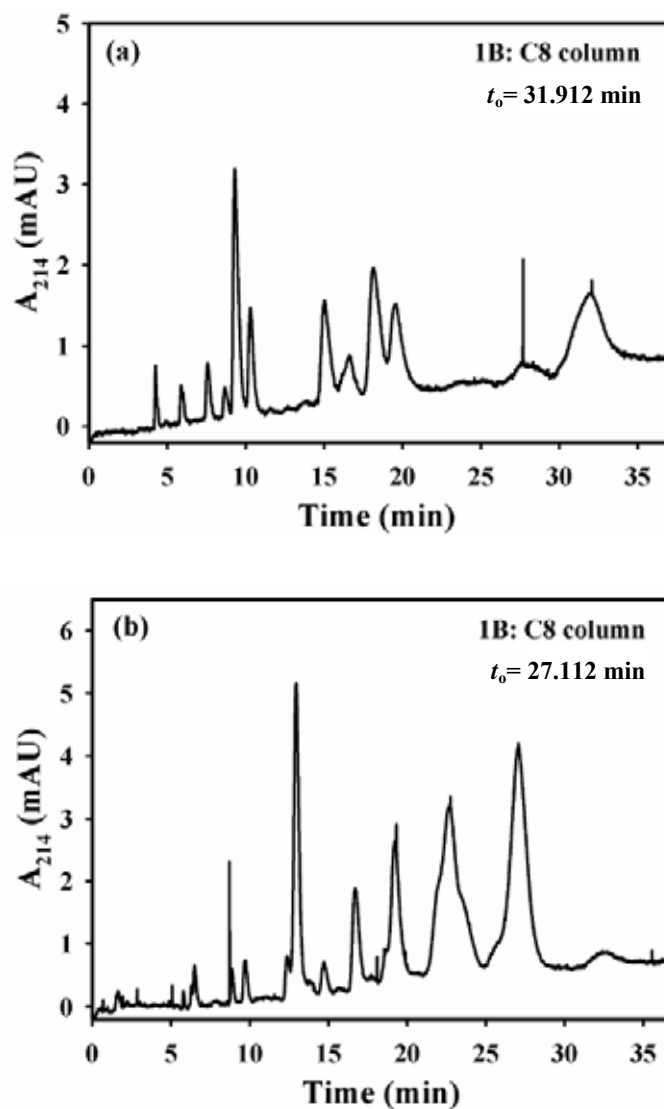
Figure 4.1 7 Electropherograms of t he t ryptic digest o f c ytochrome *C* for t hree monolithic c apillary c olumns pr epared f rom p olymerization s olution a t di fferent *n*-alkyl chain length, 20 cm effective length, 27 cm total length × 100 μm i.d., 1B: C8 column in (a and b), 2B: C12 column in (c and d) and 3B: C16 column in (e and f); hydro-organic mobile phase at 35 % ACN (v/v) in (a, c, and e) and 45 % ACN (v/v) in (b, d, a nd f), 10 mM s odium phos phate, pH 6.0 , r unning vol tage 10 kV , electrokinetic injection for 5 s at 10 kV.
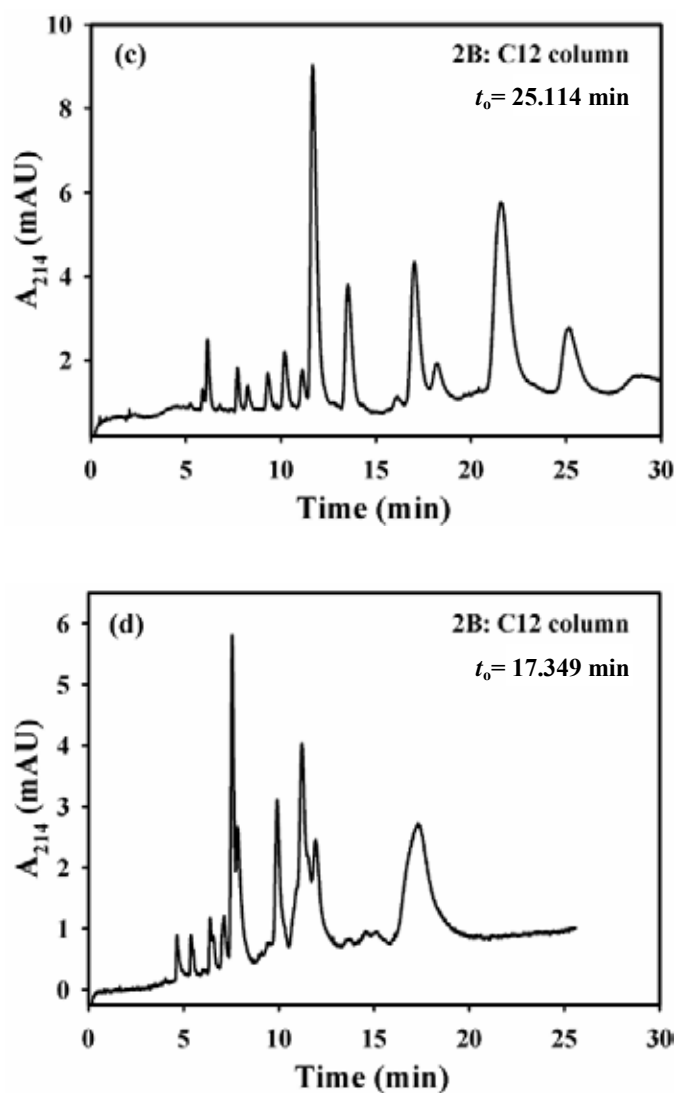
Figure 4.17 Continued. Electropherograms of the tryptic digest of cytochrome *C* for 2B: C12 monolithic column, 20 cm effective length, 27 cm total length × 100 μm i.d.; hydro-organic mobile phase at 35 % ACN (v/v) in (c) and 45 % ACN (v/v) in (d), 10 mM sodium phosphate, pH 6.0, running voltage 10 kV, electrokinetic injection for 5 s at 10 kV.
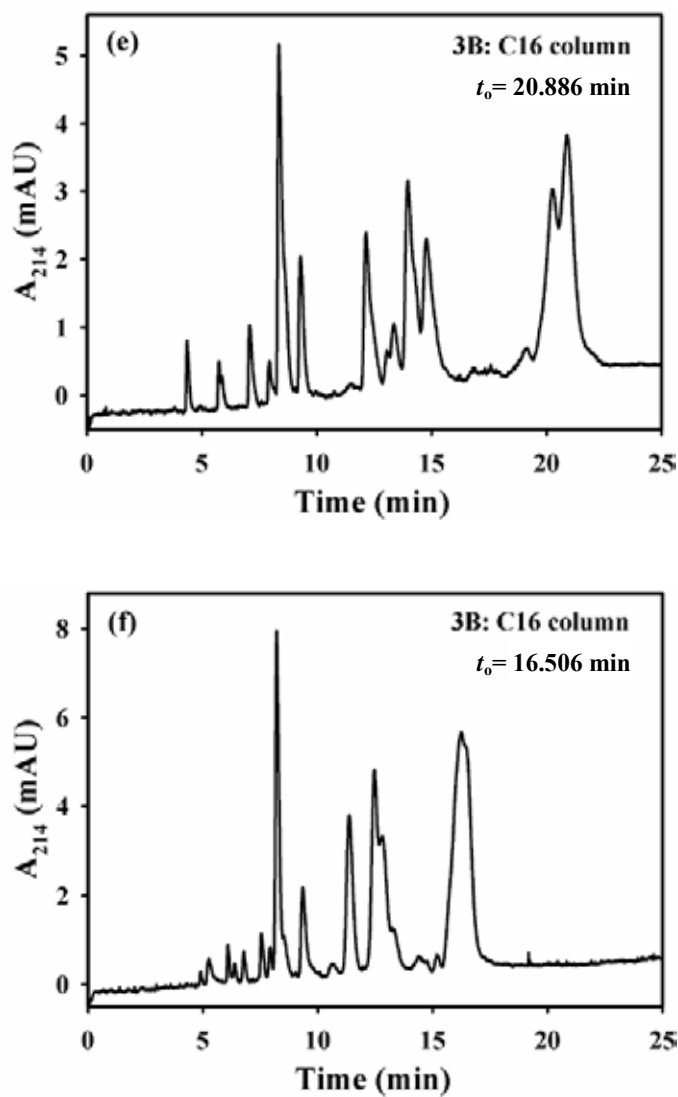
Figure 4.17 Continued. Electropherograms of the tryptic digest of cytochrome *C* for 3B: C16 monolithic column, 20 cm effective length, 27 cm total length × 100 μm i.d.; hydro-organic mobile phase at 35 % ACN (v/v) in (e) and 45 % ACN (v/v) in (f), 10 mM sodium phosphate, pH 6.0, running voltage 10 kV, electrokinetic injection for 5 s at 10 kV.
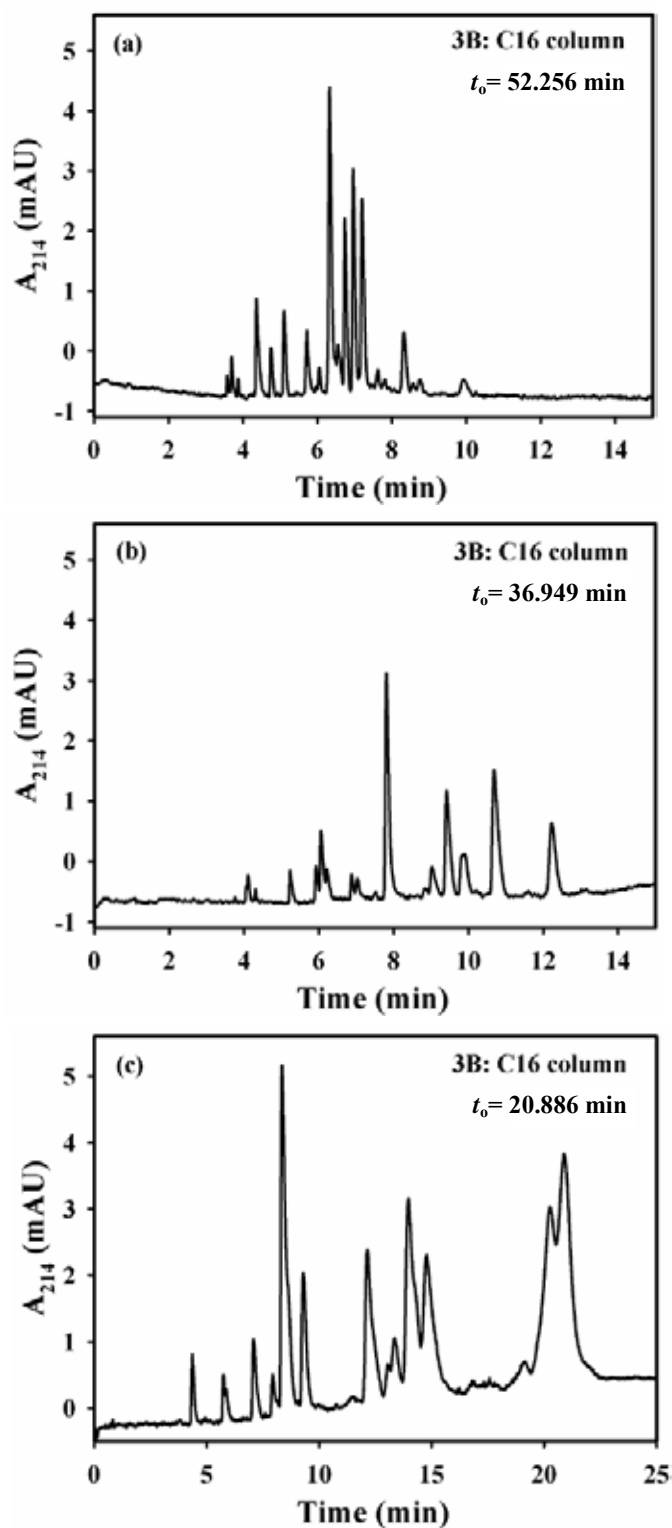
Figure 4.18 Electrochromatograms of the tryptic digest of cytochrome *C*. 3B: C16 capillary column, 20 cm effective length, 27 cm total length × 100 µm i.d.; hydro-organic mobile phase, 35 % ACN (v/v), 10 mM sodium phosphate monobasic, pH 4.0 in (a), pH 5.0 in (b) and pH 6.0 in (c), running voltage 10 kV, electrokinetic injection for 5 s at 10 kV.
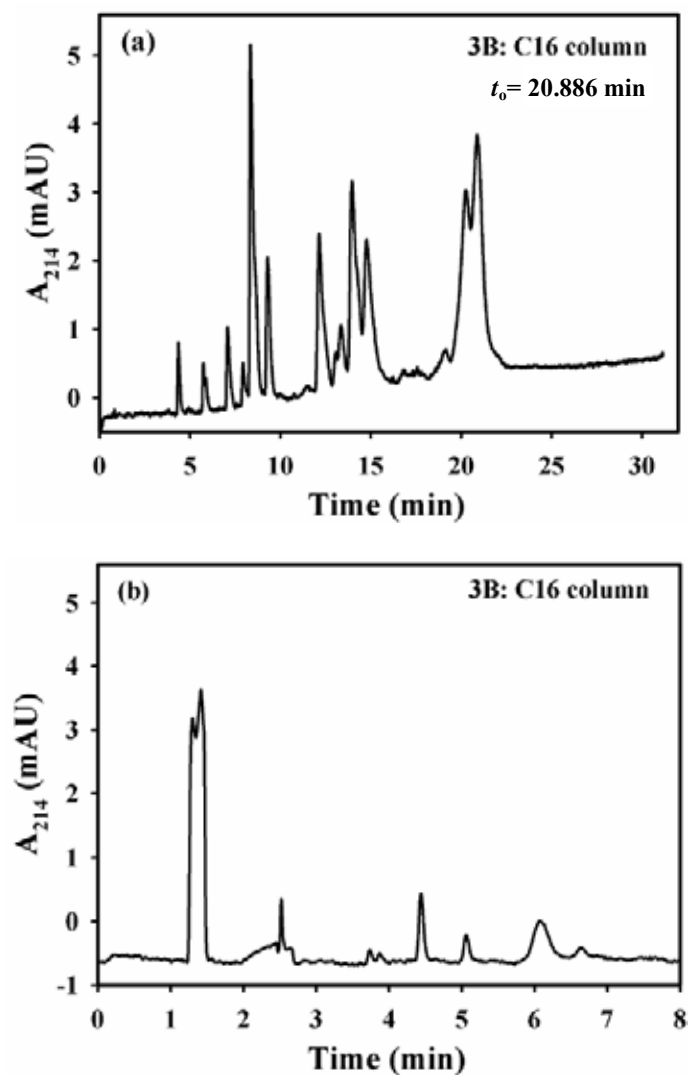
Figure 4.19 Electrochromatograms o f th e tr yptic d igest o f c ytochrome *C*. 3B : C 16 capillary c olumn, 2 0 c m e ffective le ngth, 2 7 c m to tal le ngth × 100 μm i .d.; h ydro-organic m obile pha se, 3 5 % A CN (v/v), 10 m M s odium phosphate m onobasic, pH 6.0, running voltage 10 kV, electrokinetic injection for 5 s at 10 kV in (a) and running voltage -10 kV, electrokinetic injection for 5 s at -10 kV in (b).
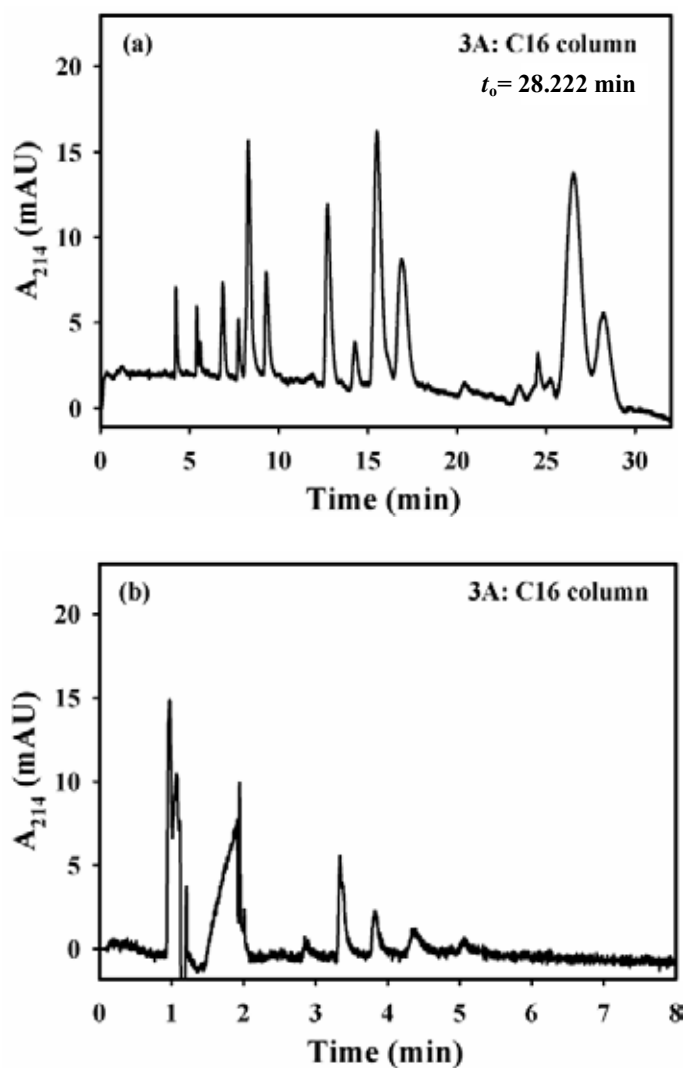
Figure 4.20 Electrochromatograms of the tryptic digest of cytochrome *C*. 3A: C16 capillary column, 20 cm effective length, 27 cm total length × 100 μm i.d.; hydro-organic mobile phase, 35 % ACN (v/v), 10 mM sodium phosphate monobasic, pH 6.0, running voltage 10 kV, electrokinetic injection for 5 s at 10 kV in (a) and running voltage -10 kV, electrokinetic injection for 5 s at -10 kV in (b).
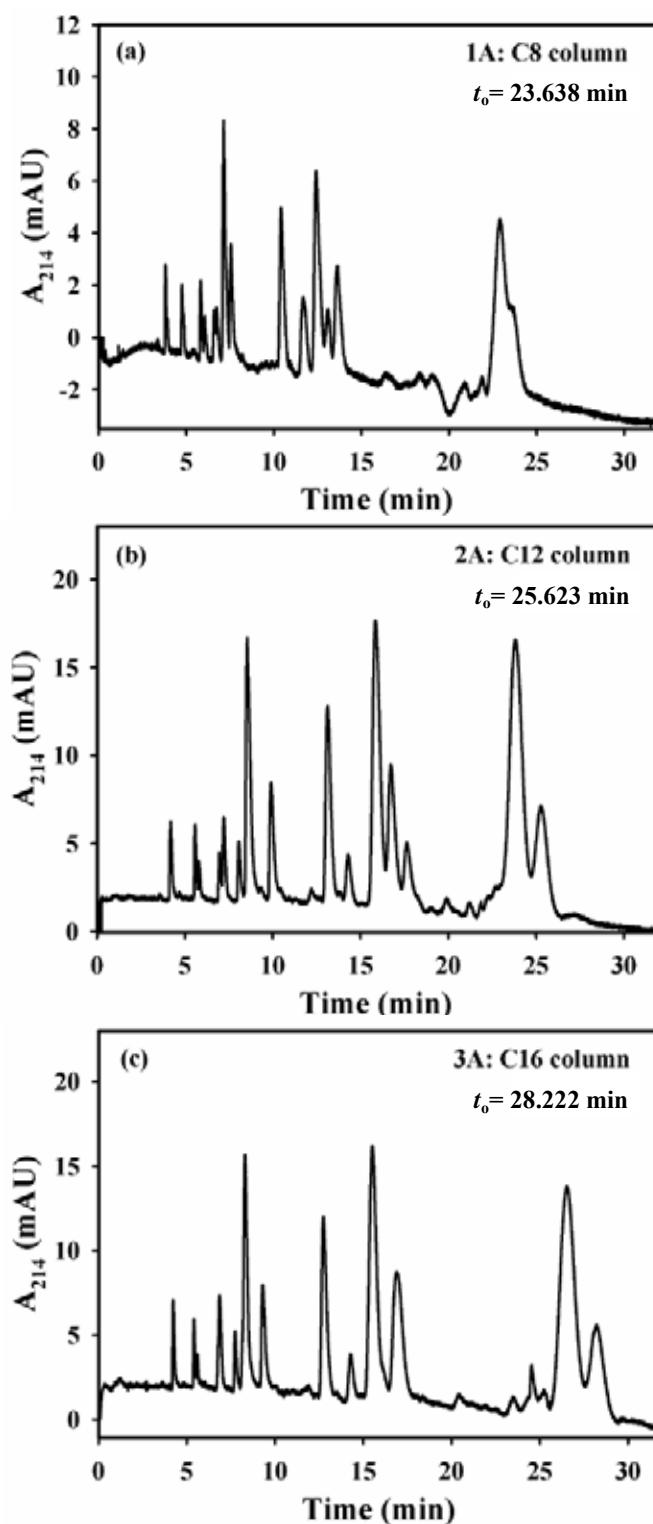
Figure 4 .21 Electrochromatograms o f th e tr yptic d igest o f c ytochrome *C* using columns with different *n*-alkyl chain length, 20 cm effective length, 27 cm total length × 100 μm i.d., 1A: C8 column in (a), 2A: C12 column in (b) and 3A: C16 column in (c); hy dro-organic m obile pha se, 35 % A CN (v/v), 10 m M sodium phos phate monobasic, pH 6.0, running voltage 10 kV, electrokinetic injection for 5 s at 10 kV.

4.4 Conclusion

In conclusions, this study has assessed the optimal *n*-alkyl chain length as well as the monomer composition for the preparation of neutral monoliths best suited for the reversed-phase capillary electrochromatography (RP-CEC) separation of peptides and proteins. In comparison with unstable monolithic columns obtained from the nitric acid initiator, the more stable monolithic columns obtained from the 2,2′-azobisiobutylronitrile (AIBN) initiator at the optimal composition of the monomers and the porogen provided comparable separation efficiency, up to 200,000 plates/m for alkylbenzene, and therefore were chosen for further study. Using AIBN as a initiator, two different neutral nonpolar monolithic columns series (designated as A and B columns series) each consisting of three columns at varying *n*-alkyl chain length were prepared by the copolymerization of the functional monomers C8-methacrylate, C12-acrylate or C16-methacrylate with the crosslinking monomer pentaerythritol triacrylate in a ternary porogenic solvent composed of cyclohexanol, ethylene glycol, and water. The magnitude of the electroosmotic flow (EOF) of A columns series depends on the pH and the ACN content of the mobile phase. This is indicative of the adsorption of electrolyte ions of the mobile phase to the monolithic surface, which imparts the monoliths with the zeta potential necessary to support the EOF. The separation efficiency for ABs obtained on the monolithic columns with the same composition of the polymerization mixture (i.e. the B columns series) was lower than that of the variable ones (i.e. the A columns series). The C16-monolith of the A series (3A column) yielded better separation efficiency towards small solutes such as alkylbenzenes, alkyl phenyl ketones, nitroalkanes, phenols and anilines, but the A columns series were inadequate for protein separation by RP-CEC. However, the C8-monolith of the B series (1B column) provided better separation efficiency for proteins while for tryptic peptide mapping, the C16-monolith of the A series (3A column) seems to provide better separation. For large protein molecules, the energetically "softer" C8 surface allowed faster sorption kinetics and in turn improved efficiency, while an energetically "harder" C16 surface favored better separation of the smaller size peptide solutes.

CHAPTER V

SUMMARY AND FUTURE WORK

5.1 Theoretical Mo dels o f Separation S electivity f or C harged C ompounds i n MEKC

The C ZE s eparation o f charged an alytes c an b e p erformed b y t he running buf fer, while t heir M EKC s eparation i s pe rformed b y the running buf fer c ontaining a surfactant as m icellar or p seudo-stationary p hase. T he s eparation s electivity or mobility s electivity in CZE (α_{CZE}) i s ba sed on t he di fference i n e lectrophoretic mobility of charged analytes, while the separation selectivity in MEKC (α_{MEKC}) arises from either the retention selectivity of the micellar phase (α_k) or α_{CZE}. In this work, equations and theoretical models for α_{MEKC} of two charged analytes were developed to predict a change in α_{MEKC} based on t he range of the mobility selectivity in CZE, retention s electivity in M EKC (α_k), s electivity ratio ($\rho = \alpha_k/\alpha_{CZE}$) and the order of the order of $|\mu|$ in CZE and k in MEKC. The proposed α_{MEKC} models were classified into four types: (I) $\rho > 1.0$, where $\alpha_k > \alpha_{CZE} \geq 1.0$; (II) $\rho \leq 1.0$, where $\alpha_{CZE} \geq \alpha_k \geq 1.0$; (III) $\rho > 1.0$, where $\alpha_k \geq 1.0 > \alpha_{CZE}$, (IV) $\rho = 1.0$, where $\alpha_k = \alpha_{CZE} = 1.0$.

In comparison with CZE, whether MEKC with normal elution mode will improve or reduce separation selectivity for two charged analytes depends on the model of α_{MEKC} and k value. Typically, better s eparation s electivity i n M EKC o ver C ZE can b e obtained f or t he α_{MEKC} Type I ($\alpha_k > \alpha_{CZE}$), o r T ype III models ($\alpha_k \gg \alpha_{CZE}$, or $\alpha_k > 1/\alpha_{CZE}$) at appropriate values of k_1, while those of Type II models result in worse of α_{MEKC} for two charged analytes. T he α_{MEKC} Type IV with α_{CZE} of 1 .0 and α_k of 1.0 ($\rho = 1.0$), no r esolution i s obtained i n either CZE or MEKC. It s hould be not ed that for a theoretical value of α_{CZE} or $\alpha_{MEKC} < 1.0$, the practical separation selectivity is equal to $1/\alpha_{CZE}$ or $1/\alpha_{MEKC}$. Therefore, an increase in k_1 may result in a r eversed order of electrophoretic mobility for two charged analytes in MEKC. Type III model

starts from less than 1.0 ($1/\alpha_{MEKC} > 1.0$) to near 1.0 (poorer separation) with increasing k_1 and then higher than 1.0 (better separation) at higher k_1 values. This indicates that reversed of $|\mu|$ in CZE and k in MEKC for two charged analytes. Using four alkylparabens as test analytes, such as IP, EP, PP and BP, excellent agreement was found between the observed α_{MEKC} and the proposed α_{MEKC} models of test analytes in MEKC over a wide range of [SDS] and values of k. It also should be noted that the direction of EOF velocity and total velocity does not affect the electrophoretic mobility of analytes and micelles, and the retention factor of analytes in MEKC. Owing to independence of the values of α_m and α_k with the direction of these velocities, these proposed selectivity models can be used for MEKC with normal, reversed and restricted modes.

5.2 Investigation of Neutral Monolithic Capillary Columns with Varying *n*-alkyl Chain Lengths in CEC

Two different neutral nonpolar monolithic columns series (designated as A and B columns series) each consisting of three columns at varying *n*-alkyl chain length were prepared by the copolymerization of the functional monomers C8-methacrylate, C12-acrylate or C16-methacrylate with the crosslinking monomer PETA to yield monoliths with surface bound C8, C12 and C16 chains. A ternary porogenic solvent consisting of cyclohexanol and ethylene glycol in various ratios at constant 3.6 wt% water was used. AIBN (1.0 wt% with respect to monomers) was added to the solution as the free radical initiator. In the A columns series, the composition of the functional monomers and crosslinker was adjusted to yield comparable chromatographic retention regardless of the alkyl chain length. In the B columns series, the composition of the functional monomers and crosslinker was kept constant yielding chromatographic retention, which increased as expected in the order of increasing the *n*-alkyl chain length.

These two different neutral nonpolar monolithic columns were characterized over a wide range of mobile phase composition. The magnitude of the EOF of A columns

series depends on the pH and the ACN content of the mobile phase. This is indicative of the adsorption of electrolyte ions of the mobile phase to the monolithic surface, which imparts the monoliths with the zeta potential necessary to support the EOF. The A columns series were evaluated for their performance by using ABs, APKs, and NAs, which are typical model solutes of high, moderate, and low hydrophobic character, respectively. Under the same mobile phase composition and applied voltage, the magnitude order of k values was ABs > APKs > NAs, which is consistent with that of the hydrophobic order of the homologous ABs > APKs > NAs. This is indicative of a reversed phase retention mechanism. It should be noted that the amount of the functional monomers for the A series such as 1A, 2A, and 3A monoliths, increased in the order C8 > C12 > C16, the shorter is the alkyl chain length the higher is the EOF velocity. This explains the slightly higher k values or slightly longer separation time on C8 and C12 than on C16 monoliths. Therefore, and for difficult separations that would require high separation efficiency, one would consider a longer alkyl chain monolith at optimal functional monomer content (e.g. C16) with slightly lower retention and faster analysis time. In the case of B columns series, the k values of ABs increased with increasing the alkyl chain length as in principle should be the case. The separation efficiency for ABs obtained on the monolithic columns with the same composition of the polymerization mixture (i.e. the B columns series) was lower than that of the variable ones (i.e. the A columns series). In the B columns series, the column made with the shorter alkyl chain length yielded higher separation efficiency than the longer one. This is due primarily to the fact that a shorter analysis time would allow less band spreading that arises from longitudinal molecular diffusion assuming that everything else has remained the same.

In comparison with C8- and C12- monoliths, the C16-monolith of the A series yielded the highest separation efficiency towards small solutes, but the A columns series were inadequate for protein separation by RP-CEC. The C8-monolith of the B series provided the best separation efficiency for proteins while for tryptic peptide mapping, the C16-monolith of the A series seems to provide the best separation. For large protein molecules, the energetically "softer" C8 surface allowed faster sorption

kinetics and in turn improved efficiency, while an energetically "harder" C16 surface favored better separation of the smaller size peptide solutes.

5.3 Future Work

Work on MEKC separation selectivity for two negatively charged analytes in thesis has proved to be useful in explaining a change in α_{MEKC} through theoretical models of α_{MEKC}. In the future work, these theoretical models could be checked in charged compounds separation in MEKC using other MEKC modes such as reversed elution mode or restricted elution mode. It is also interesting to study the other negatively charged analytes with normal elution mode or positively charged analytes with reversed elution mode. The work on the investigation of neutral monolithic capillary columns with varying *n*-alkyl chain lengths in CEC has assessed the optimal *n*-alkyl chain length as well as the monomer composition for the preparation of neutral monoliths best suited for the RP-CEC separation of peptides and proteins. The work may be extended to CEC coupled with a mass spectrometer in order to identify peptides and proteins. It is also interesting to investigate other crosslinkers and initiator to prepare the neutral monolithic capillary columns.

REFERENCES

Andrea, W., and Brown, P.R. (1997). HPLC and CE: Principles and practice. San Diego: Academic Press.

Augustin, V., Stachowiak, T., Svec, F., and Fréchet, J.M.J. (2008). CEC separation of peptides using a poly(hexyl acrylate-*co*-1,4-butanediol diacrylate-*co*-[2-(acryloyloxy)ethyl]trimethyl ammonium chloride) monolithic column. Electrophoresis 29: 3875-3886.

Bedair, M., and El Rassi, Z. (2002). Capillary electrochromatography with monolithic stationary phases: 1. Preparation of sulfonated stearyl acrylate monoliths and their electrochromatographic characterization with neutral and charged solutes. Electrophoresis 23: 2938-2948.

Bedair, M., and El Rassi, Z. (2003). Capillary electrochromatography with monolithic stationary phases. II. Preparation of cationic stearyl-acrylate monoliths and their electrochromatographic characterization. J. Chromatogr. A 1013: 35-45.

Beiler, B., Vincze, Á., Svec, F., and Sáfrány, Á. (2007). Poly(2-hydroxyethyl acrylate-*co*-ethylene dimethacrylate) monoliths synthesized by radiation polymerization in a mold. Polymer. Polymer 48: 3033-3040.

Cai, J., Smith, J.T., and El Rassi, Z. (1992). Determination of the ionization constants of weak electrolytes by capillary zone electrophoresis. J. High Resolut. Chromatogr. 15: 30-32.

Camilleri, P. (1993). Capillary electrophoresis: Theory and Practice. Boca Raton: CRC Press.

Cantó-Mirapeix, A., Herrero-Martínez, J.M., Mongay-Fernández, C., and Simó-Alfonso, E.F. (2008). Preparation and evaluation of butyl acrylate-based monolithic columns for CEC using ammonium peroxodisulfate as a chemical initiator. Electrophoresis 29: 3858-3865.

Česla, P., Blomberg, L., Hamberg, M., Jandera, P . (2006). Characterization o f anacardic a cids b y mic ellar e lectrokinetic chromatography a nd m ass spectrometry. J. Chromatogr. A 1115: 253-259.

Damić, M., and Nigović, B. (2009). Fast Analysis o f Statins in Pharmaceuticals by MEKC. Chromatographia 71: 233-240.

Dittmann, M.M., Masuch, K., and Rozing, G.P. (2000). Separation of basic solutes by reversed-phase capillary electrochromatography. J. Chromatogr. A: 887: 209-221.

Dittmann, M .M., a nd Rozing, G.P. (1997). Capillary e lectrochromatography: Investigation of t he i nfluence o f m obile pha se and s tationary pha se properties on e lectroosmotic ve locity, r etention, a nd selectivity. J. Micro Sep 9: 399-408.

Dong, J ., X ie, C ., T ian, R ., W u, R ., H u, J., a nd Zou, H . (2005). C apillary electrochromatography w ith a n eutral mo nolithic c olumn f or classification of analytes a nd de termination of b asic dr ugs i n hum an serum. Electrophoresis 26: 3452-3459.

Dong, X., Wu, R., Dong, J., Wu, M., Zhu, Y., and Zou, H. (2009). Recent progress of polar stationary phases in CEC and capillary liquid chromatography. Electrophoresis 30: 141-154.

Eeltink, S ., Rozing, G .P., Schoenmaker, P.J., a nd K ok, W . T h. (2006). Practical aspacts o f u sing m ethacrylate-ester-based m onolithic c olumns i n capillary electrochromatography. J. Chromatogr. A 1109: 74-79.

Eeltink, S., and Svec, F. (2007). Recent advances in the preparation and application of por ous pol ymer-based monolithic s tationary p hases f or capillary electrochromatography. Electrophoresis 28: 137-147.

Faure, K., Albert, M., Dugas, V., Crétier, C., Ferrigno, R., Morin, P., and Rocca, J.-L. (2008). Development of a n acrylate m onolith i n a cyclo-olefin copolymer m icrofluidic de vice f or c hip e lectrochromatography separation. Electrophoresis 29: 4948-4955.

Giddings, J.C. (1991). Unified Separation Science, New York: Wiley.

Golden, R., Gandy, J., and Vollmer, G. (2005). A review of the endocrine activity of parabens an d i mplications f or potential r isks t o hum an h ealth. Crit. Rev. Toxicol. 35: 435-458.

Grossman, P .D., and C olburn, J .C. (1992). Capillary e lectrophoresis: T heory a nd practice. Academic Press: San Diego.

Hansen, S .H. (2003). Recent applications o f mic roemulsion e lectrokinetic chromatography. Electrophoresis 24: 3900-3907.

Holdšvendová, P., Coufal, P., Suchánková, J., Tesařová, E., and Bosáková, Z. (2003). Methacrylate mo nolithic c olumns for capillary liquid c hromatography polymerized using ammonium peroxodisulfate as initiator. J. Sep. Sci. 26: 1623-1628.

Huang, H.-Y., Lai, Y .-C., Chiu, C .-W., and Yeh, J.-M. (2003). Comparing mic ellar electrokinetic chromatography an d microemulsion e lectrokinetic chromatography for the analysis of preservatives in pharmaceutical and cosmetic products. J. Chromatogr. A 993: 153-164.

Iadarola, P ., F errari, F ., F umagalli, M ., and Viglio, S . (2008). Determination o f amino a cids b y mic ellar EKC: R ecent ad vances i n method development and nove l applications t o different matrices. Electrophoresis 29: 224-236.

Karenga, S., and El R assi, Z. (2008). N eutral oc tadecyl monolith for reversed phase capillary electrochromatography o f a w ide r ange o f s olutes. J. S ep. Sci. 31: 2677-2685.

Karenga, S ., and El R assi, Z . (2010a). A nove l, ne utral h ydroxylated oc tadecyl acrylate mo nolith w ith f ast e lectroosmotic f low v elocity and its application to the separation of various solutes including peptides and proteins i n t he a bsence of el ectrostatic i nteractions. Electrophoresis 31: 3192-3199.

Karenga, S ., and El R assi, Z . (2010b). Naphthyl me thacrylate-based m onolithic column f or R P-CEC *via* hydrophobic and π interactions. Electrophoresis 31: 991-1002.

Karenga, S., and El Rassi, Z. (2010c). Naphthyl methacrylate-phenylene diacrylate-based m onolithic c olumn f or r eversed-phase cap illary electrochromatographyvia h ydrophobic a nd π interactions. Electrophoresis 31: 3200-3206.

Karenga, S ., a nd E l R assi, Z . (2011a). Mixed l igand m onolithic c olumns f or reversed-phase capillary electrochromatography via hydrophobic and π interactions. Electrophoresis 32: 1044-1053.

Karenga, S ., a nd E l R assi, Z . (2011b). Controlling r etention, selectivity a nd magnitude o f E OF b y s egmented m onolithic c olumns c onsisting of octadecyl a nd n aphthyl monolithic s egments-applications to R P-CEC of both neutral and charged solutes. Electrophoresis 32: 1033-1043.

Karenga, S., and El Rassi, Z. (2011c). Trends in nonpolar polymer-based monolithic columns f or r eversed-phase cap illary electrochromatography. Electrophoresis 32: 90-104.

Khaledi, M .G. (1998). High p erformance capillary e lectrophoresis: Theory, techniques, and applications. New York: John Wiley & Sons.

Klodzińska, E., Moravcova, D ., Jandera, P., and B uszewski, B. (2006). Monolithic continuous be ds a s a ne w ge neration of s tationry pha se for chromatographic an d el ectro-driven s eparations. J. C hromatogr. A 1109: 51-59.

Legido-Quigley, C., Marlin, N.D., Melin, V., Manz, A., and S mith, N.W. (2003). Advances i n cap illary electrochromatography an d m icro-high performance liquid chromatography monolithic columns for separation science. Electrophoresis 24: 917-944.

Li, S .F.Y. (1992). Capillary el ectrophoresis: P rinciples, p ractice an d a pplications. Amsterdam: Elsevier Science Publishers B. V.

Li, Y., T olley, H .D., and Lee, M .L. (2009). Poly[hydroxyethyl a crylate-*co*-poly(ethylene glycol) d iacrylate] mo nolithic c olumn f or efficient hydrophobic interaction chromatography of proteins. Anal. Chem. 81: 9416-9424.

Li, Y ., X iang, R ., Horváth, C ., a nd W ilkins, J.A. (2004). Capillary electrochromatography o f peptides o n a ne utral p orous m onolith w ith annular electroosmotic flow generation. Electrophoresis 25: 545-553.

Lu, M., F eng, Q., Lu, Q., C ai, Z., Zhang, L., and Chen, G. (2009). Preparation and evaluation of t he hi ghly cross-linked pol y(1-hexadecane-*co*-trimethylolpropane tr imethacrylate) mo nolithic column f or c apillary electrochromatography. Electrophoresis 30: 3540-3547.

Mallampati, S., Leonard, S., De Vulder, S., Hoogmartens, J., and Van Schepdael, A. (2005). Method de velopment a nd v alidation f or t he analysis of didanosine us ing m icellar electrokinetic c apillary chromatography. Electrophoresis 26: 4079-4088.

Matsunaga, H., Sadakane, Y ., and Haginaka, J. (2004). Identification o f di sulfide bonds a nd s ite-specific glycosylation in chicken α_1-acid g lycoprotein by ma trix-assisted la ser d esorption io nization time -of-flight ma ss spectrometry. Anal. Biochem. 331: 358-363.

McEvoy, E ., M arsh, A ., A ltria, K ., D onegan, S., a nd P ower, J . (2007). Recent advances i n t he d evelopment a nd a pplication of m icroemulsion EKC. Electrophoresis 28: 193-207.

Merhar, M., Podgornik, A., Barut, M., Žigon, M., Štrancar, A. (2003). Methacrylate monoliths pr epared from va rious h ydrophobic a nd h ydrophilic monomers-Structural and chromatographic characteristics. J. Sep. Sci. 26: 322-330.

Miola, M .F., S nowden, M.J., a nd A ltria, K .D. (1998). The us e o f m icroemulsion electrokinetic ch romatography i n p harmaceutical an alysis. J. P harm. Biomed. Anal. 18: 785-797.

Nhujak, T., Sastravaha, C., Palanuvej, C., and Petsom, A. (2005). Chiral separation in capillary el ectrophoresis u sing dual n eutral cyclodextrins: T heoretical models of electrophoretic mo bility d ifference a nd s eparation selectivity. Electrophoresis 26: 3814-3823.

Okanda, F., and El Rassi, Z. (2005). Capillary electrochromatography with monolithic stationary phases. 4. Preparation of neutral stearyl-acrylate monoliths and their evaluation in capillary electrochromatography for neutral and charged small species as well as peptides and proteins. Electrophoresis 26: 1988-1995.

Peters, E.C., Svec, F., and Fréchet, J.M.J. (1999). Rigid Macroporous Polymer Monoliths. Advanced Materials 11: 1169-1181.

Piršelová, K., Baláž, Š., and Schultz, T.W. (1996). Model–based QSAR for ionization compounds: Toxicity of phenols against *Tetrahymena pyriformis.* Arch. Environ. Contam. Toxicol. 30: 170-177.

Poouthree, K., Leepipatpiboon, N., Petsom, A., and Nhujak, T. (2007). Retention factor and retention index of homologous series compounds in microemulsion electrokinetic chromatography employing suppressed electroosmosis. Electrophoresis 28: 767-778.

Pyell, U. (2006). Electrokinetic Chromatography: Theory, Instrumentation, and Application. West Sussex: John Wiley & Sons.

Riekkola, M.-L., Wiedmer, S.K., Valkó, I.E., and Sirén, H. (1997). Selectivity in capillary electrophoresis in the presence of micelles, chiral selectors and non-aqueous media. J. Chromatogr. A 792: 13-35.

Rohr, T., Hilder, E.F., Donovan, J.J., Svec, F., and Frechet, J.M.J. (2003). Photografting and the control of surface and inner volume chemistry in three-dimensional porous polymer monoliths. Macromolecules 36: 1677-1684.

Sáfrány, Á., Beiler, B., László, K., and Svec, F. (2005). Control of pore formation in macroporous polymers synthesized by single-step g-radiation-initiated polymerization and crosslinking. Polymer 46: 2862-2871.

Štulík, K., Pacáková, V., Suchánková, J., and Coufal, P. (2006). Monolithic organic polymeric columns for capillary liquid chromatography and electrochromatography. J Chromatogr B Analyt Technol Biomed Life Sci. 841: 79-87.

Svec, F. (2009). Capillary electrochromatography: S elected d evelopments t hat caught my eye since the year 2000. Electrophoresis 30: S68-S82.

Svec, F. (2010). Porous pol ymer m onoliths: A mazingly w ide va riety o f t echniques enabling their preparation. J. Chromatogr. A 1217: 902-924.

Svec, F., P eters, E.C., Sýkora, D., and Fréchet, J.M.J. (2000). Design of the monolithic pol ymers us ed i n c apillary e lectrochromatography columns. J. Chromatogr. A 877: 3-29.

Tan, A ., B enetton, S ., a nd H enion, J.D. (2003). C hip-based s olid-phase ex traction pretreatment f or d irect e lectrospray m ass s pectrometry analysis u sing an array of monolithic columns in a polymeric substrate. Anal. Chem. 75: 5504-5511.

Tavares, R .S., M artins F .C., O liveira, P .J., R amalho-Santos, J ., and Peixoto, F .P. (2009). Parabens in ma le in fertility-Is t here a m itochondrial connection? Reprod Toxicol 27: 1-7.

Téllez, A., Fuguet, E., and Rosés, M. (2007a). Comparison of migration models for acidic s olutes in micellar el ectrokinetic chromatography. J. Chromatogr. A. 1139: 143-151.

Téllez, A ., F uguet, E ., and Rosés, M. (2007b). Optimization of t he s eparation of ionizable compounds in mic ellar e lectrokinetic chromatography b y simultaneous c hange of pH a nd S DS c oncentration. Electrophoresis 28 : 3712-3721.

Terabe, S ., O tsuka, K ., a nd Ando, T . (1989). Band br oadening i n e lectrokinetic chromatography w ith m icellar s olutions a nd ope n-tubular capillaries. Anal. Chem. 61: 251-260.

Viklund C ., Svec F ., F réchet J.M.J., and Irgum K. (1996). Monolithic, "molded", porous ma terials with h igh flow c haracteristics f or s eparations, catalysis, or solid phase chemistry: Control of porous properties during polymerization. Chem. Mater. 8: 744-750.

Vlakh, E.G., and Tennikova, T.B. (2007). Preparation of methacrylate monoliths. J. Sep. Sci. 30: 2801-2813.

Wang, M.-M., Wang, H.-F., Jiang, D.-Q., Wang, S.-W., and Yan, X.-P. (2010). A strong inorganic acid-initiated methacrylate polymerization strategy for room temperature preparation of monolithic columns for capillary electrochromatography. Electrophoresis 31: 1666-1673.

Wen, E., Asiaie, R., and Horváth, C. (1999). Dynamics of capillary electrochromatography: II. Comparison of column efficiency parameters in microscale high-performance liquid chromatography and capillary electrochromatography. J. Chromatogr. A. 855: 349-366.

Wilson, C.O., and Gisvold, O. (1998). Textbook of Organic Medicinal and Pharmaceutical Chemistry. Philadelphia: Lippincott-Raven.

Zhang, L., Ping, G., Zhang, L., Zhang, W., and Zhang, Y. (2003). Preparation and characterization of monolithic columns for capillary electrochromatography with weak electroosmotic flow. J. Sep. Sci. 26: 331-336.

BIBLIOGRAPHY

Publications

1) C. Puangpila, A. Petsom, T. Nhujak "Theoretical models of separation selectivity for ch arged co mpounds i n m icellar el ectrokinetic ch romatography" *Electrophoresis*, 32 (2011) 203-209. Impact factor = 3.569

2) C. Puangpila, T. Nhujak, Z. El Rassi "Investigation of neutral monolithic capillary columns w ith va rying n -alkyl ch ain l engths i n capillary electrochromatography" *Electrophoresis*, accepted. Impact factor = 3.569

International Presentations

1) C. P uangpila, T. N hujak, Z . E l Rassi "Methacrylate-based m onoliths a t va rying alkyl chain l ength f or C EC of pr oteins a nd pe ptides m apping–preparation, chromatographic characterization an d p erformance" P oster P resentation, 10th Asian-Pacific International S ymposium o n M icroscale S eparations an d A nalysis, 10-13 December, 2010, Hong Kong University, Hong Kong, China.

2) C. Puangpila, A. Petsom, T. Nhujak "Theoretical models of separation selectivity for ch arged co mpounds i n m icellar electrokinetic ch romatography" P oster presentation, 17 [th] International S ymposium o n Electro- and Liquid P hase-separation T echniques, 29 A ugust-1 S eptember, 2010, T reat M ont H otel, Baltimore, Maryland, USA.

3) C. P uangpila, T. N hujak, Z . E l R assi "Methacrylate-based m onoliths a t va rying alkyl chain l ength f or C EC of pr oteins a nd pe ptides m apping–preparation, chromatographic ch aracterization an d p erformance" Poster p resentation, 17 [th] International Symposium on Electro- and Liquid Phase-separation Techniques, 29 August-1 September, 2010, Treat Mont Hotel, Baltimore, Maryland, USA.

National Presentations

C. Puangpila, A. Petsom, T. Nhujak "Theoretical models of separation selectivity for charged compounds in micellar electrokinetic chromatography", Poster presentation, 85th RGJ S eminar S eries Contemporary A nalytical C hemistry and A nalytical Technology, 9 September, 2011, Mahidol University, Bangkok.

VITA

Chanida Puangpila was born in Sakonnakhon, Thailand, on Monday 13rd June, 1983. She received Bachelor's degree of Science in Chemistry, from Khon Kaen University in A pril, 2006. S he c ontinued he r s tudy for a D octoral d egree of S cience i n Analytical C hemistry, the D epartment o f C hemistry, th e F aculty o f S cience, Chulalongkorn University in June, 2006 and completed the program in 2012.